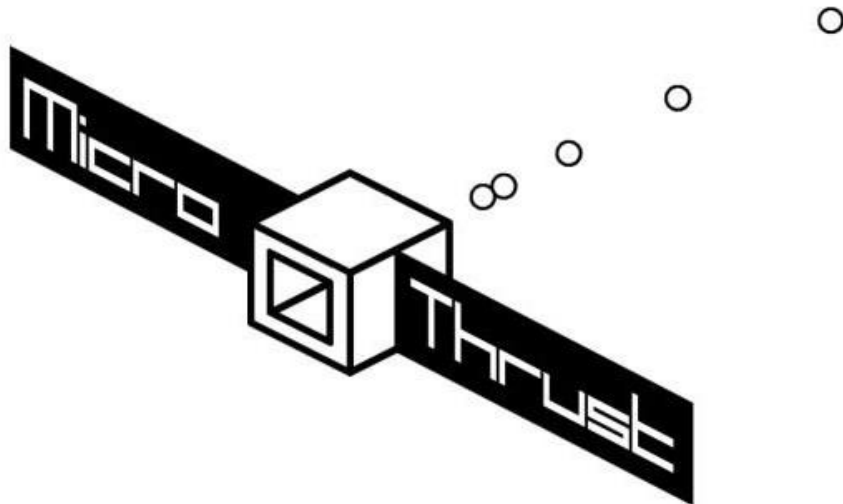


# Hardware and Software Design of the Microthrust Power and Control System



Submitted in partial fulfillment of the requirements for the degree  
of

MASTER OF SCIENCE

in

COMPUTER ENGINEERING

by

Jan Timmerman

CE-MS-2014-05

This work has been supported by the MicroThrust project, grant agreement number 263035, funded by the EC Seventh Framework Program theme FP7-SPACE-2010

# Abstract

The Microthrust project aims to deliver an efficient and scalable electric propulsion system for very small form factor satellites. For this aim, a thruster chip (THC) is being developed at EPFL, Switzerland, that uses a strong electric field to accelerate charged particles from hollow 'needles'. The particles are emitted from the propellant, a liquid that consists of positive and negative ions.

To propel these charged particles, both an 'extraction voltage' is needed that extract the particles from the liquid and an 'accelerator voltage' that accelerates and focuses the beam. A small form factor of 80x80x20mm is required for the power and control system (PCS) to generate these voltages and control the THC.

The voltage of the accelerator plane is defined as 0V while a voltage is applied to the 'particle emitter', so in fact an emitter voltage and an extraction voltage are generated.

The emitter voltage, which is typically between 3kV and 4kV, is generated using a Royer circuit combined with a voltage doubler. The Royer circuit generates an AC voltage from 12V DC input through a self-oscillating circuit that is fed in a transformer. A doubler circuit doubles and rectifies this output. To regulate the output voltage, the 12V supply of the Royer circuit is periodically interrupted using a 16kHz PWM signal, which is generated by a microcontroller. The controller continuously monitors the emitter voltage and adjusts the PWM signal accordingly based on PID control software. As efficiency was initially not good, a lot of effort has been spent to improve this circuit which eventually succeeded using a careful component selection

Extraction voltage is generated from the emitter voltage by using a controllable resistor divider. This is possible since the extractor plane of the thruster chip should not draw a current. The control of this bypass is a similar, but not identical, to the PID control for the emitter voltage.

As the spacecraft needs to remain electrically neutral, both a positive and negative stream of particles needs to be emitted simultaneously. Functionality was therefore split among two boards, one creating two opposite emitter voltages of up to 4kV and the other creating up to four extraction voltages. Communication between boards was done using a serial bus and a state machine as command parser. A graphical user interface on a PC allows user control of the PCS.

The PCS is able to produce two opposite emitter voltages and four extractor voltages on two 80x80mm boards with an efficiency of >50% above 1W. The accuracy requirement (1%) and ripple regarding the emitter voltage has been met, but that of the extraction voltage (0.1%) not fully. We were able to successfully generate thrust using our PCS and the microthrust thruster chip.

# Table of Contents

Table of Contents.....	4
1 Introduction.....	9
1.1 Goals.....	10
2 Background.....	11
2.1 Electrospray thruster.....	11
2.2 Taylor cone.....	11
2.3 Ionic Liquids.....	12
2.4 History of electrospray.....	12
2.5 Overview of electric propulsion methods.....	13
2.5.1 Field Emission Electric Propulsion (FEEP).....	13
2.5.2 Ion Engine.....	13
2.5.3 Projects with great similarity to microthrust.....	13
2.5.3.2 <i>Ionic Electronic Propulsion System (IEPS)</i> .....	14
2.6 The microthrust thruster chip.....	15
2.7 Emitter voltage generation methods.....	16
2.7.1 Multiplier circuits.....	16
2.7.2 Transformer based circuits.....	17
2.7.3 Generation methods used in other projects.....	19
3 System Design.....	20
3.1 Overview of board implementations.....	21
3.1.1 Initial board.....	21
3.1.2 Extended initial board.....	21
3.1.3 Size compliant boards.....	22
3.1.4 Modified size compliant boards.....	22
3.2 Setup.....	23
3.3 Requirements.....	24
3.3.1 Hardware requirements.....	25
3.3.2 Emitter voltage generation.....	25
3.3.3 Emitter voltage switching.....	25
3.3.4 Current and voltage sensing.....	25
3.3.5 Extractor voltage.....	26
3.4 Design selections.....	27
3.4.1 Emitter voltage generation.....	27
3.4.2 Emitter voltage switching.....	27
3.4.3 Sensing of $V_{\text{emitter}}$ , $I_{\text{emitter}}$ and $V_{\text{extractor}}$ .....	27
3.4.4 Extractor voltage generation.....	28

3.4.5	Control.....	28
3.4.6	Communication .....	28
4	Implementation and Design .....	29
4.1	Emitter voltage generation .....	29
4.1.1	Resonant flyback implementation .....	29
4.1.2	Royer implementation.....	30
4.2	Emitter voltage switching.....	33
4.2.1	Gate voltage generator .....	34
4.3	Extractor voltage generation.....	35
4.4	Software setup and structure.....	36
4.4.1	Structure.....	36
4.4.2	Command parser .....	37
4.4.3	Communication .....	37
4.5	Emitter voltage control .....	39
4.5.1	Software implementation .....	40
4.5.2	ADC reliability testing .....	42
4.5.3	Testing and identifying software and hardware problems .....	42
4.6	Extractor voltage control.....	42
4.7	Fault detection .....	43
4.7.1	Overcurrent detection.....	43
4.7.2	Overvoltage detection.....	43
4.8	Graphical User Interface.....	44
5	Results .....	46
5.1.1	Emitter voltage measurements.....	46
5.1.2	Extractor voltage measurements .....	46
5.2	Emitter voltage generation .....	47
5.2.1	Ripple of $V_{emitter}$ .....	48
5.2.2	Efficiency .....	49
5.3	Emitter voltage switching.....	50
5.4	Extractor voltage generation.....	51
5.4.1	Ripple.....	52
5.5	Electrospray thruster testing with the PCS .....	53
5.5.1	Spray results .....	54
6	Conclusion .....	56
6.1	Contributions.....	56
6.2	Future work .....	57
6.2.1	Controller.....	57
6.2.2	ESA voltage generation .....	57

## Nomenclature

ADC	=	Analog Digital Converter
BB	=	BreadBoard (model)
CPCB	=	Central Power and Control Board
COTS	=	Commercial off the shelf
ESA	=	Extractor Switch Assembly
EIFB	=	Electrical Interface Board
EPFL	=	Ecole Polytechnique Fédérale de Lausanne
ESTEC	=	European Space Research and Technology Engineering Center
FEEP	=	Field Emission Electrospray Thruster
FET	=	Field Effect Transistor
FM	=	Flight Model
HVPS	=	High Voltage Power Supply
IA	=	Instrumentation Amplifier
iEPC	=	International Electric Propulsion Conference
Isp	=	Specific Impulse
I <sup>2</sup> C	=	IIC, inter integrated circuit communication protocol
IDE	=	Integrated Development Environment
MTPS	=	Microthrust Power System
PCB	=	Printed Circuit Board
PCS	=	Power and Control System
PWM	=	Pulse Width Modulation
S/C	=	Space Craft
THC	=	Thruster chips (microfabricated thruster arrays)
TMS	=	Thruster Module System, which is the THC plus holder and peripherals
TRL	=	Technology Readiness Level
UART	=	Universal asynchronous receiver/transmitter

## Preface

This document is the conclusion of a thesis project that started for me in May 2012 at a company that had an interesting project involving a “novel and experimental space thruster”. This description is what one envisions when starting an engineering study and I was happy to take part of this project as graduate project.

Microthrust had already started a year earlier in 2011, so my work began with digging through, not always relevant, documentation and viewing puzzling schematics. After some time and a few brief meetings, I knew enough to start testing on the initial prototype, which contained a bit of software and circuits that were not quite functional. After many iterations of testing, developing software and hardware modifications by Martin the Jong, a heavily modified prototype was flown to Switzerland in November 2012 to combine with the 2012 version of the microthrust thruster chip. It took almost a day of tweaking using a lab-supply and trying several thruster chips before an electrospray was detected and the thruster chip was deemed operational, so our microthrust Power and Control System (PCS) could be tested. This version of the thruster chip usually operated only for a few minutes and never longer than 30 minutes, so it was surprising that after two hours of operation the chip was still generating thrust. The setup was left to run overnight and was still in operation the next morning.

In January 2013 the new PCS was presented during a meeting at TNO. This PCS was a miniaturized version of its predecessor with many improvements. With great improvements comes great risk, and indeed during development of new software to control the different components, problems like noise and crossover due to the tight margins were identified and mitigated. When the PCS was finally stable a test was planned in May 2013 and we went to Queen Mary London where a vacuum thruster chip test setup was available. The board was placed in vacuum, and broke down. After repairs and modifications a new test in London was planned resulting in another breakdown. After two unsuccessful trips to the UK a local high vacuum testing location was needed to simulate operating conditions in vacuum as apparently the board was affected by this. Testing facilities were found in the form of a vacuum deposition oven and later at a small start-up at the TU-Delft. After several of these tests, and more iterations of improvements, a new trip to London was due. Finally in October 2013, near the end of the project a successful test was booked. The project ended in December 2013. Although the level of readiness was not as advanced as initially was aimed at, the response from ESA was very positive and development on the microthrust thruster chip is still ongoing.

I am honored to have been part of a project that finished with glowing review from the European Space Agency, a very complex piece of equipment, a number of papers that feature my name and a t-shirt. I am thankful to Richard Visee and SystematIC who have entrusted me with the responsibility of controlling this challenging piece of equipment and Hugo Biersma, for introducing me to this project. I have gained a lot of experience with regard to electronics and hardware testing for which I have also to thank Martin de Jong who showed me the hands on approach to PCB design and testing. I would like to mention Single Quantum and Everest Coatings for providing high vacuum testing facilities and Arjan van Genderen for his guidance during the unorthodox process that led to this document. Lastly thanks to family and friends that have supported me and of course Marleen Kelder whose patience was tested during this entire process.

Delft University, September 2014

*Jan Timmerman*

# 1 Introduction

Small spacecraft like the Delfi-N3xt<sup>6</sup> and the SwissCube project<sup>2</sup>, provide a low-cost access to space. In recent years more and more functionality available to the full sized counterparts became available for this type of spacecraft<sup>29</sup>. Currently however, there is still a lack of a flexible and efficient propulsion system that is capable of carrying them beyond their initial orbit. Electro spray thrusters are seen as one of the promising technologies to fill this gap and are included in NASA's Space Technology Roadmap for In-Space Propulsion Systems<sup>21</sup>. To provide such a propulsion the microthrust project was initiated with the aim to deliver an efficient and scalable electric propulsion system for this type of satellites. The involvement of SystematicC and this thesis is the development of a power and control system (PCS) for the microthrust electric propulsion system.

In 2007, Neuchatel Switzerland, at the new Microsystems for Space Technologies Laboratory, the development of a novel micromachined propulsion system started with the goal to create a 'thruster on a chip'. In 2011, with support of the European Space Agency (ESA) and supervised by Herbert Shea a team of five project partners, including SystematicC, started microthrust. A project to develop not only a chip, but a fully functional, modular, thruster system directly applicable to cubesat sized spacecrafts.

The microthrust consortium consists of five partners:

<i>Partner</i>	<i>Tasks</i>
TNO	systems engineering, business development
Queen Mary University of London (QMUL),	integration, thruster chip performance testing
École Polytechnique de Fédérale Lausanne, Switzerland (EPFL)	thruster chip development, mission proposals
Nanospace, Sweden	holders for components and propellant, housing and interconnects for components
SystematicC	power and control system (PCS)

The thruster chip (THC) that is developed by École Polytechnique Fédérale de Lausanne (EPFL) and the Queen Mary University of London (QMUL) needs a stable controllable alternating supply that delivers both a voltage of at least 1 kV to create a stream of ions and a voltage of 3-4kV that accelerates and focuses the beam. A simple view of this thruster principle can be seen in figure 1. Additionally, the PCS should deliver two of these alternating accelerator voltages and four extraction voltages. This poses a significant challenge as the form factor of the PCS should stay within two 10x10cm circuit boards and the PCS needs to control and monitor the currents and voltages provided. Multiple microcontrollers control and monitor the high voltage generators and communicate with

the spacecraft controller. The software for this project is another challenge as improper control is likely to cause severe damage to the hardware, mandating costly repairs.

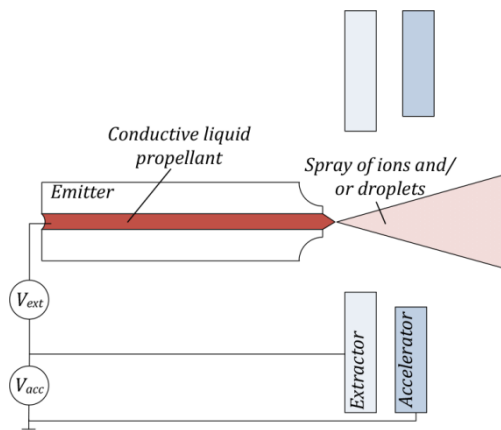


**Figure 1: Emitter, extractor and accelerator**

The microthrust PCS should deliver at least 3-4kV with an efficiency of 50%. Details of the specifications of this supply and controller will be presented later.

## 1.1 Goals

The goal of this thesis is to design and build hardware and software for a microthrust power and control system. The development of the hardware is not part of the activities leading to this thesis but debugging and improvements are, and were done in concert with the hardware developer, M.C.J. de Jong.

The final goals are:

- To develop a PCS that operates in concert with the electrospray chip to generate thrust.
- Get familiar with the hardware and complexities of the components
- Help creating a fully functional microthrust prototype board
- Design infrastructure and software for a scalable prototype

These goals should be achieved with an operating voltage of around 3-4 kV with sufficient efficiency and with all functionality on only a board of cubesat proportions (10x10 cm)<sup>24</sup>

The main challenge in this project is the control and development of both hardware and software as problems can be addressed only with a proper comprehension of both domains. This thesis will illustrate the different topics involved and the evolution of the microthrust power and control system (PCS) from concept to final breadboard model.

The project is structured iteratively. Before the involvement of this thesis project early concepts were already built on breadboards to experiment with different components. In a second phase these concepts are combined on a breadboard to prove feasible operation, my involvement started in this phase. The last phase is the production of a PCS that adheres to all the requirements as specified in 0.



Figure 2: The microthrust project group

## 2 Background

### 2.1 Electro spray thruster

The microthrust thruster chip is part of the electro spray thruster family, which are all thrusters that produce thrust through the emission of ions or charged droplets that are extracted from a liquid through means of an electric field. This in contrast to ion thrusters that extract ions from a plasma. As the mass of a single ion is very small the mass/acceleration ratio or  $Isp$  for electro spray and similar propulsion systems can be 3-10 times higher as an chemical propellant system. An electro spray thruster operates by feeding propellant into an ion emitter, which commonly has the form of a sharp needle. An electric field is established between the tip of this needle (emitter) and the opposing electrode. The electrically conductive propellant is then distorted into a sharp so-called Taylor cone as a result of the surface tension and electrostatic force that balance each other.

### 2.2 Taylor cone

The physical principle that is used in electro spray thrusters like the microthrust thruster chip is the so called Taylor cone. When an electric field is applied on an ionic liquid (or otherwise electrically conducting liquid) either cations or anions will gather at the surface depending on the applied polarity. When the electric field is strong enough, slight variations will cause small extrusions of liquid. These extrusions will, in turn, be more strongly influenced by the electric field further strengthening this effect. Shape and size of a Taylor cone is determined by the electric field versus the surface

tension of the liquid. At the point where the force of the electric field exceeds the force of surface tension the tip of this cone will emit a jet of liquid. This effect is used in several types of electrospray thrusters to generate thrust. An example is shown in figure 3 where in figure 3c a Taylor cone is formed<sup>13</sup>.

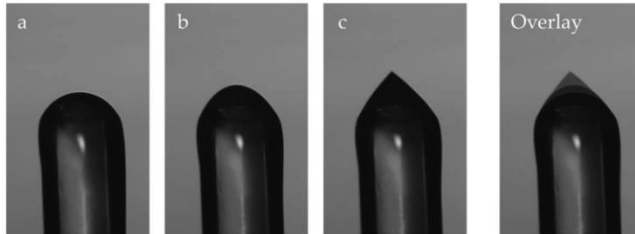


Figure 3: Sharpening of ionic liquid when electric field is applied.

### 2.3 Ionic Liquids

Ionic liquids are molten salts composed of a combination of positively and negatively charged ions. The special property of these salts is that they are liquid at or close to room temperature<sup>20</sup>. Applying an electric field will result in the gathering of cations or anions at the surface of the liquid. An advantage over metals as used in the FEEP thruster is the lower melting point compared to indium or easier handling compared to the extremely reactive cesium.

### 2.4 History of electrospray

The concept of ion propulsion is credited to R.H. Goddard in 1906<sup>28,34</sup> but the origins of electrospray can be traced back to experiments performed in the 1910's by John Zeleny. He observed that when a charged conductive liquid inside an hollow glass tube was placed opposite a grounded metal plate, the liquid tip would deform. The deformation would be in the form of a cone with a spray of particles from its tip when the voltage was high enough. In 1964 a physical description of this cone was presented by Sir Geoffrey Taylor<sup>20</sup>. After this paper, the American and European space agency's saw a great potential in this technology as they expected an high specific impulse and several projects were started in attempts to build a operational thruster system. In Europe, ESTEC produced an emitter with an Isp of 1223 seconds and a thrust of 0.5mN using +12.5kV and -2.6kV and in the US in 1974 an emitter was demonstrated producing a total of 4.45 mN of thrust with an Isp of 1365 seconds and operating point of 12kV<sup>17</sup>. After this period it took almost 25 years before in 1995 in Moscow an article was published on the iEPC about propulsion systems for small satellites. Then in '97 and '98, Martinez et al. published an overview on respectively electric propulsion and colloid thrusters. Furthermore in 1998 J. Perel, who published earlier on colloid thrusters in 1970, published an article called "Micro-electric propulsion using charged clusters"<sup>23</sup>. After these publications the interest in electric propulsion for micro satellites increased, resulting in a number of electric micro propulsion systems in development or in an experimental stage today. An extensive survey of

cubesat sized propulsion methods is provided in 2010 by Mueller et al.<sup>22</sup> showing over 15 different propulsion types. This introduction will only cover thruster types that are similar to the microthrust project with respect that only thrusters using charged particles as a means of generating thrust are considered.

## 2.5 Overview of electric propulsion methods

A number of electric propulsion methods suitable for cubesat sized satellites have been conceived and are in various stages of development. The common denominator for all projects is that they rely on an electric field to accelerate charged particles but the source of these particles varies. A number of propulsion methods like the microcavity discharge thruster<sup>5</sup> and the Teflon based pulsed plasma thruster<sup>4</sup> are omitted as some of these are either too dissimilar to microthrust or development seems to have stalled in recent years.

### 2.5.1 Field Emission Electric Propulsion (FEEP)

FEEP uses an alkali metal with a low melting point like indium or cesium that is propelled in a similar manner as the electrospray thruster. A high electric field is applied present above the liquid resulting in a Taylor cone and atoms are ionized at the tip of the jet and accelerated. Feeding of the liquid metal is either done through wetting of the needle or feeding through a small channel in the needle. FEEP results typically in very high Isp's of over 8000 seconds. Interestingly an FEEP engine has been equipped with ionic liquid which results in a similar behavior as an electrospray array<sup>19</sup>.

### 2.5.2 Ion Engine

Ion engines generate plasma in a small chamber from an inert gas like xenon and ions are extracted from this plasma through an electrostatic grid and accelerated in an electric field. Although plasma generation methods differ, a popular method is the use of a high frequency antenna that excites the few ions always present in a gas thus generating more ions and eventually resulting in a plasma<sup>22</sup>. A kickstarter project was running in July and August of 2013 to raise an amount of \$200,000 for the CubeSat Ambipolar Thruster (CAT) project, which is a cubesat suitable ion engine that is being developed at the University of Michigan and was promised to be completed within 18 months<sup>16</sup>. The goal for the fundraiser has not been met but development is still in progress.

### 2.5.3 Projects with great similarity to microthrust

Microthrust is one of a few projects focusing on building a high Isp thruster of cubesat proportions using ionic liquid as propellant. Three other projects show great similarity to the way ions are produced and propelled.

### 2.5.3.1 Busek Electrospray Thruster

Busek has already produced an 0.5U cubesat sized emitter that claims a thrust of 0.7 mN, and an efficiency of 800 seconds but up to 1300s<sup>3</sup>.

Busek uses emitters with a large diameter but adds a porous material on top of the emitter to create multiple Taylor cones which form in a fluidic layer on top of the porous material<sup>7</sup>. This thruster is available commercially.

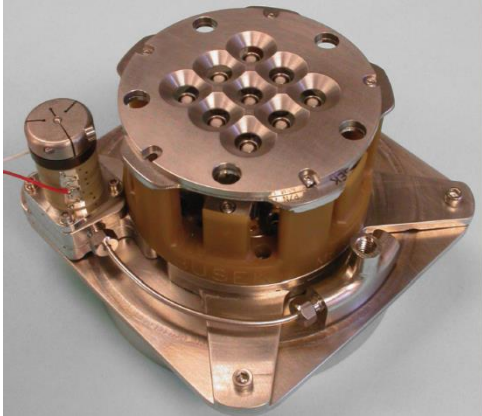


Figure 4: Busek electro-spray thruster

### 2.5.3.2 Ionic Electronic Propulsion System (iEPS)

The iEPS project is run at Michigan University and uses an ionic liquid that is accelerated using an electronic field generated with emitters and opposing plates with a high voltage<sup>15</sup>, which is almost identical to the technique used in the microthrust project. One difference is the production method, which uses a material with many small channels that are not created using etching and bonding techniques but rather due to the use of a porous substrate as base material. Although the location of the channels is not controllable, it has the advantage that it produces a great number of channels compared to the number of channels used in microthrust.

### 2.5.3.3 Ionic Liquid FEEP

Based on FEEP technology but uses ionic liquid instead of alkali metals<sup>19</sup>. Also this project uses a slit instead of multiple emitters, which, according to the creators, has the advantage of a greater operating range as the shape and number of Taylor cones varies. As the system is based on already existing FEEP technology authors claim high readiness level for this project. This project has very similar requirements regarding a high voltage, low power supply and uses a commercial off-the-shelf (COTS) EMCO F101 10kV power supply.



Figure 5: An COTS EMCO supply capable of up to 10 kV

## 2.6 The microthrust thruster chip

The microthrust thruster chip is also a chip that creates a Taylor cone and accelerates charged particles from its emitters. Microthrust uses a small hollow pillars that uses the principle of capillary force to draw liquid to the tip. Near the tip an electric field is applied to extract ions and droplets and a second field concentrates and accelerates the particles. The principle of the microthrust emitter is shown in figure 6. As the size and thrust of a single emitter is very limited, typically in the range of 10  $\mu\text{N}$ , the thruster chip combines an array of these emitters, currently up to 91, to generate enough thrust as the aim was a thrust of at least 1mN per chip.

A disadvantage with early electrospray systems is that is that the propellant was emitted in droplets rather than single ions which lowers the nozzle velocity of the particles and thusly the  $I_{sp}$ . To address this, a solution is to increase the fluidic impedance of the nozzle, for instance by making the channel smaller. As the channels need to be produced reliably, resolution of the technology was often a problem. An earlier solution was to clog the channel with small beads<sup>14</sup>. This later evolved in a smaller channel that has a high fluidic impedance by itself.

The Thruster Chip (THC) is produced at local facilities of EPFL and due to complexity of the chip is produced in two separate parts that are bonded together. One part consists of the emitter and the extractor layer, an insulator and accelerator layer are bonded on top of this layer to create the THC.

In figure 6 is a cross-section of the THC. The bonding material is the polymer layer shown in red. The accelerator and extractor layers are relatively thin conductive layers enclosed in a thicker layer of  $\text{SiO}_2$ .

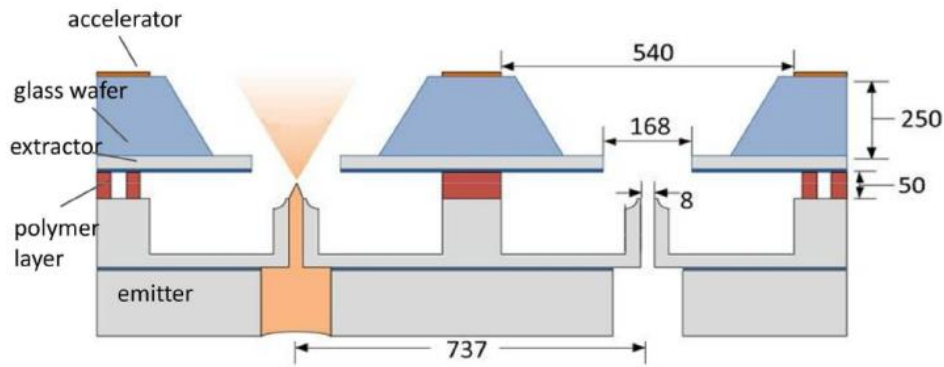


Figure 6: Cross cut of the THC (sizes in  $\mu\text{m}$ )

The size of the emitter needs to be small enough generate a capillary force to draw in propellant and as explained also defines the fluidic impedance which in turn determines the propellant flow. A high fluidic impedance will result in a small droplet size and as a result, a high  $I_{sp}$ . The size of the channel and the shape of the tip have changed during the project.

## 2.7 Emitter voltage generation methods

Two common methods are available to generate a high voltage, one uses a multiplier circuit the other a transformer based circuit.

### 2.7.1 Multiplier circuits

A Cockcroft Walton multiplier was initially developed in 1930 to produce a high voltage for particle accelerators. The circuit can consist of any number of stages where each stage doubles the initial voltage<sup>8</sup>

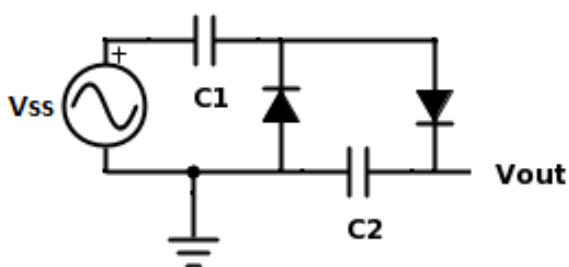


Figure 7: A single-stage of a Cockcroft-Walton voltage multiplier

In figure 7 a single-stage Cockcroft-Walton voltage multiplier is shown. These stages can be cascaded, with each stage providing double of its input voltage. For simplicity we consider the operation of a single stage.

The circuit operates as follows: On a negative voltage from  $V_{ss}$  the right hand side of  $C_1$  is charged with charge  $Q$ . Then when  $V_{ss}$  is positive the equally positive charge at the right hand side of  $C_1$  will be repelled and due to the direction of the diodes, move to the right-hand side of  $C_2$ . Another

negative voltage from  $V_{ss}$  will charge the right-hand side of  $C_1$  again and will be released on a positive cycle effectively adding to the charges in the network, thus propagating further through the network with each cycle. To understand the multiplying function of the network observe the situation where the right hand side of  $C_2$  is already charged with charge  $Q$ . Now, when  $C_1$  is charged and  $V_{ss}$  is positive the potential over  $C_1$  will be zero but charge  $Q$  is still present and therefore will be equally distributed over  $C_1$  and  $C_2$  resulting in  $1\frac{1}{2}Q$  at  $C_2$ . The 3th cycle this will be  $1\frac{3}{4}Q$  and this will continue until the total charge is  $2Q$  and thus a double output voltage. An additional advantage is that this circuit also delivers a DC voltage, therefore it can be used without the need for a rectifying diode bridge.

2.7.2 Transformer based circuits

Small, high turn ratio transformers are used commercially for backlighting purposes and transformers with an 1:100 or 1:125 turn ratio are easy to obtain at various suppliers.

2.7.2.1 Flyback circuit

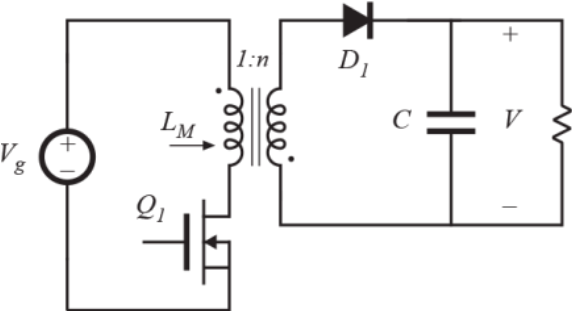


Figure 8: Flyback circuit

The flyback circuit shown in figure 8 is used commonly to generate high voltages and has the advantage that it is simple and uses few components and also that it is quite efficient. One of the disadvantages is that it tends to produce quite a lot of ripple<sup>18</sup>.

In the example of figure 8 a signal, for instance from a PWM source, is used to switch Q1 on and off generating an alternating voltage over  $L_m$  which is coupled to the secondary transformer winding and generates an secondary  $V$  which is  $n$  times  $V_{Lm}$

2.7.2.2 Royer circuit

A Royer circuit is more complex but has better noise characteristics. It needs to be noted that what commonly is referred to as ‘Royer circuit’ is actually a modified Royer circuit as an additional oscillation capacitor is added to the primary side of the circuit. This results in a sinusoid primary waveform instead of a square waveform, which improves noise and characteristics<sup>35</sup>.

Also, as the Royer input waveform is controlled through a feedback from the transformer, this circuit operates on its natural frequency of the oscillation which is determined by the capacitance of  $C_1$  and the inductance of the transformer where the natural frequency is

$$\frac{1}{2\pi * L_{trans} * C_1} \tag{1}$$

In literature sometimes a secondary ‘matching’ capacitor is shown which should help create a secondary LC circuit with roughly the same natural frequency as the primary.

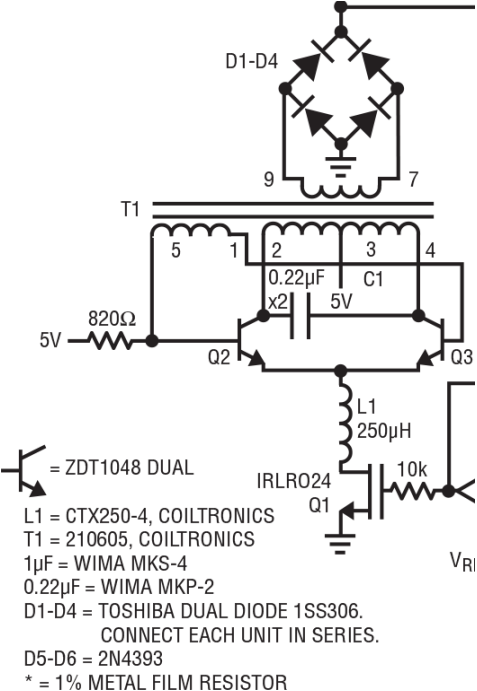


**Figure 9: A Royer based circuit**

In figure 9 an example of a Royer circuit is shown<sup>35</sup>.

A current is fed in a central transformer tap (3) and is shorted to ground through one of two transistors (Q2, Q3) which are controlled using a special feedback coil from the transistor. One of these transistors is connected to the uppermost tap of the transformer and the other the bottom tap. This effectively generates either a positive or negative voltage at the output. When a voltage is applied the system starts when one of the transistors opens, e.g. Q2, due to minute unbalance in the system and a current starts to flow from 5V to ground.

To analyze further operation it is easiest to distinguish the states through which the circuit cycles:

1. The transistor generating a positive voltage (Q2) at the secondary side of the transformer is on and remains on through positive feedback from the transistor.
2. The transformer coil saturates causing the positive voltage to drop that causes a drop in current as Q2 closes, creating a negative voltage at the secondary side of the transformer and the feedback acts on Q3.

3. Q3 is generating a negative voltage and the feedback voltage keeps Q3 on
4. The coil saturates causing the voltage to rise again creating a positive feedback voltage which in turn drives Q2.

To limit the current into the system an combination of a coil(L1) and a FET(Q1) or transistor is used, where Q1 can be controlled with a PWM signal from a chip or microcontroller.

### 2.7.3 Generation methods used in other projects

The FEEP project uses a COTS EMCO F101 supply which was analyzed by our Swiss partner EPFL and has a transformer based design. That a Cockcroft-Walton design is also feasible is shown by our iEPS competitors at MIT, where an examination of photographs of the power supply shows a long cascade of diodes and capacitors.

### 3 System Design

Producing a prototype with stringent size constraints and large complexity as is the case in the microthrust PCS is difficult. Therefore a development prototype was produced which does not comply to size and contains a limited number of the required components so will contain only a single extraction voltage instead of four as required by the specifications. The first prototype consists of the following blocks:

- Positive emitter voltage generator
- Negative emitter voltage generator
- Switching between positive and negative voltage
- Extractor voltage generator
- Microcontroller
- Current and voltage measurement circuits

Prior to this thesis a test breadboard has been produced to experiment with different concepts. This chapter does not contain a complete design exploration as many design choices have already been taken or are influenced by this prototype.

In this chapter the requirements for the system and high level design options and setup will be addressed.

### 3.1 Overview of board implementations

For a more comprehensive understanding of the development stages and the point where my contributions started an overview of the different boards:

#### 3.1.1 Initial board

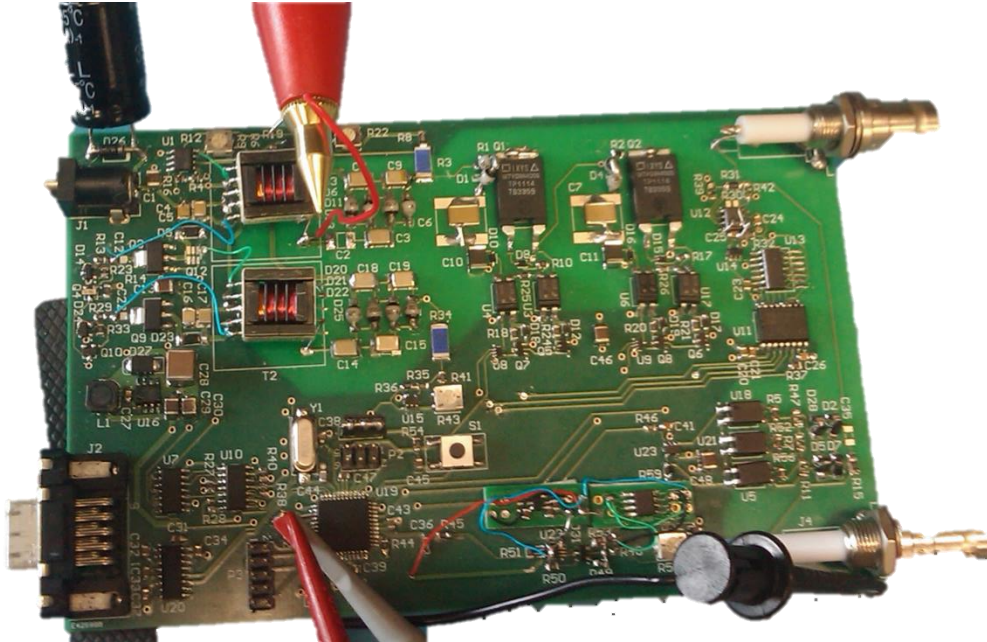


Figure 10: Initial board with resonant flyback circuit

My involvement started when the initial board was just finished and this board intended to contain all required functionality. It was based on earlier tests using separate breadboard circuits and simulations. The board contains a  $V_{emitter}$  and  $V_{extractor}$  generator circuit, a circuit to switch polarity and a microcontroller to control the circuits and measure voltages. Most of this was not functional or functioning problematically. The board depicted in Figure 10 was already slightly modified as is visible from the additional wiring on the board.

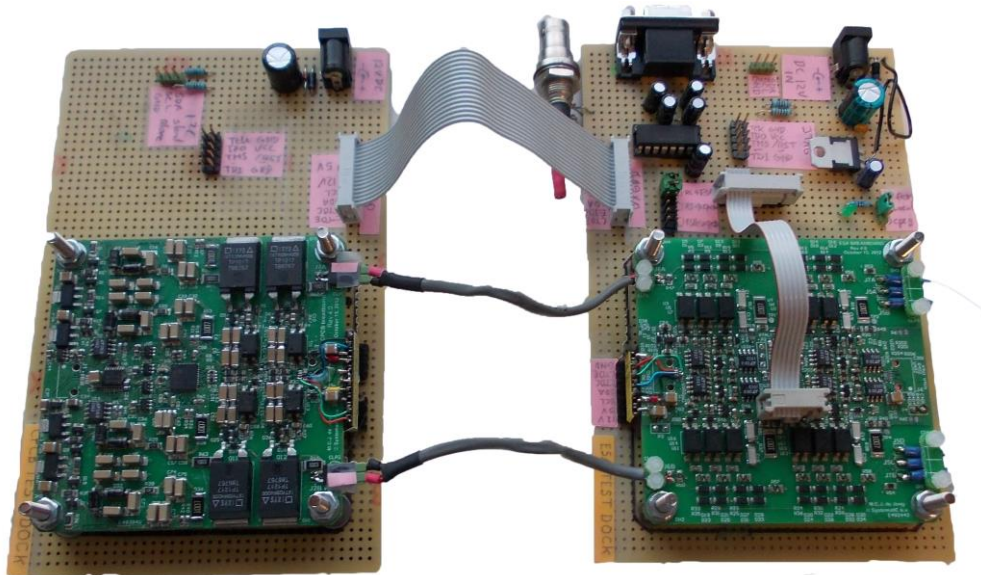
#### 3.1.2 Extended initial board



Figure 11: Initial board with extension boards

Figure 11 shows the extended initial board where the problems regarding high voltage generation, switching and measuring were solved. The extension boards contain alternative circuits for high voltage generation and rectification. The batteries are used as floating supply voltage to control the high voltage FET's that are present on the board. This version was successfully tested with a microthrust thruster chip in November 2012 at our partner EPFL, Switzerland.

### 3.1.3 Size compliant boards



**Figure 12: CPCB (left) and ESA (right) dock mounted**

The initial board was succeeded by two separate boards, produced at the beginning of 2013. The board on the left contains the circuits to generate emitter voltages and the board on the right generates the extraction voltages.

A switch was made from serial communication on the initial board to the required I<sup>2</sup>C communication, test docks helped that transition and made communicating and programming of the separate boards easier. Also it prevented strain on the programming headers when connecting and disconnecting the programmer. Another reason to build these docks was the fact that there proved to be an issue with one of the programming headers missing a 5V line which was artificially added on the test dock. In May 2013 a set of boards without docking extensions was used to test in London and after the resulting improvements and fixes the functionality of the boards on the dock diverged from functionality of the boards used for testing in vacuum so they were not used anymore.

### 3.1.4 Modified size compliant boards

The resulting board contained modifications for noise reduction and measurement and numerous fixes for different problems as is visible from the wiring and stacked components shown in figure 13. This board has a multitude of fixes including an all new current detector, different diodes, increase

robustness and many patches to prevent crosstalk and noise. We stopped development on this board in November 2013 after a successful test in London.

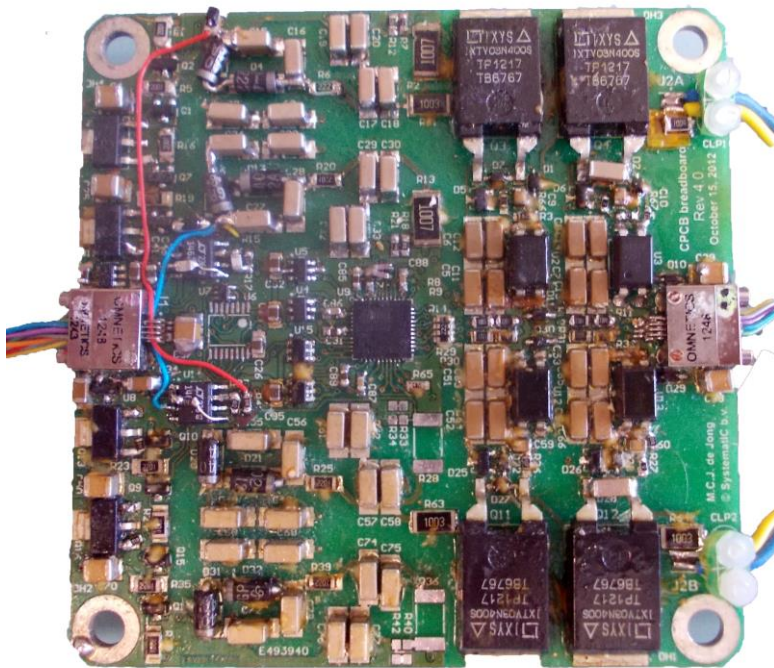


Figure 13: Modified CPCB board

### 3.2 Setup

The maximal number of thruster chips that is specified to be supplied by a single PCS is 'up to 24' and as every chip needs to be separately controlled, the PCS needs to provide 'up to 24 extraction voltages'. The number of control channels on a single microcontroller is limited so the setup is modular and the functionality of the PCS is split in separate boards.

The Central Control and Power Board (CPCB) containing:

- 4 Emitter voltage supplies
- Polarity switching circuits
- Measurement and control of current and voltages

Up to 6 Extractor Switching Assembly (ESA) boards containing:

- 4 extraction voltage supplies
- Measurement and control of extraction voltages

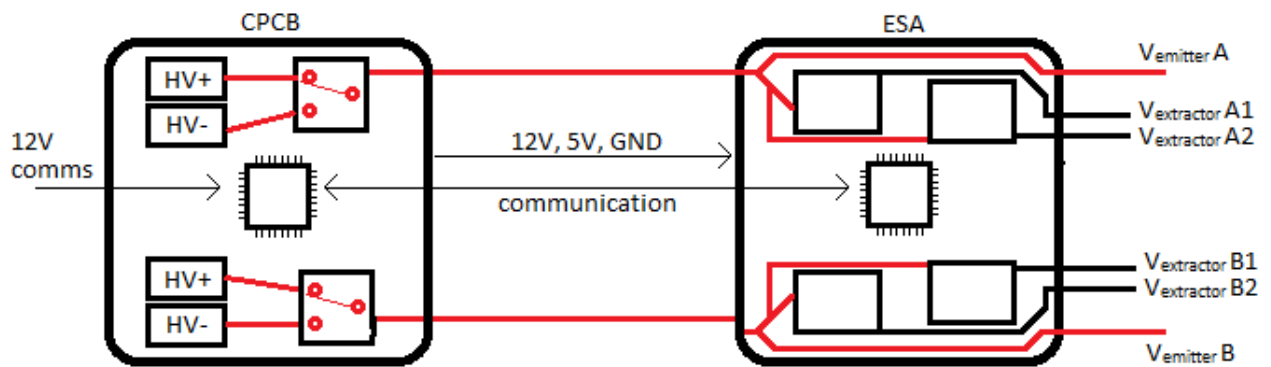


Figure 14: Abstract representation of CPCB and ESA board

Figure 14 shows an abstract of the planned setup of the CPCB and ESA boards respectively. The emitter and extraction voltages will be connected as shown in figure 15. The CPCB board features four high voltage generators and two polarity switching circuits. The ESA board uses four identical circuits to control the separate extraction voltages A1, A2, B1 and B2 providing control for a total of four thruster chips. The emitters will be connected to the voltage from the CPCB board (see figure 6) so the extraction voltage is the voltage relative to the emitter voltage.

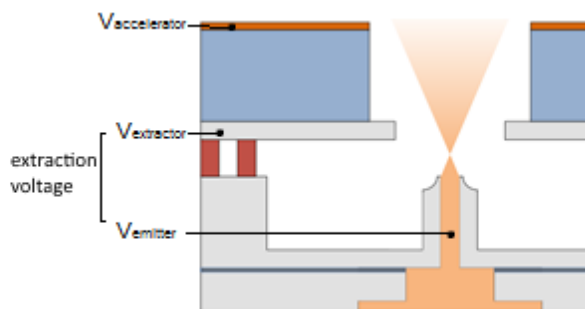


Figure 15: Emitter and Extraction voltages with an extraction voltage of 800V and emitter voltage of 3000V.

Figure 15 shows this relation.  $V_{emitter}$  is the HV output (e.g. 3kV).  $V_{extractor}$  refers to the voltage with respect to too ground (0V), where the term ‘extraction voltage’ refers to  $V_{emitter} - V_{extractor}$  as this is the potential difference used for extracting ions from the ionic liquid. The extraction voltage in this example 800V so  $V_{extractor}$  is at a potential difference of 800V relative to  $V_{emitter}$  resulting in a  $V_{extractor}$  at pin A1 of  $3000 - 800 = 2200V$

### 3.3 Requirements

The verification and cross-reference matrix, created by microthrust partner TNO contains all the formal requirements set for the microthrust project and is shown in 0. The requirements listed in this chapter are a combination of formal requirements and additional ‘soft’ requirements set during bi-weekly conference meetings with microthrust partners as not all requirements are formalized in detail.

### 3.3.1 Hardware requirements

L2-PCS-INT-R5	The PCS shall mechanically interface with the spacecraft
L2-PCS-INT-R6	The PCS shall mechanically interface with the TMS
L2-PCS-PHY-R2	The PCS envelope is limited to 80x80x20 mm (single TMS configuration)

**Table 1: PCS requirements**

A number of general requirements are hardware design. The project partners need to agree on connector interfaces and screw holes to mount the PCS. The 80x80 is the inner diameter that is agreed upon for this project as this leaves room for cables that can safely be used for higher voltages. The TMS that the requirements refer to is the Thruster Module System which is the combination of 4 thruster chips with housing and propellant tanks.

### 3.3.2 Emitter voltage generation

L2-PCS-FUN-R4	The power efficiency of the high voltage section of the PCS shall be more than 50% at its design envelop (factor of 3 input power range)
L2-PCS-FUN-R7	The extractor to accelerator voltage shall be controlled between 0 and 4kV
L2-PCS-QUA-R2	The extractor to accelerator voltage shall be controlled with an accuracy of 1%

**Table 2: Requirements emitter voltage generation**

In the requirement in table 2 the emitter voltage is denoted by ‘the extractor to accelerator voltage’. The factor of 3 means the efficiency should be above 50% between a factor 3 range so for instance between 1.33 and 4 watts. The emitter voltage is the voltage provided by the CPCB and this is specified to be controllable up to 4kV. In the course of the project this requirement is informally somewhat relaxed to 3kV.

### 3.3.3 Emitter voltage switching

L2-PCS-FUN-R2	The PCS shall enable bipolar operation of the MTPS
L2-PCS-FUN-R8	The PCS shall be able to operate at a frequency of up to 1 Hz

**Table 3: Switching requirements**

MTPS is the microthrust power system. To maintain neutrality of the spacecraft and to both extract positive and negative ions from the ionic liquid it is necessary to produce opposite, alternating positive and negative emitter voltages.

### 3.3.4 Current and voltage sensing

--	Average $V_{\text{extractor}}$ voltage accuracy <0.1% (3V at 3kV) <sup>12</sup>
--	Current sensing with eight bits accuracy

**Table 4: Sensing requirements**

The  $V_{\text{extractor}}$  requirement originates in the fact that the absolute output at  $V_{\text{extractor}}$  is between 2 and 3kV.

Calculations show that the operating point where the extractor starts spraying is around 720 volt for an early version of the microthrust emitter<sup>13</sup>. As tests with the thruster chips show variation and also to change the operating point from ionic to droplet mode, an extraction voltage of 1000V should be sufficient. Figure 16, shows the 4 operating modes for electrospray emitters. This particular image is from an electrospray system that uses higher extraction voltages. In pure ion mode the absolute thrust is low but the  $I_{sp}$  (mass/acceleration) is high. In droplet mode the absolute thrust will be higher due to spray of droplets.

The current of  $V_{\text{emitter}}$  is an indication of the thrust that is produced and high currents are also an indication that something is wrong. Therefore they need to be measured with reasonable accuracy which is specified as eight bits of accuracy.

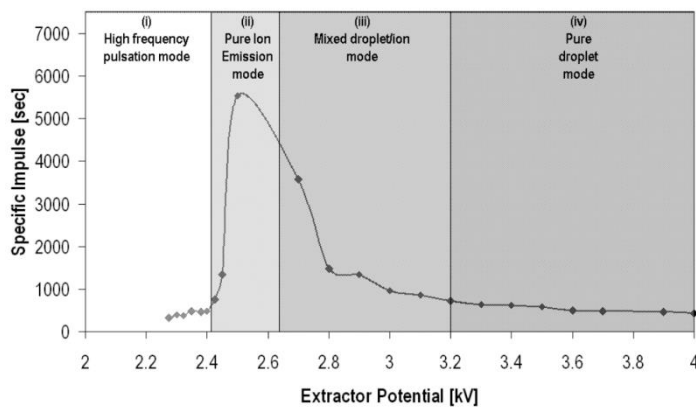


Figure 16: Variation in operating points of an electrospray system<sup>25</sup>

### 3.3.5 Extractor voltage

L3-ESA-FUN-R5	The ESA shall be able to handle at least [9] THC's per polar side
L3-ESA-FUN-R9	The ESA shall control the emitter to extraction voltage between 0-1kV
L3-ESA-CON-R1	The ESA shall be able to operate and control up to [6] TMS

Table 5: Extractor switching assembly requirements

In these requirements 'The ESA' refers to one or more ESA boards. To accommodate a various number of THC's the ESA boards will be designed to be modular. Since it is expected that in designs with multiple Thruster Module Systems (TMS) not all thrusters will operate at the same time and a TMS will contain 4 THC's the total amount of THC's controllable will be 24 and the total amount of THC's operational at the same time will be a maximum of 9 per polarity so 18 THC's in total.

## 3.4 Design selections

### 3.4.1 Emitter voltage generation

Commercial HV generation circuits like backlighting for LCD screens are commonly based on a transformer design like the Royer circuit, so a lot of components and circuitry are easily obtainable. In literature a number designs can easily be found and efficiencies of over 85% when combined with a CCFL tube are not uncommon<sup>11,30</sup>. These were reasons to select a Royer topology as high voltage generation circuit. For analysis and implementation, a COTS Texas Instruments CCFL supply was obtained and also used in a modification of the first board.

### 3.4.2 Emitter voltage switching

To switch polarity of the emitter voltage it is not sufficient to stop generating a positive voltage and start generating a negative voltage or vice versa as the voltage doubler circuit for one polarity inherently provides a path to ground for the other. (For clarification notice the direction of the diodes in figure 7). In many applications it would be sufficient to use a relay switch but as this type of mechanical component is prohibited for space applications and also since these switches generally have an high weight this is not feasible for the microthrust PCS. A solution using HV FETS would be another option but these FETs require an extra  $V_{\text{threshold}}$  with respect to  $V_{\text{drain}}$ . In essence this type of circuit requires a floating supply voltage.

### 3.4.3 Sensing of $V_{\text{emitter}}$ , $I_{\text{emitter}}$ and $V_{\text{extractor}}$

For voltage sensing a resistive voltage divider will be used as it is simple and components are relatively easy to obtain. As power requirements for the circuit are limited and multiple voltages need to be measured, the voltage divider should have sufficiently high impedance so not much energy is lost. A 1:1000 voltage divider would be a good ratio as it fits in the desired 5V range and allows for some room to detect overvoltages. By using a  $1\text{G}\Omega/1\text{M}\Omega$  resistor at a voltage of 3.5kV this will result in  $\frac{3500^2}{1\text{G}} = 12,5\text{mW}$  which is acceptable on an expected power budget of several watts, with the exact amount not currently specified in the requirements. For the current detection of  $I_{\text{emitter}}$  initially the selection was made for a high side current detection, i.e. in the path of the emitter voltage. This is changed to a low side current detector in a later stage, based on a small resistor to ground in the HV generation circuit.

To measure with the desired 0.1% accuracy at least 10 bits on the microcontroller ADC are required.

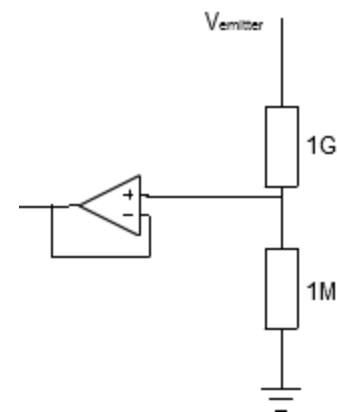


Figure 17: 1:1000 voltage divider

#### 3.4.4 Extractor voltage generation

Because it would be space and weight inefficient and energy consuming to have a separate HV generator for each extractor, the extraction voltages are generated by division of the emitter voltages. A voltage divider of this kind could be created using a FET<sup>26</sup> but the challenge still remains that the control signal from a 5V domain is used to control a high voltage. An optocoupler combines the best of both worlds as it is able to control a high voltage but also allows for a low-voltage control signal.

#### 3.4.5 Control

The type of microcontroller used has already been defined prior to my arrival and is an Atmel 8 bit atmega164p. A disadvantage of this type of microcontroller is the fact that the ADC is relatively slow with a sample frequency of 12.5 kHz (dependent of clock speed). An advantage is prior experience with 8-bit Atmel microcontrollers in a separate SystematIC space project, where it proved to be quite resilient to space radiation.

For the emitter voltage generator an alternative would be to use a dedicated controller chip. This is similar to a CCFL topology used for LCD backlighting although little modifications are needed, as CCFL topologies observed do not control on voltage. Disadvantages would be an extra number of components and some extra power consumption.

#### 3.4.6 Communication

The microcontrollers on the CPCB and ESA boards have only one I<sup>2</sup>C channel available and one serial communications channel. As the communication with spacecraft control is mandated to be I<sup>2</sup>C the communication between boards is done using the serial bus.

## 4 Implementation and Design

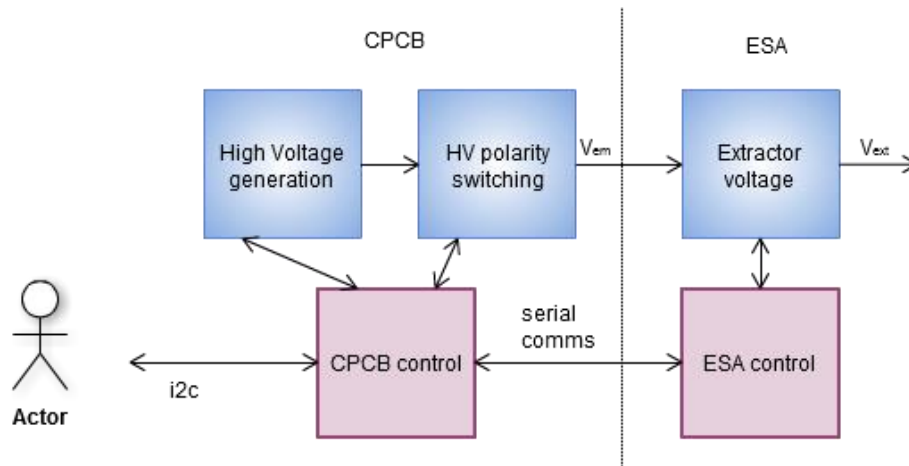


Figure 18: microthrust components

Figure 18 shows an abstract view of the components within microthrust and their interaction. The CPCB controls both the emitter voltage and polarity switching and is the primary interface for the actor which is either a person as in our testing, or the spacecraft control using an I<sup>2</sup>C interface. The ESA creates and controls the extraction voltage and communicates with the CPCB through the serial interface.

In this chapter the implementation of the different components will be presented as well as implementation issues and their solutions and what techniques have been used to prevent problems.

### 4.1 Emitter voltage generation

#### 4.1.1 Resonant flyback implementation

In advance of this thesis project a variant on the flyback circuit was built, namely a resonant flyback circuit, a variant on the circuit described paragraph 2.7.2.1. The only additions are an extra capacitance to create an oscillating LC circuit and feedback to the controller to time the frequency of the pulse on the FET (Q1 in figure 8)

##### 4.1.1.1 Timing issues

In the microthrust project the microcontroller is designated to handle control of the HV generation circuit. In the case of a resonant flyback circuit this means actively monitoring the feedback and generating a pulse for every oscillation of the flyback circuit and as the oscillation frequency of the resonant flyback circuit was in the order of 60kHz this meant 60.000 hard time interrupts per second which needed to be handled within  $\frac{1}{4}$  of the cycle so the response time is  $\frac{1}{4 * 60k} = 4\mu s$  which includes

delays in the circuit that generates a interrupt pulse from the feedback signal. Based on a clock frequency of 16 MHz this roughly translates to only 50 computational cycles to generate a pulse on a output pin.

As the time constraint limits the options for a software implementation, the only viable implementation is an interrupt handler that enables Q1 within  $4\mu s$ , waits a certain number of cycles, within the interrupt routine and exits, where the length of the wait corresponds with the output voltage.

Initially the timing constraints could not be met. A breakdown of the assembly code showed that additional registers were stored at the beginning of the interrupt and the register allocation was suboptimal. Improving this solved the issue partially but it was still difficult to control and unstable. As the timing constraints were so limited that no other interrupts would be available on the controller this implementation was abandoned.

#### 4.1.2 Royer implementation

The next implementation was a Royer based implementation. As time was limited and an early test was planned at the EPFL Switzerland, a COTS CCFL Royer circuit was modified so it could be switched on and off using a microcontroller and a voltage doubler was added to rectify and increase the output voltage. The test in Switzerland was done using a thruster chip with only a single emitter. In reality this means the load is a magnitude lower than even the load of the sensing resistors so for this first version the output for the circuit was fixed using hardware.

The next version was fully controllable and the circuit was based on the Willaims application note<sup>35</sup> but initial results proved unsatisfactory as the efficiency was typically below 50% in stark contrast to the efficiencies mentioned in the application note.

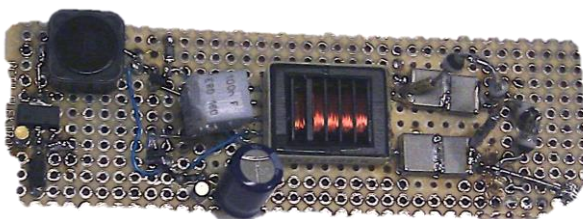


**Figure 19: Royer testboard, high voltage output at right hand side**

In figure 19 the testboard used for Royer efficiency testing is shown. As simulations delivered no clue why losses were higher than anticipated, this board was used to test different components. Several types of capacitors and diodes where tested. With the main categories

- Derating capacitor 10nF (XR7)
- Non-derating capacitors 1nF (COG)

- Normal diodes (4kV, 2kV)
- Fast recovery diode (1.75 kV)

On the primary side a lot of high performing components were available. For the secondary side the number of components was very limited due to the high potential and small form-factor requirement.

For the diodes only one manufacturer is available that delivers diodes for up to 4kV and for the capacitors none could be found that adhered to the form factor desired and none above 10nF.

Furthermore the characteristics of these capacitors proved to be such that they derated to 20% of its original capacity when the specified voltage was applied. Meaning that two 10nF capacitors in series with an applied voltage of 4kV would have a remaining capacity of only 1nF. Capacitors that did derate very little were also tested but these were only available in 100pF.

For the diodes between 1.5kV and 2kV more manufacturers were available but this would mean diodes need to be used in series. When using multiple diodes in series the potential hazard exists that diodes are dissimilar in leakage and the voltage is not evenly distributed. To help prevent this, only diodes of the same order batch were used in series.

	Efficiency
XR7 capacitor, normal diodes	43%
C0G capacitor, normal diodes	43%
C0G capacitor, fast recovery	62%

**Table 6: Efficiency results with different diode and capacitor configurations**

Table 6 shows the results of tests with different components for the voltage doubler. To control the board a frequency generator was used and the tested voltage was 2.5kV with a load of 1.25W. The results show that a proper diode selection is of great importance for this circuit.

#### 4.1.2.1 Secondary resonance capacitor

Occasionally a secondary oscillator capacitance was seen in Royer designs. Intuitively this can be explained as matching the oscillation frequency at the primary with the oscillation frequency at the secondary side of the transformer.

The relation between input and output using a secondary capacitance is:

$$C_{sec} = C_{pri} / turns^2 \quad (2)$$

As the turn ratio is 100. The  $C_{sec}$  should be  $\frac{68n}{10000} = 6,8pF$ . In reality a 6.8pF capacitor that is suited for the voltages involved could not be found so a number of combinations with 15pF capacitors and 30pF capacitors was tested. This resulted in an erratically functioning circuit where occasionally the performance was equal to a circuit without secondary oscillation capacitor and occasionally the performance was drastically reduced. When adding a single 10pF capacitance, the performance was

always severely negatively impacted with only 10% efficiency at 700V. This directly contrasted with results that have been obtained from simulations.

This also illustrated the earlier observation that measurements on the secondary side of the transformer were impacting performance, as the probe itself has a parasitic capacitance and small capacitances show to have a strong impact on performance. In the final Royer circuit no secondary oscillation capacitor was added as a positive effect could not be found.

4.1.2.2 Simulations of Royer Circuit

To get a better understanding of the functioning of a Royer circuit and see if there are other possibilities for improvement, LTspice was used.

A preexisting design containing a controller chip<sup>31</sup> was modified to match the PWM controlled Royer circuit of the CPCB. The resulting schematic, depicted in figure 20 closely resembles the physical implementation that was used.

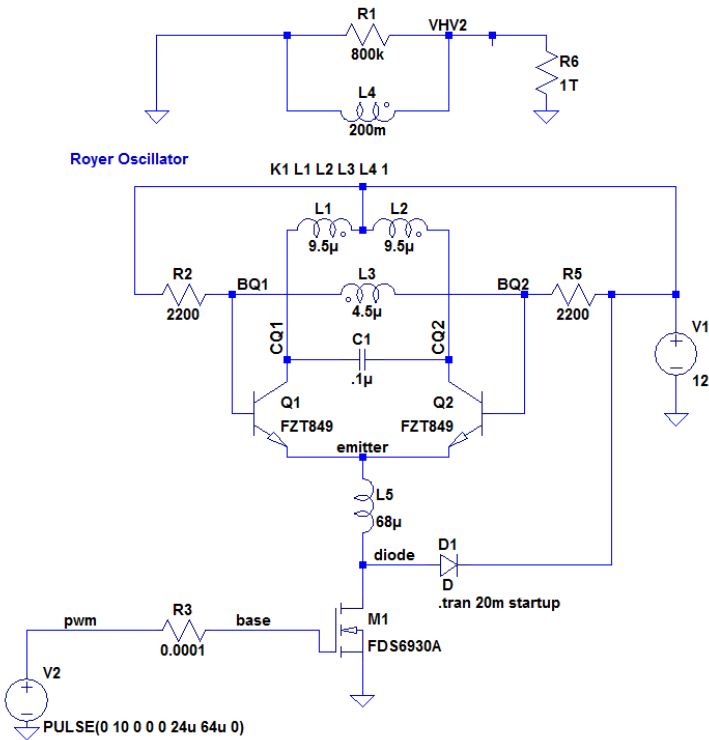


Figure 20: Royer implementation in LTspice without secondary oscillation capacitor

Results in simulations showed little influence of a secondary capacitor parallel to R6, but practice showed a significant decrease in efficiency when using the wrong capacitance and no improvement when using the calculated capacitance. Also the influence of different PWM frequencies was negligible. The results are shown in table 7.

PWM dutycycle	V <sub>out</sub> (RMS)	Load ( $\Omega$ )	P <sub>in</sub>	P <sub>out</sub>	Efficiency
9,96%	1.1804KV	10M $\Omega$	418.01 mW	139.33mW	33,33%
20,00%	1.5807KV	10M $\Omega$	758.66 mW	249.87mW	32,94%
31,25%	1.7773kV	10M $\Omega$	966.19 mW	315.88 mW	32,69%
31,25%	1.7535kV	5M $\Omega$	1262.9 mW	614.95 mW	48,69%
31,25%	1.7214kV	3M $\Omega$	1636.1 mW	987.76 mW	60,37%
31,25%	1.6803kV	2M $\Omega$	2.0684W	1.4117W	68,25%
31,25%*	1.6803KV*	2M $\Omega$	2.0704W*	1.4118W*	68,19%*
37,50%	1.6071KV	800k $\Omega$	4.0567W	3.2285W	79,58%
37,50%*	1.6067kV*	800k $\Omega$	4.0571W*	3.2267W*	79,53%*
* With secondary oscillation capacitance					

Table 7: Efficiency simulations for different loads

## 4.2 Emitter voltage switching

As noted in the previous chapter, it is not possible to use relays to switch the polarity of the emitter voltage. A possible solution was found in a high power FET capable of withstanding 4000V with relative low leakage and a suitable form factor. To prevent breakdown of this FET the emitter voltage generation circuit needs to be discharged before the opposite voltage can be generated. Otherwise, for instance when switching to a positive emitter voltage, the combination of the residual negative voltage and the positive voltage exceeds the limit of the HV FETs. As the positive doubler circuit provides a path to ground for the negative voltage and vice versa, discharge can be provided by enabling both of the FETs. The hazard in this case is the fact that high voltage generation should not be enabled as it is short circuited.

The switching of polarity consists of four steps. For the case when switching from negative to positive these steps are:

- Disable negative HV generation
- Enable FET for positive emitter voltage (negative discharge)
- Disable FET for negative emitter voltage
- Enable positive HV generation

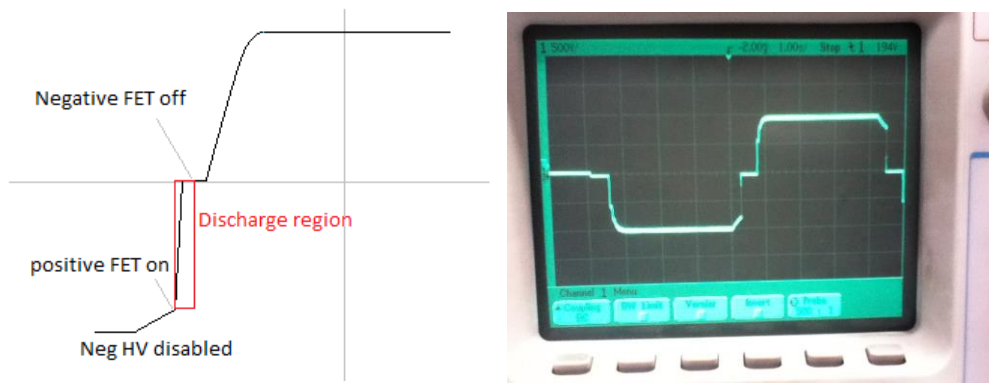


Figure 21: Polarity switching of the HVPS

Figure 21 shows the switching behavior of the CPCB where the effects are illustrated. With on the right a scope image of the CPCB, generating +2kV and -2kV with a period of approximately 8 seconds. The period is a combination of the on-time of the HV generators and the wait states for discharging and switching.

Note from the scope image that without an active discharge the discharge-time would be significant as the wait between switching off the HV generator and active discharge is 300ms and the voltage drop is only very limited, showing that an active discharge is necessary. To limit discharge current, a 100kΩ resistor is inserted in both HV paths, which is low enough to disregard in normal operation but limits the discharge to about 30mA.

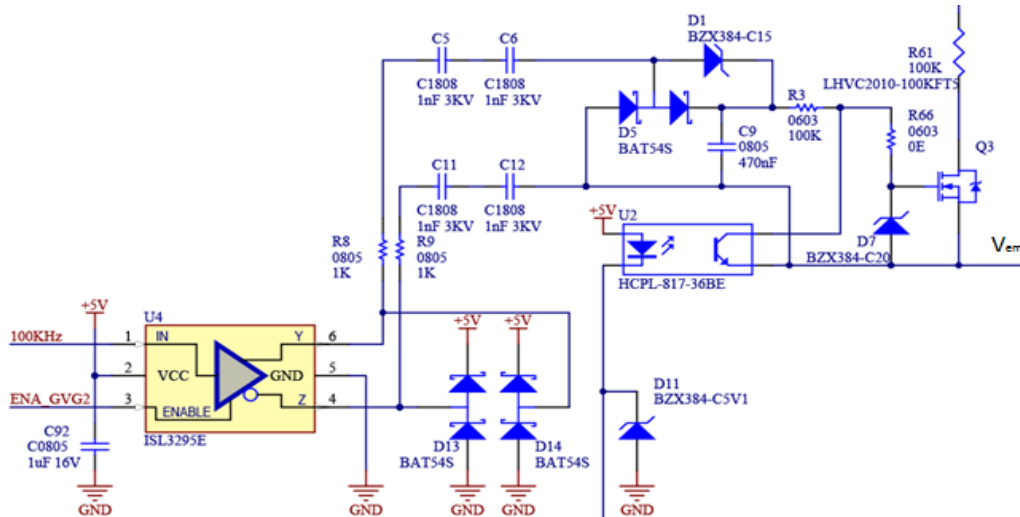


Figure 22: switching circuit including gate voltage generator

#### 4.2.1 Gate voltage generator

To switch the FET (Q3 in figure 22) to an on state, a gate voltage of at least 6,5V above  $V_{source}$  is needed, but this supply should also be floating since the FET is going to switch high voltages resulting in a similarly high  $V_{source}$ . To create such a floating voltage supply a battery was used in early tests. Later this was replaced with capacitors in series to create a barrier for the DC voltage and an alternating signal that is rectified after crossing the barrier. Using a PWM signal and a driver (U4)

which produces 2 inverted alternating 5V signals, a theoretical 10V extra on the gate of the HV FET is generated to open it, shown as Q3 in figure 22. Using optocoupler U2, the gate can be connected to the drain which closes the FET. As the circuit draws over 10mW of power, the circuit can be switched on and off by the controller using the ENA\_GVG signal.

### 4.3 Extractor voltage generation

The total extraction voltage ( $V_{emitter} - V_{extractor}$ ) that needs to be created is 1/3th of  $V_{emitter}$ . A resistive divider to limit the maximum voltage, paired with an optocoupler for control, is a feasible solution. Still no small form factor, low leakage optocouplers are available that can withstand large voltages, in fact 350V was the highest that was found, and furthermore it would be undesirable to have the full emitter voltage available as a control-range as effects of this voltage on the extractor plane are unknown and could result in a breakdown of the thruster chip.

According to the chip designers the extractor has a theoretical power consumption of 0, meaning that even a high impedant resistive divider could be used. Figure 23 shows an representation of the control implemented. An optocoupler is combined with a resistor to limit the maximum extraction voltage.

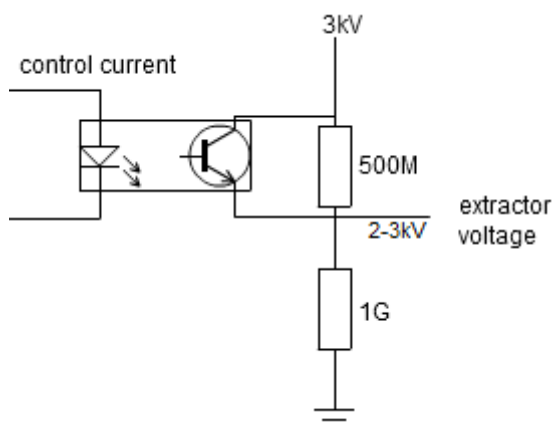


**Figure 23: Abstract representation of the extractor control**

The top resistor is scaled so that it is one third of the bottom resistor at maximum resistance, or around 500M max. It has been designed for an emitter-extractor voltage of about 1 kV when an emitter voltage of 3kV is available. To control the extraction voltage three identical optocouplers were used with phototransistors that can withstand  $350V_{collector-emitter}$  and have a low “dark current” when completely off. This is necessary to get the maximum resistance of 500M without influence on the resistance due to the phototransistors in parallel.

To control the conductivity of the phototransistors a control loop regulated current is sent through the LEDs of the opto-isolators. To achieve reasonable efficiency the three LEDs are connected in

series, but because it would take at least six volt through three such LEDs a circuit is powered with the 12V rail.

## 4.4 Software setup and structure

### 4.4.1 Structure

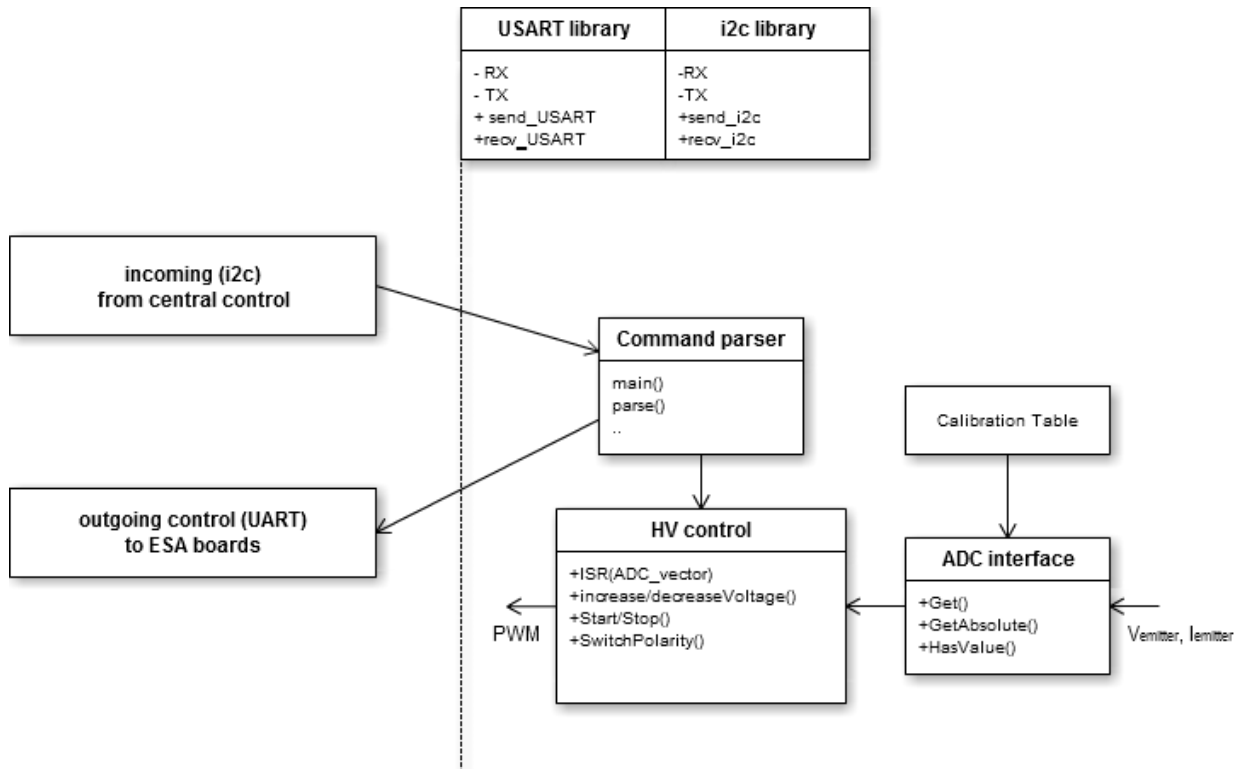


**Figure 24: CPCB software structure**

Figure 24 shows a diagram of CPCB software with the components involved. The commands from the central control are parsed by the command parser which also initiates high voltage generation and switching behavior. The control blocks use an ADC library to get results from the ADC that are compensated with results from a calibration table.

Although the number of blocks and amount of code involved is not very large, both hardware and software are developed concurrently which requires continuous testing and a defensive approach to software development to prevent software bugs disguising as hardware problems. This means that every line of software had to be tested extensively. Setting up communication, setting up a PWM signal, controlling it, evaluating the effect on the hardware, and this also means that with every problem both hardware and software need to be investigated for problems. Every new iteration of hardware showed that it is almost impossible to build a perfectly functional new board of this complexity, so a first phase is always about identifying problems and improving functionality.

#### 4.4.2 Command parser

During early prototyping a simple way to control the hardware was by assigning operations like ON/OFF or lower/higher to single characters. As complexity increased and more control options were necessary, a solid design of a command parser was needed. To parse input, there are tools available called *command line parser generators* that generate a command parser based on a rule list<sup>32</sup> or table<sup>10</sup>. Configuring these takes time to gain familiarity and none could be found that are directly suited for use in this project and to get familiar with one, to be able to integrate it into the workflow adds complexity. To keep parsing relatively simple, commands should be kept short. This also saves overhead as less characters need to be transmitted, although it is a bit more error prone when applying manual control. In the bases, the parser parses a character and based on the current state and the character read, it either enters a new state and is ready for the next character, or is finished and will enter the default state and call a procedure based on the command received. The list of states and commands is shown in Appendix E .

As the number of commands is relatively limited there is the option to create single byte commands which would greatly simplify the software to parse commands. The main risk in this case would be the inadvertently pressing of a wrong button during testing could result in unintended and possibly dangerous behavior when unexpectedly a high voltage generator starts running. The other disadvantage of single byte commands is that it is hard to remember when controlling microthrust and to comprehend when reviewing logs. Late in the project a graphical user interface or GUI, which is shown in chapter 4.8, would replace the need for command line control.

#### 4.4.3 Communication

As for an implementation of an I<sup>2</sup>C library, writing a new software library would take quite a lot of time and might introduce new bugs. Another solution is to use a standard library. Atmel does not provide such a library, but the code used in arduino<sup>1</sup> board is freely available and has been borrowed for use in this project. It does need modification as the Arduino framework uses a C++ layer where Arduino developers can set properties and specifics for their communication. The library mostly consists of an interrupt routine that implements the different states of the I<sup>2</sup>C protocol and puts the received data in a buffer.

##### 4.4.3.1 Communication Setup

For I<sup>2</sup>C communication 3 different structures are available.

- The CPCB functions as master in a master-slave environment
- The CPCB functions as master in a multi-master environment
- The CPCB functions as slave in a master-slave environment

Although no specifications are defined regarding the state of the CPCB, a multi-master environment is complex and error prone as no standard contention mechanism is defined. The simplest solution for CPCB software development would be to define the CPCB as master. In that role, the CPCB can send data without delay, and poll for data whenever it has resources. This means also a shift of complexity to the space craft controller that will control the CPCB and needs to poll continuously for data. Furthermore, when one considers the microthrust system as a peripheral the CPCB should be slave as peripherals are commonly slave. Therefore the CPCB communication is set up with CPCB as slave and S/C control, or during testing, human control with an Arduino board as I<sup>2</sup>C master.

#### *4.4.3.2 Receiving data at the controller*

As the master sends data, on receipt of a byte, an interrupt is called to read the data from the register and write it in a buffer. To prevent overwriting data, the buffer needs to be emptied as soon as possible. An easy solution would be to copy the buffer at the end of a transmission to a new buffer so the buffer is available immediately afterwards. This has the disadvantage that this copying operation needs to be atomized as the buffer is not accessible when not all data has been copied, with the consequence that the copying might cause a large delay. Another solution is emptying the buffer on a FiFo basis. This has the disadvantage that it might overflow when 'read out' is not occurring quickly enough and bytes are lost. Still, as the expectation is that communication is quite limited this is currently the implementation that is selected.

#### *4.4.3.3 Sending data from the controller*

The arduino that functions as master controller polls for data every 10 ms. As the default implementation of the I<sup>2</sup>C protocol does not allow the slave to return no data, the slave will return '0x0' when no data is available. Partly due to this, but also to make debugging easier, the protocol uses only ascii, requiring that all measurement data is converted to ascii before it is put in the transfer buffer. To prevent accesses to the send buffer while transmission is in operation, there are two sendbuffers called sendbuffer and i2c\_sendbuffer. The sendbuffer is copied to the i2c sendbuffer in small chunks of 14 bytes when a data request is made, which helps to ensure that there are no big copy actions occurring the interrupthandler. The 14 bytes size restriction is a legacy parameter based on early message size in the project, where the biggest was 14 bytes, and has the consequence that the master also needs to request 14 bytes per transaction. This is in line with the way I<sup>2</sup>C commonly is used, namely to request data which often is also of a predefined size. Whenever an overflow occurs because the data is not requested rapidly enough, or the read data is not read fast enough from the buffer, the buffer is full and data will be dropped.

#### 4.4.3.4 CBCB to ESA communication

Although in an I<sup>2</sup>C environment multiple boards and multiple masters are possible, the microcontroller family selected has only one I<sup>2</sup>C channel available. This would mean that the S/C controller would also receive all internal communication.

To solve this, the serial channel could be used. The serial protocol also allows multiple boards to be addressed using 'Multiprocessor Communications Mode' where a stop bit is used as 'broadcast' bit that indicates if a packet sent contains address or data information. When an address arrives the intended receiver sets it's mode to 'receive data' otherwise it will keep ignoring data packets.

### 4.5 Emitter voltage control

The most optimal way to control a system is to analytically model all the components in the loop and make a control appropriately for this system. The controller that is implemented is usually the well-known PID controller.

Applying a practical approach to PID control, the basic formula for a controller is<sup>27</sup>:

$$P(t) = K_p e(t) + K_i \int_0^t e(\tau) d\tau + K_d \frac{d}{dt} e(t)$$

The control signal  $P(t)$  is composed of the error signal  $e(t)$ , which is the deviation from the desired value and is multiplied by  $K_p$ . As  $K_p$  is finite there is no control signal when the error  $e(t)$  equals but when there is no control signal, there is no output voltage, so the net result is a steady state error.

This is solved with an extra factor  $K_i \int_0^t e(\tau) d\tau$  which is the sum of all the errors. Optionally a differentional factor  $K_d \frac{d}{dt} e(t)$  can help prevent overshoot as it limits the control signal when the error is rapidly changing, e.g. during startup, though it can also increase instability when not carefully modeled<sup>27, 33</sup>. As the nature of the HV generator is quite difficult to model and subject to change and various loads, a heuristic approach to determine the constants in the control equation seemed more suitable. In literature this approach is commonly found<sup>9, 27</sup> for instance in Ziegler-Nichols tuning. The standard approach used is to tune a purely proportional controller to the point where the system starts to oscillate, tune it back a bit, and continue with an integrational factor to prevent a steady state error. Lastly a differentiator part can be used to prevent overshoot but might also add instability. Optimal tuning parameters are dependent on constraints regarding overshoot, energy consumption etc. In microthrust, the HV generator must not overshoot during startup to prevent damage to components and also because the system is not symmetrical so overshoot will take a relative long period to settle. This is mainly caused by 10nF filter capacitors that are used to filter the voltage produced and also some energy is retained in the 68uH snubber coil at the primary side of the Royer circuit.

In our implementation a similar approach is used. Instead of reaching oscillation the proportional factor of the PID controller is experimentally increased up to the point where the signal almost overshoots and lowered again. Then the integrator is increased. Lastly different load tests are applied to see if the system is behaving as intended under load.

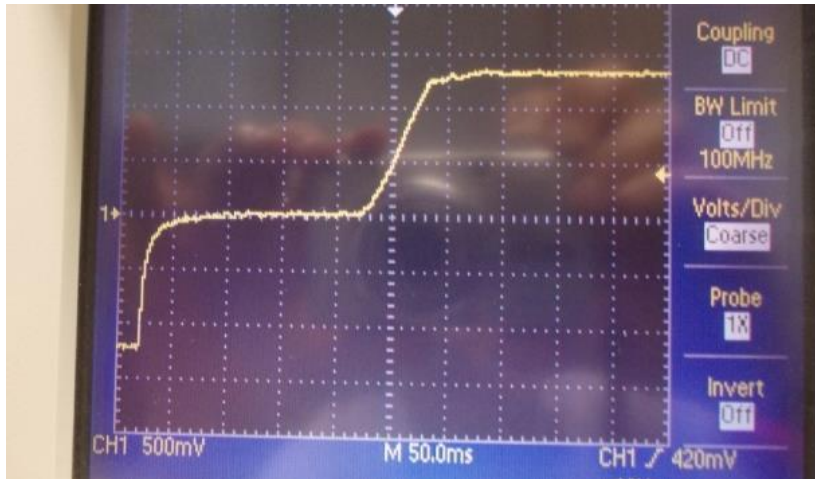


Figure 25: Transient behavior Emitter voltage generation at 2750V

#### 4.5.1 Software implementation

The control is constantly adjusted whenever a new data sample arrives. For the best measurement results an ADC clock of below 200 kHz is needed, and since the clock speed is based on the clock speed of the microcontroller divided by a power of 2 the optimal clock speed is  $16M/128 = 125$  kHz. With 13 cycles per sample this means a sample frequency of around 10 kHz. To verify operation, a first version was developed while monitoring only a single ADC channel and controlling only a single PWM channel. A later version needed control switching to measure different channels and control different PWM signals.

Whenever a sample is ready the interrupt ensuing is as follows:

- The 'sample ready' interrupt routine checks which channel was read
- A safety check to see if the sample is not out of bounds
- A control algorithm produces a new control signal
- The corresponding PWM is adjusted
- The channel is changed and a new sample is requested.

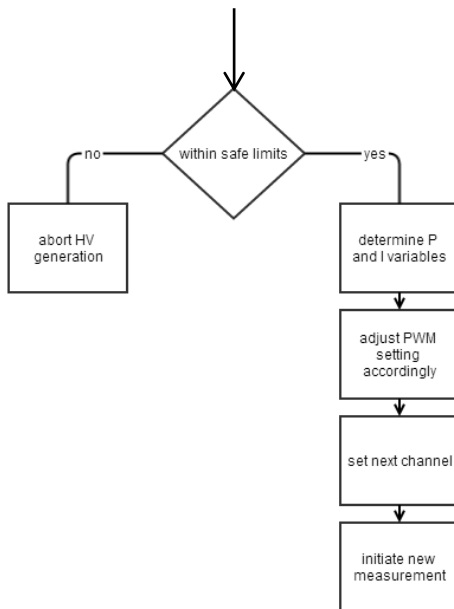


**Figure 26: Steps when a sample is ready**

As the same interrupt routine also handles the current measurements, when a current sample is read:

- A safety check is done to see if an overcurrent and possible short is occurring
- The result is stored

The current and voltage samples are read in alternating sequence so after every voltage sample a current sample is generated.

#### 4.5.1.1 *Sample and control matching*

A major source of damage could be a mismatch between the channel that is read and the channel that is controlled. Whenever there would be a mismatch between these, the controller would control a different HV circuit than it was measuring, meaning there would be no feedback and the HV generator would be running at full power within milliseconds.

To prevent accidents in this respect, a solution was necessary that somehow would match the ADC sample read to the PWM signal controlled. Preferably a solution that is as simple as possible so it could be positively verified as being absolutely correct. The solution selected was creating a 'GetADC(channel)' and a 'SetOCR(channel, dutycycle)' method, the latter controlling the PWM. The goal was to no longer think of a separate PWM and ADC pin but to see both as in- and output of a single channel.

The channel is retrieved and used as the only argument throughout the interrupt handler, reducing formal verification of the match of ADC channel and PWM channel to only the GetADC and SetOCR routine which are both 9 lines of code.

To verify if all the hardware components in the control loop were functional, a separate test program has been used to control the PWM manually and inspect corresponding samples from the ADC.

#### 4.5.1.2 Calibration table for hardware compensation

There is a significant non-linear effect present in the system, which is the voltage coefficient (VCR) of the 1:1000 resistor divider used to transfer voltages to the low voltage domain. The worst case VCR of the high ohm resistors used is up to  $7ppm/V$ . This results worst case at 3kV to  $\frac{7ppm}{V} * 3000V = 21000ppm$ . This is equal to 2.1%. The solution in the microthrust project is the use of a lookup-table with compensation for ADC values. This table is generated based on measurements in a controlled test environment which has the additional advantage that other system nonlinearities, for instance from protection diode leakage can also be mitigated. The calibration table needs to be manually filled using measurements some intermediary values are then extrapolated using an excel sheet. An example of this table is shown in 0on page 72.

#### 4.5.2 ADC reliability testing

In early implementations the measured noise could stretch in hundreds of millivolts. To test the reliability of the Atmel processor, a simple test setup with the ADC pins wired to a different supply voltages was executed to see if the performance of the microcontroller was as expected. Also the effect of channel switching between the ADC channels was unknown and therefore needed to be tested. The test results showed only a single bit of variation and a very stable operation.

#### 4.5.3 Testing and identifying software and hardware problems

When a new board is finished or large changes are applied, operation needs to be verified. This starts with using modified control software that actuates different components and allows for fixed PWM settings to carefully enable the Royer circuit and verify that the feedback signals arrive correctly. As not every component is working immediately, an oscilloscope in conjunction with the hardware design documents is used to analyze the signals involved and try to isolate the problem. As hardware is difficult to modify and test, it is crucial that software is operating correctly, therefore when issues arise, its corresponding software components are checked to verify if they are operating correctly.

### 4.6 Extractor voltage control

For extractor control, a similar approach has been taken as described in paragraph 4.5. A PI controller switches between the four controlled channels and adjusts accordingly. Also similar is the channel matching abstraction. So instead of PWM and ADC, both are addressed using the same channel.

As the effect of adding a thruster chip was unknown with respect to parasitic capacitances, the control variables are adjustable by the user, so the system parameters could be adjusted if needed. Some results are given in Appendix G on page 75.

During the first test in Switzerland it was concluded that operational parameters of the THC could be different for positive and negative voltages. For that reason both negative and positive voltages are separately controllable. As the voltages are rectified, the CPCB needs to indicate which polarity is present. When the CPCB also sends the command to apply an extraction voltage, the current extraction voltage setting is saved and a new one, corresponding to the indicated polarity is loaded. The implementation in software for the ESA board is in the basis the same PID code, with the major difference that the control variables have different presets and can be controlled. Another important difference is the fact that in this case a higher control signal means a lower voltage and vice versa so the control was inverted.

## 4.7 Fault detection

### 4.7.1 Overcurrent detection

In case of overly high power consumption, HV generation should be turned off immediately. To detect high power consumption the current detector code generates an error. For this error detection two separate phases are identified

- Change of voltage (usually startup)
- Steady state

During change-of-voltage, the emitter current can often be high enough to reach the maximum that the current detector is able to detect. This has the consequence that during 'change of voltage' high currents are permitted. In the steady state high currents should not occur so only a few samples of high current are allowed to account for load changes before an overcurrent is detected.

A solution to reach 'steady state' was based on the positive derivative of the emitter voltage. When the change of voltage was within 50V for 16 samples, the controller was in steady state, as the voltage changes relatively slow and otherwise it is difficult to distinguish with noise. Reentry in the change-of-voltage state occurs when the measured voltage is off with more than 50 V for 4 consecutive samples. Due to noise problems, occasionally the control reached steady state too early so a simpler solution is also implemented that uses the absolute value to determine steady state. A disadvantage of the latter method is that an overcurrent is not easily detected when steady state is not yet reached.

### 4.7.2 Overvoltage detection

Preventing overvoltage was crucial also during the development stage where an occasional software fault is more likely to occur and could otherwise result in damage to the hardware. In normal operation an overvoltage should not occur but will also prevented in the same manner when it occurs.

Overvoltage is defined as 300V above set voltage to account for load changes and noise. This value is changeable. When an overvoltage is detected the system is switched off.

## 4.8 Graphical User Interface

As the amount of features increased on the microthrust PCS, the status feedback also increased and the samples of measurements were harder to read, so it would be very useful if a comprehensive control interface would be available. The interface should allow for control through buttons instead of typed commands and provide feedback by parsing and showing the measured samples. Also would a GUI make it easier for microthrust partners to control the PCS and perform tests.

To develop a GUI, a platform was needed with the following features

- Drag and drop GUI creation
- Library for serial communication
- Language and IDE experience
- Run on microsoft windows
- No financial costs involved

The microthrust frontend should provide a graphical interface where button actions result in commands at the serial interface of the computer connected to the 'serial to I<sup>2</sup>C' translator that passes the commands to the PCS.

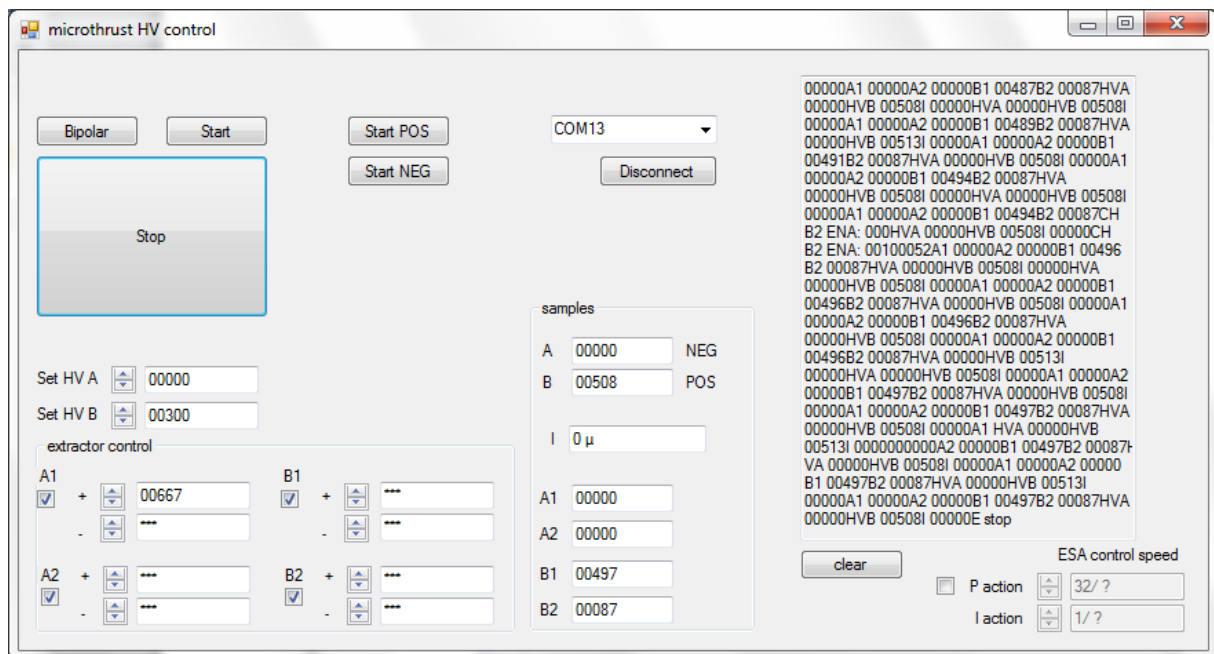


Figure 27: Microthrust control GUI

Preferably the time to get up to speed with the platform should be limited, which left basically three options: Borland RAD studio, Microsoft Visual Studio, or Java Netbeans. As RAD studio is not free this left NetBeans and Visual Studio. Both have proper serial libraries and should be equally suited for this

purpose. Based on the fact that the author has no experience with Visual C# but does have experience with Visual C++, this seemed as an opportune moment to gain knowledge of the language and attempt a simple first implementation to estimate effort and complexity. This attempt proved to be on par with expectations, so C# was used for the microthrust GUI and no efforts were made to evaluate other platforms.

In the final version the entire list of commands is implemented and incoming samples are parsed and corresponding fields are updated. A list of these commands is shown in Appendix E .

## 5 Results

The results presented here are a combination of the data gathered by QMUL where the board was tested in a vacuum environment and the results from tests in the Systematic lab. As a result of limited time and a tight schedule regarding tests and flights to QMUL, some of the tests were performed cautiously to make sure the board would not get damaged. This means that only limited test data is available around operating voltages. As key parameters of this project were efficiency and overall performance, these are the focal points of this chapter.

### 5.1.1 Emitter voltage measurements

Making accurate measurements of high voltage is an extra challenge as normal oscilloscopes are not equipped to this.

The probe used for measurements was a large 1:1000 HV probe suited for measurements up to 40kV. This probe was created to measure with multi-meters that usually have a  $10\text{M}\Omega$  impedance as is shown in figure 28. To analyze transient behavior and stability, a multimeter is not sufficient so a scope is needed. Most scopes do not have an impedance of  $10\text{M}\Omega$  but only  $1\text{M}\Omega$  which resulted in a 1:1900 factor instead of 1:1000.

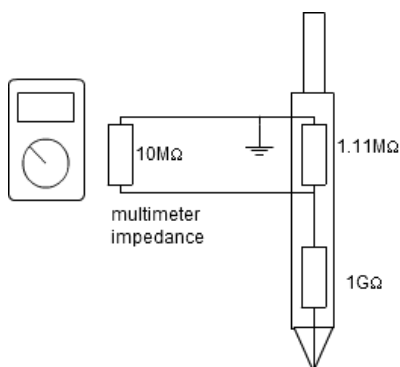


**Figure 28: Internal resistances probe with multimeter resulting in 1:1000 measurements**

The measured signal often contained noise but due to the size and the high impedance, the probe was prone to pick up noise so it was difficult to determine if a 100mV noise signal was in fact a disturbance of 190V on the board or just noise picked up by the probe.

### 5.1.2 Extractor voltage measurements

As the extraction voltage is created using a high voltage resistive divider, any measurement load would impact the result. Two different approaches have been used. One is to measure the buffered signal that is part of the control loop as was described in section 3.4.3. This is reasonably accurate but the disadvantage is that any errors present there will go undetected as the controller uses

exactly the same signal. So when the control is operating as expected the signal of the scope and the controller behavior will match, but this does not prove the output is correct.

The second method is to measure using the high voltage probe. This has the disadvantage that it impacts the result as the  $1\text{G}\Omega$  of the probe parallel at the  $500\text{M}\Omega$  of the extractor control (see Figure 23, p35) results in an effective resistance of  $333\text{M}\Omega$  for the extractor controller, thus reducing its range.

Another disadvantage is the fact that voltage measurements are not done with respect to voltage and ground but between two high voltages. The latter means that the equipment needs to be floating which in practice means that only battery powered multi-meters are available for this type of measurement.

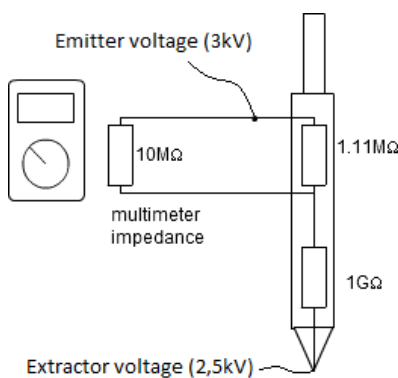


**Figure 29: Extractor measurement requires floating measurement equipment and influences maximal extraction voltage**

As the multimeter could not deliver much information about dynamic behavior, extra hardware was built that could measure the AC component of the extraction voltage using a normal probe. This circuit consisted of blocking capacitors and an instrumentations amplifier to amplify the difference between  $V_{\text{emitter}}$  and  $V_{\text{extractor}}$

## 5.2 Emitter voltage generation

L2-PCS-FUN-R4	The power efficiency of the high voltage section of the PCS shall be more than 50% at its design envelop (factor of 3 input power range)
L2-PCS-FUN-R7	The extractor to accelerator voltage shall be controlled between 0 and 3,5kV
L2-PCS-QUA-R2	The extractor to accelerator voltage shall be controlled with an accuracy of 1%

**Table 8: PCS high voltage generation requirements (revisited)**

As specified by the requirement L2-PCS-FUN-R7 the CPCB is capable in generating a voltage up to 3-4kV. The exact voltage is dependent on the version of the diodes installed as described in table 6, p31.

### 5.2.1 Ripple of $V_{emitter}$

Accurately measuring ripple is difficult, so as with the extractor measurement, a construction using blocking capacitors and protection diodes was used to measure stability. These tests were done with two different loads of  $400\text{M}\Omega$  and  $30\text{M}\Omega$ . The requirements show that the ripple should stay within 1% or 30V at 3kV.

The noise at 1000V is typically around  $12V_{\text{peak-peak}}$ , or about  $4.25V_{\text{RMS}}$  with a frequency of about 14Hz likely caused by the speed of the royer generator in combination with the controller. Worst case occasionally a  $20V_{\text{peak-peak}}$  is seen.

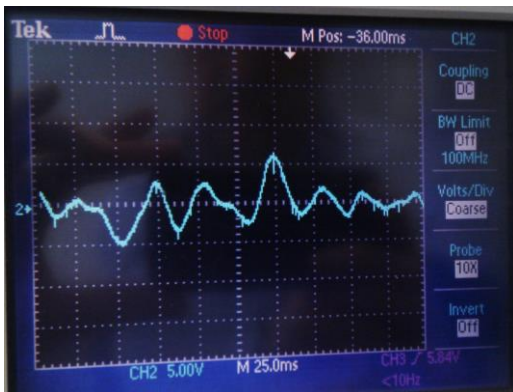


Figure 30: CPCB supply ripple (5V/division)

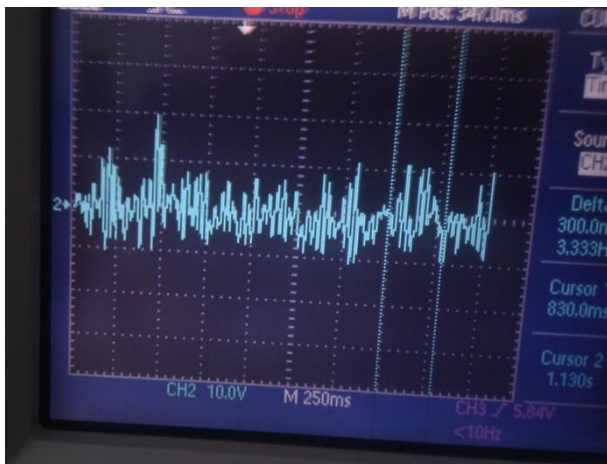


Figure 31: CPCB supply ripple at 3kV (10V/division)

Increasing the voltage also increases the ripple. Typically the ripple above 2000V is around  $20V_{\text{peak-peak}}$  with an occasional ripple at  $30V_{\text{peak-peak}}$ . The frequency is now around 33Hz.

One advantage of the slow ripple frequency is the fact that for the overall system the extraction voltage accuracy is more important than the emitter voltage and due to the slow fluctuations the extraction voltage will partially be able to compensate for these fluctuations.

To review the worst-case performance over voltage we see that the 1% requirement as described by L2-PCS-QUA-R2 in table 8 is met considering the PCS has an output of 3kV.

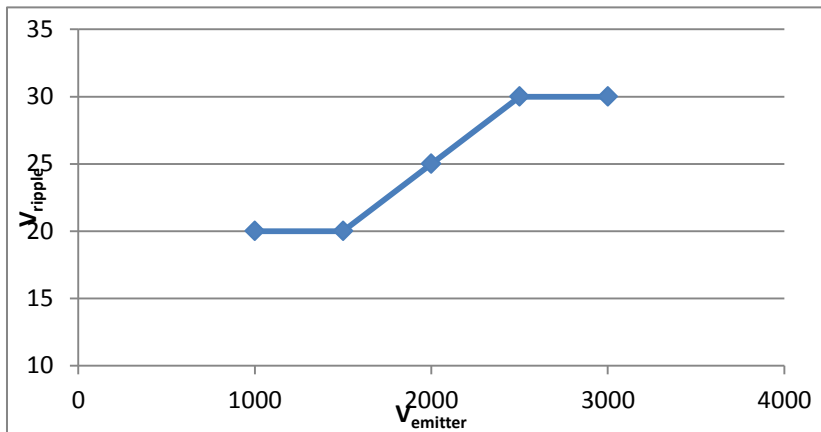


Figure 32: Ripple vs. output voltage

### 5.2.2 Efficiency

To measure efficiency the input current of the 12V supply line was measured as well as the output voltage as shown in table 9.

$P_{in}$ (12V)	Load	$P_{out}$ with $V_{emitter}$ at approx. 2.5kV	Efficiency (without steady state power consumption)
0,83W	25M $\Omega$	0.25W	25,3%
1.12W	15M $\Omega$	0.41W	37%
2W	6M $\Omega$	1,02W	51%
3W	3,333M $\Omega$	1,75W	58%

Table 9: Efficiency of CPCB HVPS

Higher loads have not been successfully tested on 2.5kV. The reason this value was selected was for safety as the tests were performed in a critical phase days before an integration test in London and those tests would only run up to 2 kV.

Table 10 shows the efficiency of the first version of the CPCB and a significant improvement is made, mainly caused by selecting more suitable diodes.

$P_{in}$ (12V)	Load	$P_{out}$ with $V_{emitter} = 2.75kV$	Efficiency (without steady state power consumption)
0.85W	30M $\Omega$	0.25W	29.5%
1.39W	15M $\Omega$	0.50W	36.4%
2.95W	6M $\Omega$	1.26W	42.8%

Table 10: First CPCB HVPS efficiency

The results in Table 9 do not show efficiency over a factor of 3 voltage range as required by the specification. The efficiency requirements are not strictly met for requirement L2-PCS-FUN-R4 since the efficiency requirement is met from output powers of 1W and higher but no successful tests were performed at 3W output.

### 5.3 Emitter voltage switching

L2-PCS-FUN-R2	The PCS shall enable bipolar operation of the MTPS
L2-PCS-FUN-R8	The PCS shall be able to operate at a frequency of up to 1 Hz

**Table 11: HVPS switching requirements**

The speed of switching between voltages is controllable in steps of 500ms and the L2-PCS-FUN-R8 requirement can be technically met although losses are quite high with a half-period of only 500ms. Although dead time between polarities should not be too high, the circuit must be fully discharged before a different polarity HV generator is started, otherwise the sum of the residual voltage and the generated voltage could exceed the specifications of the FETs. Another source of delay is the gate voltage. As shown in chapter 4.2.1, a gate voltage generator is used to create a voltage to open the FET. When this gate voltage generator is started some time is needed to create a high enough voltage at the gate of the FET.

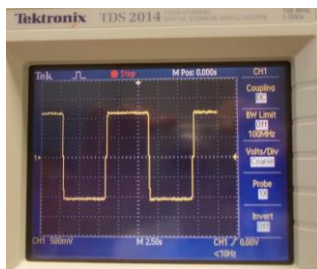


**Figure 33: Polarity switching with an emitter voltage of 2 kV**

To prevent any possible problems liberal wait times are applied. The timings for switching from positive to negative (and vice versa) are:

- Disable negative HV generator and enable positive gate voltage generator
- 100ms
- Discharge by enabling positive HV FET
- 100ms
- Disable negative HV FET
- 100ms
- Enable positive HV generator and disable negative gate voltage generator

Before the extractor can be started the emitter voltage needs to be stable, meaning within 95% of its end value before the extractor is switched on. Figure 34 shows that reaching a stable voltage takes approximately another 50ms, resulting in a total switch time of 350ms.

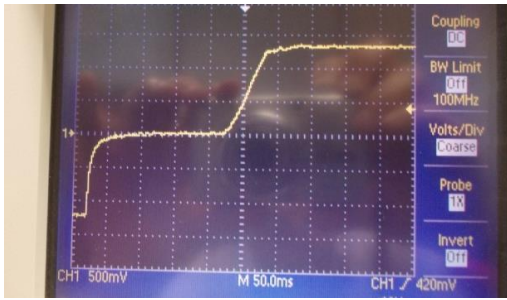


**Figure 34: Emitter voltage switching behavior at 2750V**

A half-period of 500ms as requirement L2-PCS-FUN-R8 states is therefore not advisable although still feasible. Figure 34 shows that the discharge time could be improved and also switching times are quite liberal and could likely be improved without negative consequences. But since the capacitive load of a thruster chip with ionic liquid is unknown, exact discharge requirements are unknown. For tests with the thruster chip a period of 10 seconds was typically used so these timings were sufficient and improving was not a priority.

#### 5.4 Extractor voltage generation

Extractor ripple testing proves an extra challenge due to the high impedance of the extraction voltage generation circuit. As there is no power consumption, efficiency is not an issue and the most significant parameter is ripple and transient behavior.

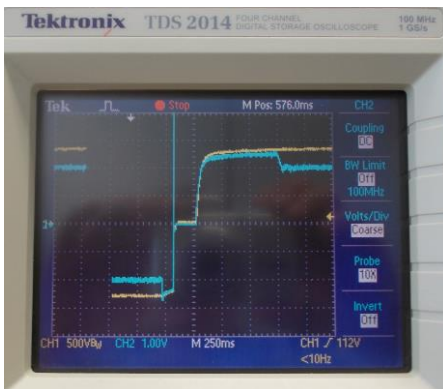


**Figure 35:  $V_{emitter}$  (yellow) at 2,5kV and  $V_{emitter} - V_{extractor}$  (blue) at approx. 700V**

Figure 35 shows the generation of extractor and emitter voltages. The extraction voltage, formally the voltage difference between  $V_{emitter}$  and  $V_{extractor}$  is 700 volts. The voltage is measured using the buffered signal in the 5V domain of the board.

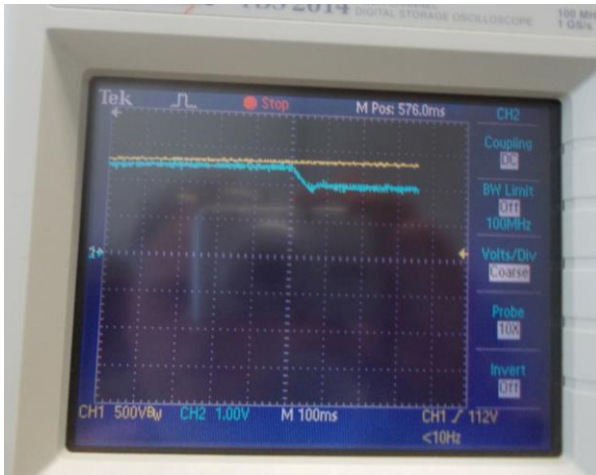


**Figure 36: extraction voltage generation**

The generation of the extraction voltage also takes about 50ms and shows a slight overshoot which is not a problem. As the influence of the thruster chip on the behavior is unknown, the control variables can be modified. An overview of the effects has been made in advance of the final test in Londen and is shown in the appendices on page 75.

#### 5.4.1 Ripple

The ripple at  $V_{\text{extractor}} - V_{\text{emitter}}$  is measured using blocking capacitances and an instrumentations amplifier to amplify the difference between  $V_{\text{emitter}}$  and  $V_{\text{extractor}}$ . The results were suboptimal as the ripple was around  $4.2V_{\text{peak-peak}}$  which is significantly above the 1V as per specification. A possible culprit lies in the fact that the PWM of the ESA board microcontroller has only 8 bits resolution which results in a maximal control accuracy of 0.25%. Another big factor is the fact that the ripple of the CPCB supply is propagating into the extraction voltage.

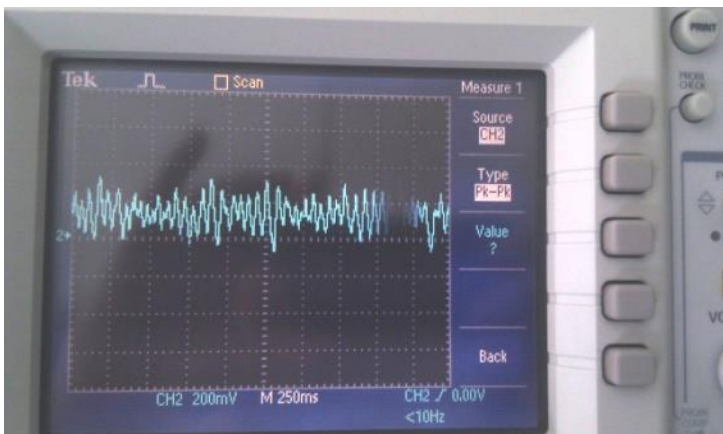


**Figure 37: Extractor ripple**

A separate version of the CPCB, that has not been part of this thesis and was produced near the end of the microthrust project, was controlled using a separate controller chip instead of the microcontroller. This resulted in an extractor showing only  $250mV_{\text{peak-peak}}$  indicating that the extractor

ripple is sufficiently compensated when using an analog chip to control HVPS. However this board has other issues.

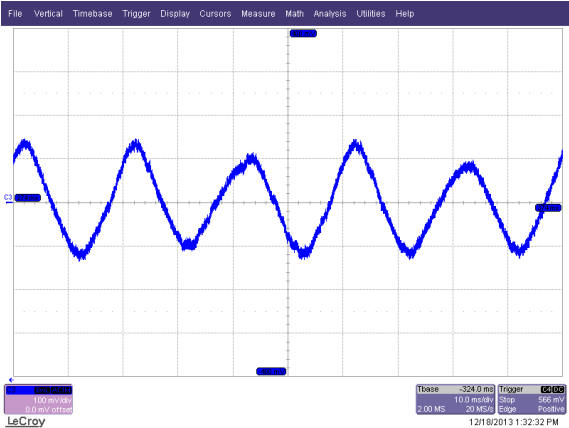


Figure 38: Extractor ripple using TL5001 controlled HVPS

### 5.5 Electro spray thruster testing with the PCS

At Queen Mary University in London the electro spray research group has a test setup with a vacuum chamber, mounting brackets and a ionic liquid feeding system where the PCS and thruster chip can be mounted for testing. The vacuum chamber also contains a Faraday cup that catches the electrons so a current is measured when the thruster chip starts spraying. When the PCS is not connected, two high voltage supplies provide the voltages for testing of the thruster chip. The thruster chip has been produced in different versions: A single emitter, to prove the principle, and 19 and 91 emitter chips.

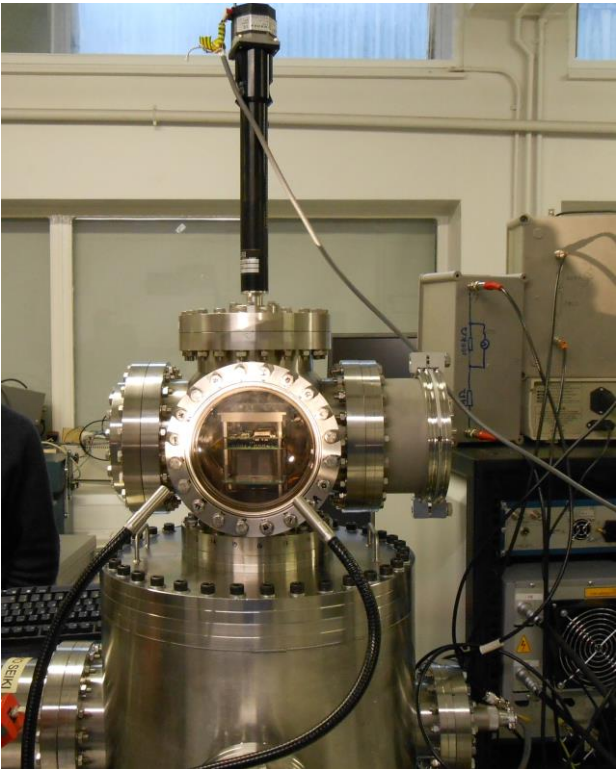


Figure 39: Vacuum chamber with fully assembled microthruster thruster system inside

### 5.5.1 Spray results

Figure 40 shows functional spray results from a test using a thruster chip with a single emitter. An imbalance is present between negative and positive current. It is not exactly known what causes this, but the phenomenon has been observed throughout the project. The results are stable with a little ripple.

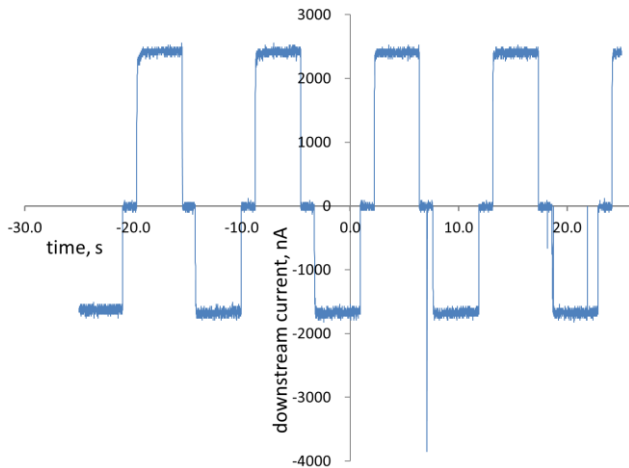


Figure 40: Single emitter,  $V_{\text{emitter}}=2\text{kV}$ ,  $V_{\text{emitter}}-V_{\text{extractor}}=880\text{V}$ . Half-time period: 5 seconds, large collector plate.

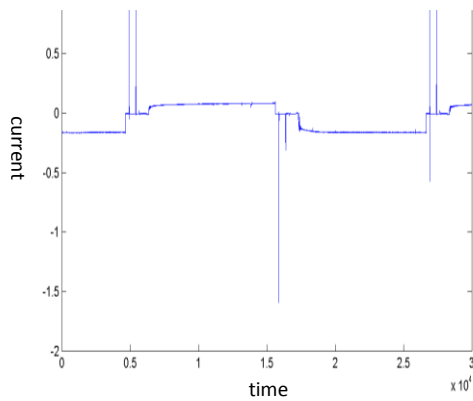
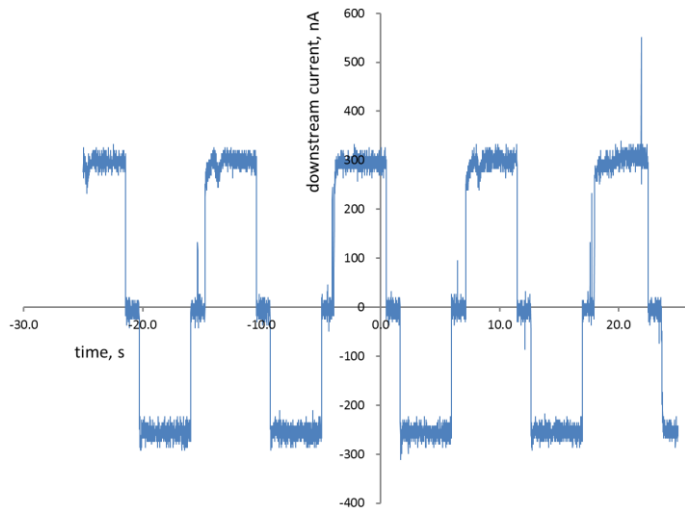


Figure 41: test with early prototype in 2012, single emitter, polarity is inverted

Early prototyping tests in Neuchatel, Switzerland show the same pattern. The polarities are inverted so the negative polarity shows a lower current as the positive polarity. The peaks are suspected to be switching noise.



**Figure 42: 19 emitters, 2000V emitter, 870  $V_{\text{emitter}} - V_{\text{extractor}}$ , half-time period: 5 seconds, small collector cup.**

Tests using a 19 emitter array were also successful although the noise is more emphasized.

## 6 Conclusion

In this thesis the development aspects and design of a novel, CubeSat sized, high voltage power and control board is described. The board creates multiple positive and negative high voltages and shows that, starting from 0V, within 50ms a stable voltage can be generated. The software structure and components are described as well as the control methods and determination of the control parameters.

Shown is that SystematicCs microthrust PCS successfully delivers an alternating voltage of at least 3kV, depending on configuration, and can be controlled using an intuitive interface that provides comprehensible control for partners in the project.

The results are mostly satisfactory although not all the requirements regarding ripple have been met, with the note that a mostly functional successor is created that does adhere to ripple specifications.

The thruster chip produced by our partner EPFL in Switzerland is a novel product that is still very much under development. During the process of this project different iterations of chips have been used with various degrees of success, but final results are promising, showing that the microthrust thruster chip combined with the described PCS is capable of producing stable thrust.

A paper 'Miniaturized HV Power Supply' was submitted to iEPC 2013 conference and awarded with a recommendation for outstanding paper.

### 6.1 Contributions

In this project I have worked in close collaboration with M. de Jong on building an innovative small form factor power and control board. I have identified and helped to solve the diverse array of problems that arise when developing a small form-factor board with controllable high voltages.

My contribution did not consist of designing and soldering of the PCS. I did contribute in discussing possible improvements, testing and simulating the Royer circuit, including building a test board, reviewing and discussing CPCB and ESA design documents, searching for suitable components and I carried main responsibility for the design, implementation and testing of software for the first PCS as well as the successive CPCB and ESA boards and the frontend interface. Also I wrote a part of the paper that was submitted to the International Electric Propulsion Conference 2013 and can be found in Appendix H .

## 6.2 Future work

Although the future is uncertain as funding for this project was available for a limited period only, the development of the thruster chip continues at EPFL and the PCS might gain traction in the future. Some difficulties in the current design still remain and could be addressed in future iterations.

### 6.2.1 Controller

Currently the CPCB and ESA board are both controlled using an 8-bit Atmel microcontroller which has a comparatively slow ADC and is not radiation-tolerant. As interest in CubeSat sized projects is growing, small microcontrollers might be applied that are radiation tolerant and will help guarantee correct operation. A rad-hard controller is already available in the FPGA domain, produced by ACTEL. This would significantly differ from the current controller implementation but could be a good alternative.

### 6.2.2 ESA voltage generation

The current extraction voltage generator is vulnerable for load changes. As shown in Appendix I the load is much higher than anticipated so to create a more robust extraction voltage an alternative is desired. An idea was posted to use a FET as 'emitter follower' and  $V_{\text{extractor}}$  to control the gate of a FET. The FET will then 'follow' the voltage that is applied at the gate and start going off when the output voltage nears the gate voltage. One challenge is the fact that this is difficult to achieve for both polarities.

### 6.2.3 Radiation testing

Microthrust is ultimately targeted for space applications and should be radiation tested to evaluate the effects of radiation.

## References

- 1 Arduino, 'Arduino Sourcecode' <<https://github.com/arduino/Arduino>> [Accessed 31-7-2014].
- 2 Maurice Borgeaud, Noémy Scheidegger, Muriel Noca, Guillaume Roethlisberger, Fabien Jordan, Ted Choueiri, and Nicolas Steiner, 'Swisscube: The First Entirely-Built Swiss Student Satellite with an Earth Observation Payload', in *Small Satellite Missions for Earth Observation* (Springer, 2010), pp. 207-13.
- 3 Busek, 'Busek Electro Spray Thruster', (2013).
- 4 M Coletti, F Guarducci, and SB Gabriel, 'A Micro Ppt for Cubesat Application: Design and Preliminary Experimental Results', *Acta Astronautica*, 69 (2011), 200-08.
- 5 Mark de Chadenedes, Drew Ahern, John Alaimo, Jin-Hoon Cho, Sung-Jin Park, J Gary Eden, Rodney L Burton, Je Kwon Yoon, Stephen Garrett, and Hariswaran Sitaraman, 'Advances in Microcavity Discharge Thruster Technology', in *Proc. 46th AIAA/ASME/SAE/ASEE Joint Propuls. Conf* (2010).
- 6 S De Jong, GT Aalbers, and J Bouwmeester, 'Improved Command and Data Handling System for the Delfi-N3xt Nanosatellite', in *Proceedings of the 59th International Astronautical Congress, Glasgow, Scotland* (2008).
- 7 Nathaniel Demmons, Vlad Hruby, Douglas Spence, and Thomas Roy, 'Electrospray Source', (Google Patents, 2013).
- 8 Edgar Everhart, and Paul Lorrain, 'The Cockcroft-Walton Voltage Multiplying Circuit', *Review of Scientific Instruments*, 24 (1953), 221-26.
- 9 Chang C Hang, Karl Johan Åström, and Weng Khuen Ho, 'Refinements of the Ziegler–Nichols Tuning Formula', in *IEE Proceedings D (Control Theory and Applications)* (IET, 1991), pp. 111-18.
- 10 Stewart Heitmann, 'Argtable'2011) <<http://argtable.sourceforge.net/>>. Accessed 1-7-2014
- 11 Diodes Inc., 'Ap2001 Ccfl Inverter', in *Application Note* (2002).
- 12 M.C.J. de Jong J. Timmerman, 'Deliverable D5.3.2: Test Report of Fabricated Board', (2013).
- 13 Renato Krpoun, and Herbert R Shea, 'A Method to Determine the Onset Voltage of Single and Arrays of Electro Spray Emitters', *Journal of Applied Physics*, 104 (2008), 064511.
- 14 Renato Krpoun, and HR Shea, 'Integrated out-of-Plane Nanoelectrospray Thruster Arrays for Spacecraft Propulsion', *Journal of Micromechanics and Microengineering*, 19 (2009), 045019.
- 15 Robert S Legge, and Paulo C Lozano, 'Electrospray Propulsion Based on Emitters Microfabricated in Porous Metals', *Journal of Propulsion and Power*, 27 (2011), 485-95.
- 16 Benjamin Longmier, 'Cat: A Thruster for Interplanetary Cubesats'2013) <[www.kickstarter.com/projects/longmier/cat-a-thruster-for-interplanetary-cubesats](http://www.kickstarter.com/projects/longmier/cat-a-thruster-for-interplanetary-cubesats)> [Accessed 8-12-2013]
- 17 José Mariano López Urdiales, 'Progress in Colloid Propulsion' (Massachusetts Institute of Technology, 2004).
- 18 Westcoast Magnetics, 'Flyback Converter Design'.
- 19 S Marcuccio, P Pergola, and N Giusti, 'Il–Feep: A Simplified, Low Cost Electric Thruster for Micro–and Nano–Satellites', *Journal of Propulsion and Power*, 14 (1998), 774-81.
- 20 KN Marsh, JA Boxall, and R Lichtenthaler, 'Room Temperature Ionic Liquids and Their Mixtures—a Review', *Fluid Phase Equilibria*, 219 (2004), 93-98.
- 21 Mike Meyer, Bryan Palaszewski, Dan Goebel, Harold White, and David Coote, 'In-Space Propulsion Systems Roadmap', *NASA Headquarters, Washington, DC*, 20546 (2012).
- 22 Juergen Mueller, Richard Hofer, and John Ziemer, 'Survey of Propulsion Technologies Applicable to Cubesats', (2010).
- 23 Julius Perel, and John F Mahoney, 'Micro-Electric Propulsion Using Charged Clusters', in *Advanced Space Propulsion Workshop, 9 th, Pasadena, CA* (1998), pp. 355-63.
- 24 The CubeSat Project, 'Cubesat Specification Drawing', ed. by cubesat\_standardrev12\_1.jpg <[www.cubesat.org](http://www.cubesat.org)>.

- 25 R. Kearney R. Visee, 'Deliverable 5.1.3 Electrical System Model', (2011).
- 26 Vishay Semiconductor, 'Fets as Voltage Controlled Resistor', in *Application Note* (1997), p. 6.
- 27 Sigurd Skogestad, 'Probably the Best Simple Pid Tuning Rules in the World', in *AIChE Annual Meeting, Reno, Nevada* (2001).
- 28 Ernst Stuhlinger, *Ion Propulsion for Space Flight* (McGraw-Hill New York, 1964).
- 29 Hyperion Technologies, 'Product Page' <<http://www.hyperiontechnologies.nl/styled-2/page2.htm>> [Accessed 6-6-2014].
- 30 Linear Technology, 'High Power Ccfl Controller for Wide Dimming Range and Maximum Lamp Lifetime', (LT1768 datasheet), p. 1.
- 31 ———, 'Lt Spice' <<http://www.linear.com/designtools/software/#LTspice>> [Accessed 18-6-2014].
- 32 Suzuki Tetsuya, 'Line Guide' <<http://www.spice-of-life.net/lineguide/>> [Accessed 01-07-2014].
- 33 Antonio Visioli, *Practical Pid Control* (Springer, 2006).
- 34 R. Joseph Cassady W. Andrew Hoskins, Olwen Morgan, Roger M. Myers, Fred Wilson, David Q. King and Kristi deGrys, '30 Years of Electric Propulsion Flight Experience at Aerojet Rocketdyne', in *33th International Electric Propulsion Conference* (Washington: 2013).
- 35 J. Williams, 'High Voltage, Low Noise, Dc/Dc Converters', in *Application Note* (2008).

## Appendix A Overview of problems during PCS development

### *Magnetic coupling*

During early development of the CPCB board, occasional sparks were seen when running at voltages above 2kV. As margins were tight, this was not totally unexpected though some attempts were made to find the cause. The design of the Royer circuits for positive and negative voltages were equal, as was the case at the first board but due to size constraints the distances between the positive and negative Royer circuit was reduced to about 1 mm. When testing the feedback of the circuit we noted that both the positive and negative were reporting a voltage, which should be impossible. Also when measuring the control signal it proved to be correctly controlled by the microcontroller. The culprit was found in the magnetic coupling of the tightly packed Royer circuits which both resonated on the same frequency. By changing the resonation frequency of one of the circuits the problem was solved.

### *Measurements and Noise*

Noise has been an consistent problem during the project as the CPCB board features multiple 66kHz oscillating voltages of  $2000V_{\text{peak-peak}}$  while measurements should be accurate to a few millivolts. A number of filters have been added to mitigate this but not without difficulty as an unfortunate side-effect of the ATMEGA32u4 microcontroller that is used on the CPCB board is the fact that this chip combines the programming header with the ADC inputs. This means that direct filters on the ADC signal are prohibited although the tracks for the programmer are picking up quite a lot of noise. A special cap was built that could be placed on the programming header when not in use.

### *Discharge sparking*

During tests we were always very conscious of the sharp 'tick' of a spark occurring on the board. Although surprisingly often these sparks did not cause damage.

Most notably when we tried to measure the temperature effect on the  $1G\Omega$  measurement resistor using cooling liquid (not conductive) which arced nonetheless, likely due to condensate. This temporarily created a 1:1 divider instead of 1:1000 which was not very positive for the 5V components on the other side. Initially a protective diode was present to prevent this but it was removed earlier as the measurement current was only about  $3000V/1G\Omega = 3\mu A$  and the leakage of the protection diode influenced the result. Eventually quite a lot of components needed to be tested and a few needed replacement.

### *Breakdowns of current detector*

After the first unsuccessful test in QMUL one of the components that was broken was the current detector. The high-side current detector was an intricate circuit that had its own floating supply voltage and a instrumentation amplifier to detect currents. The entire floating circuit contained a number of resistors and capacitors. This should not be a problem but could become a problem during discharge when not all the capacitors were discharged exactly equal, which was possible as not all capacitors and resistances were equal although calculations showed that the values were not of such significance that it could break down.

After 6 attempts on making this detector more robust an alternative was coined which already came up during earlier discussions: a low-side current detector and the component was removed.

### *Grounding problems during QMUL tests*

In May 2013 a PCS was finished that seemed functional and capable of controlling the microthrust thruster chip. However a number of failed tests followed, of which the cause was difficult to identify as the board stopped communicating and started sparking violently in air when trying to diagnose afterwards, almost as if the programming memory was corrupted. More problems were present and needed addressing but nonetheless this behavior was puzzling and troubling and could not be reproduced in the lab.

The schematic was reviewed extensively, a lot of tests were performed and other issues were identified and addressed, also possible causes were (preventively) addressed to make the board more robust.

In the second last test, instead of breakdown, the board stopped communicating but was still running. This almost certainly had to be a grounding problem and a lot of external wiring was added to make sure that all grounds were properly connected. The first successful test was the result. This leaves of course the question: how many tests were impacted by this oversight, as earlier test could have ended less disastrous and more informative or even successful.

### *High vacuum problems and the Paschen curve*

What commonly is considered a vacuum has an interesting effect on breakdown voltages for arcing. In a pure vacuum no electrons are present to provide a conductive path. The effect of low pressure and electric conductivity is described in the Paschen curve which shows that the breakdown voltage of air in a near vacuum is significantly lower as under normal pressure. This would be disastrous for our PCS. In attempts to find a local site to perform vacuum tests this effect was often unknown and the exact pressure required (lower than one millibar) could not be guaranteed, which was one of the reasons that for a long time no local high vacuum testing facilities were available and is also the

cause of at least one destructive failure as during the first test of the CPCB and ESA board the vacuum was not yet perfect when an emitter voltage was generated and a spark in the vacuum chamber was observed by bystanders.

# Appendix B Full list of requirements

This list is created by TNO. During the project some requirements were relaxed as being more practical for testing or from component point of view.

MicroThrust VCRM (Verification and Cross-Reference Matrix)									
Version 3	Legend	Yellow Cells contain updated values w.r.t. previous version			A = Applicable	T = Test			C = Compliant
Date: 1-Nov-2013	Legend	Orange cells need elaboration of requirements in the future			NA = Non-Applicable	M = Measurement			NC = Non Compliant
	Legend	Deleted requirement			PA = Partial Applicable	A = Analysis			PC = Partial Compliant
Requirement ID	Requirement description	Justification	Parent Requirement	Functional criticality [High / Medium / Low / Goal]	Applicability for Breadboard [A/NA/PA]	Applicable values for breadboard	Verification Method (VM) if Applicable for BB	Description of verification	Breadboard Verification Status [C/NC/PC]
L0-PR-R1	The MicroThrust (Colloid) Propulsion System shall be able to provide thrust for velocity changes and position control for a variety of spacecraft	The main function of a propulsion system is to deliver thrust for spacecraft attitude control and spacecraft velocity changes.	-	High	NA	-	-		
L0-PR-R2	The MicroThrust Propulsion System (MTPS) enables high efficient electric propulsion for small spacecraft enabling new missions	From the analysis of a set off missions, a set of typical requirements will be deducted.	-	High	NA	-	-		
L0-PR-R3	The MTPS design comprises of at least a thruster module, the power control electronics and optionally an electrically isolated external refill tank	The MicroThrust Propulsion System offers the potential to have a miniaturized electric (so high specific impulse) propulsion system which requires small amounts of propellant.	-	High	NA	-	-		
L0-PR-R4	The MTPS shall be a modular system and have flexibility in placement, thrust, configuration and total impulse delivery	The aim is to develop a complete system and not only a thruster or so.	-	Medium	NA	-	-		
	The MTPS shall not be optimized for a specific mission, but will be designed for a set of typical	The principle of the colloid propulsion system is such that for a significant part it can be build using the same technologies as used for micro electronics enabling easy production of identical components ideal for modular building blocks. Multiple modules combined with a centralized tank give a flexible usage of							
L0-PR-R5	missions	the system.	-	Medium	NA	-	-		
L0-PR-R6	In this FP7 Program a breadboard model will be build, tested and demonstrated. The breadboard model will comply a sub set of the requirements relevant for the flight type propulsion system	The requirement that are relevant for the Breadboard are marked in this matrix	-	High	A	See below	T,M,A	Several	PC
L0-MI-R1	In this FP7 Program a breadboard model will be build, tested and demonstrated. The breadboard model will comply a sub set of the requirements relevant for the flight type propulsion system	See D1.3 Mission Requirements and Propulsion System Specifications	Mission Analysis	High	NA	-	-		
L0-MI-R2	The MicroThrust propulsion system shall be designed to provide accelerations at 1AU that are greater than or equal to [0.1] mm/s <sup>2</sup> . This minimum acceleration ensures feasibility of the low-thrust trajectory in space and controllability of the satellite during cruise.	See D1.3 Mission Requirements and Propulsion System Specifications	Mission Analysis	High	NA	-	-		
L0-MI-R3	The power utilised by the MicroThrust propulsion system shall be less than or equal to [80%] of the average power produced by the satellite in cruise mode.	See D1.1 Mission Requirements and Propulsion System Specifications	Mission Analysis	Medium	NA	-	-		
L0-MI-R4	The design of the MicroThrust propulsion system shall accommodate a decrease of input power by a factor of [3] during the duration of the mission without major impact on its Isp performances (Isp decrease shall be less than TBD)	See D1.3 Mission Requirements and Propulsion System Specifications	Mission Analysis	High	PA	Vemitter variation from [TBD]-3800V (in case accelerator is present) and 1 or 2 THC's	T	Investigation of the effect of reduced Vemitter on the BB performance, by measurement of currents. Variation of number of THC's in use	TBC
L0-MI-R5	The total dry mass of the overall MicroThrust propulsion system (including TMS, PCS, and EPS external tank and all feeding systems) shall be lower than [100] gr per kg of launch mass (10% mass fraction). This mass fraction does not include solar panel masses.	See D1.3 Mission Requirements and Propulsion System Specifications	Mission Analysis	Medium	NA	-	-		
L0-MI-R6	The total wet mass of the overall MicroThrust propulsion system (including TMS, PCS, EPS, and total propellant) shall be lower than [300] gr per kg of launch mass (30% mass fraction). This mass fraction does not include solar panel masses.	See D1.3 Mission Requirements and Propulsion System Specifications	Mission Analysis	Medium	NA	-	-		
L0-MI-R7	The MTPS in its smallest configuration shall fit the constraints of a 3U CubeSat.	See D1.3 Mission Requirements and Propulsion System Specifications	Mission Analysis	High	NA	-	-		
L0-MI-R8	The MTPS shall operate for at least [4] years in space.	See D1.3 Mission Requirements and Propulsion System Specifications	Mission Analysis	High	PA	1 month life time	T	1 month continuous testing in vacuum chamber, measuring currents downstream and at thruster module. NOTE: duration length may change due to operational feasibility.	NC
L0-MI-R9	The solar panel mass inherent to the use of the MicroThrust propulsion system shall be book-kept at the system level and taken into account in the analysis.	See D1.3 Mission Requirements and Propulsion System Specifications	Mission Analysis	High	NA	-	-		
L0-MI-R10	The MTPS shall consume less than [5]W per kg of spacecraft launch mass.	See D1.3 Mission Requirements and Propulsion System Specifications	Mission Analysis	High	PA	5W down rated with actual number of emitters	A, T	Confirmed on BB by measurement of currents and voltages	NC

MicroThrust VCRM (Verification and Cross-Reference Matrix)									
Version 3	Legend	Yellow Cells contain updated values w.r.t. previous version		A = Applicable	T = Test				C = Compliant
Date: 1-Nov-2013	Legend	Orange cells need elaboration of requirements in the future		NA = Non-Applicable	M = Measurement				NC = Non Compliant
	Legend	Deleted requirement		PA = Partial Applicable	A = Analysis				PC = Partial Compliant
Requirement ID	Requirement description	Justification	Parent Requirement	Functional criticality [High / Medium / Low / Goal]	Applicability for Breadboard [A/NA/PA]	Applicable values for breadboard	Verification Method (VM) if Applicable for BB	Description of verification	Breadboard Verification Status [C/NC/PC]
L1-FUN-R1	The produced thrust to power ratio of the MTPS shall be greater than [20] $\mu\text{N/W}$ (50 mW/ $\mu\text{N}$ ) when considering the power as the total input power to the propulsion system.	See D1.3 Mission Requirements and Propulsion System Specifications	L0-MI-R2, L0-MI-R10	High	A	[20] $\mu\text{N/W}$	A, T	Thrust analysed using ToF and possibly direct thrust measurement. Power measurement from voltages and currents.	C
L1-FUN-R2	The propulsion specific impulse at full power shall be greater than or equal to [3000] sec for interplanetary exploration missions.	Deduction from dV and total allowable propulsion system mass	L0-MI-R1, L0-MI-R6	High	A	[3000] s	A, T	ToF measurements, and possibly direct thrust measurements.	NC
L1-FUN-R3	The MTPS shall be able to deliver thrust during at least [17000] hrs.	See D1.3 Mission Requirements and Propulsion System Specifications	Mission Analysis	High	PA	1 month	T	1 month continuous testing in vacuum chamber, measuring currents downstream and at thruster module. NOTE: duration length may change due to operational feasibility.	NC
L1-FUN-R4	The MTPS should not contribute to spacecraft charging. MTPS should be emitting a neutral charged plasma.	When emitted beam is not neutral, spacecraft is getting charged and at high level of charging ions start decelerating and go back towards S/C reducing Thrust and Isp (To be reviewed with SMART-1 description) Main function of the MTPS will be long duration thrusting to propel the spacecraft, however, short duration pulses might be needed for small adaptations, attitude control or formation flying.	-	High	NA	-	-	-	-
L1-FUN-R5	The MTPS shall be able to deliver thrust in both pulse mode and quasi-static continuous mode (= bipolar continuous operation)	See D1.3 Mission Requirements and Propulsion System Specifications	L0-PR-R1	Medium	PA	-	T	Testing of BB in pulsing mode and continuous mode	C
L1-FUN-R6	The MTPS system shall be designed to survive and be able to operate during [4] years after launch.	See D1.3 Mission Requirements and Propulsion System Specifications	L0-MI-R8	High	PA	1 month	T	1 month continuous testing in vacuum chamber, measuring currents downstream and at thruster module. NOTE: duration length may change due to operational feasibility.	NC
L1-CON-R1	Thrust orientation shall be 90 degrees with respect to the surface of the spacecraft to which the system is attached	It is likely the thruster module will be attached to the surface of the spacecraft, which is generally orientated as the spacecraft coordinate system	-	Medium	A	90	T	Measurement of plume angle, using EPFL segmented array and QMUL linear translator.	C
L1-CON-R2	The MTPS shall be able to operate with up to [6] TMS connected to 1 CPCB	System shall be modular, but to limited the possible number of connections and limit the requirements on the control systems the amount of modules is limited to a maximum of 6	L0-PR-R1, L0-PR-R2, L0-PR-R4, L0-PR-R5	Medium	PA	1 TMS, 4 THC's	T	BB testing	TBC
L1-INT-R1	The MTPS shall accommodate a satellite [5] V or [12] V regulated bus.	See D1.3 Mission Requirements and Propulsion System Specifications	-	Low	PA	12V	T	General BB design and testing	C
L1-INT-R2	The MTPS shall accommodate a satellite I2C, CAN or RS422 data bus.	See D1.3 Mission Requirements and Propulsion System Specifications	-	Low	PA	I2C	T	General BB design and testing	C
L1-INT-R3	The potential of accelerator grid shall be equal to external spacecraft, which is assumed to be ground level (= 0V)	Since the MTPS work in bipolar mode, a common potential of the accelerator grid is required to prevent ions from quickly returning to the spacecraft. Normally the outside of the spacecraft is also a neutral potential to prevent significant amount of ions to be attracted to spacecraft. Both effect together make it logical to set the accelerator grid to the outside potential of the spacecraft, which is assumed to be at 0V. In reality this voltage might be a few hundred volts above or below the local space potential.	-	High	A	Vacc=0	M	General BB design and initial electrical tests.	C
L1-INT-R4	The MTPS shall electrically interface with the spacecraft	Power and partial control delivered by spacecraft	L0-PR-R3	High	PA	ICD	T	BB design	C
L1-INT-R5	The MTPS shall mechanically interface with the spacecraft	It has to be mounted into a spacecraft	L0-PR-R1	Low	PA	ICD	T	BB design	C
L1-PHY-R1	The total dry MTPS mass shall be less than [300] gr in its smallest configuration.	See D1.3 Mission Requirements and Propulsion System Specifications	L0-MI-R5, L0-MI-R7	High	A	[300] g	M	Weighing relevant components of the BB	C
L1-PHY-R2	In its smallest configuration, the MTPS shall be able to process [520] gr of propellant, including 10% reserve and residuals.	See D1.3 Mission Requirements and Propulsion System Specifications	L0-MI-R1, L0-MI-R7	Medium	PA	D6.1.3	A	General design and testing of BB	C
L1-PHY-R3	The MTPS in its smallest configuration shall fit in a volume defined by 1U out of the 3U CubeSat volume. This volume is approximately 10 x 10 x 10 cm <sup>3</sup> . This volume excludes solar panels.	See D1.3 Mission Requirements and Propulsion System Specifications	L0-MI-R7	High	PA	ICD	M	Measurement of BB dimensions	C
L1-PHY-R4	The plume divergence for the MTPS shall ideally be in the lower segment of the range of [25-40] degrees half angle.	The smaller this angle, the closer external equipment can be placed near the MTPS.	-	Goal	A	-	M	Measurement of plume angle, using EPFL segmented array and QMUL linear translator.	C
L1-PHY-R5	The MTPS shall consume less than [5] W per kg of spacecraft launch mass.	See D1.3 Mission Requirements and Propulsion System Specifications (to be included)	L0-MI-R10	High	A	5W down rated with actual number of emitters	A, T	Testing of power input and relate this to calculated thrust from TOF traces and current	PC
L1-PHY-R6	Materials are selected on the basis of ECSS-E-30 Part 8	Unless there are good reasons, like i.e. for the propellant, ECSS-E-30 is applicable.	-	Medium	NA	-	-	-	-

MicroThrust VCRM (Verification and Cross-Reference Matrix)									
Version 3	Legend	Yellow Cells contain updated values w.r.t. previous version			A = Applicable		T = Test		C = Compliant
Date: 1-Nov-2013	Legend	Orange cells need elaboration of requirements in the future			NA = Non-Applicable		M = Measurement		NC = Non Compliant
	Legend	Deleted requirement			PA = Partial Applicable		A = Analysis		PC = Partial Compliant
Requirement ID	Requirement description	Justification	Parent Requirement	Functional criticality [High / Medium / Low / Goal]	Applicability for Breadboard [A/NA/PA]	Applicable values for breadboard	Verification Method (VM) if Applicable for BB	Description of verification	Breadboard Verification Status [C/NC/PC]
L1-ENV-R1	As a first assumption, the electronic units shall survive external temperatures in the range of [-30 to +60] oC (operational and non-operational).	See D1.3 Mission Requirements and Propulsion System Specifications	-	High	NA	-	-	-	
L1-ENV-R2	As a first assumption, the TMS thrusters chips shall survive external temperatures in the range of [-80 to +90] oC (operational and non-operational).	See D1.3 Mission Requirements and Propulsion System Specifications	-	High	NA	-	-	-	
L1-ENV-R3	The MTPS shall survive the mechanical load and vibration environment as defined by the [TBD] launch vehicle.	See D1.3 Mission Requirements and Propulsion System Specifications	-	High	NA	-	-	-	
<b>Additional requirements to be reviewed before insertion and numbering</b>									
L1-FUN-R	For AOCs applications, the MEMS EP thruster impulse bit shall be equal or less than [10-6] Ns.								
L1-ENV-R	Pressure and gas environment (N2 dissolving in to EMI-BF4)								
L1-ENV-R	electrical (ESD, EMI)								
L1-QUA-R	Thrust resolution TBD The MEMS EP thrust resolution shall be consistent with a [8 bit] data system.								
L1-QUA-R	Thrust accuracy TBD								
L1-QUA-R	Thrust response time TBD								
L1-QUA-R	Thrust noise TBD Thrust noise mN/Hz0.5 (requirement TBD)								
L1-QUA-R	The EMC produced by the MPTS shall be compatible with normal EMC requirements								
L1-QUA-R	Spillage/leakage								
L1-OPE-R	Autonomy i.e. Requirement on the way to handle power going down or communication with spacecraft								
L1-OPE-R	Failure detection and management								
L1-OPE-R	Available propellant sensing								
L1-OPE-R	Temperature regulation								
L1-SUP-R	Logistics								
L1-SUP-R	Transport								
L1-SUP-R	Filling								
L2-TMS-FUN-R1	The TMS integrates the thruster chips, the local propellant storage and feeding chips and is the structural interface to the spacecraft	See parent requirement	L0-PR-R3	High	PA	Spacecraft interface will be interface to BBTS, see ICD	M, T	BB design and assembly en integration of BB in BBTS	C
L2-TMS-FUN-R2	The TMS shall enable bipolar operation mode of the MTPS	See parent requirement	L1-FUN-R5	High	A	-	T	BB testing	C
L2-TMS-FUN-R3	The produced thrust to power ratio of the TMS shall be greater than [51] μN/W (19.6mW/μN) when considering the power as the total high voltage input power to the TMS	See D.2.5.1 (M36 update) Preliminary propulsion system design	L1-FUN-R1	High	A	[51] μN/W	A, T	Thrust analysed using ToF and possibly direct thrust measurement. Power measurement from voltages and currents.	NC
L2-TMS-FUN-R4	The TMS shall be able to deliver a minimum thrust of 300 μN in its smallest configuration.	Bases on minimum acceleration and minimum size of spacecraft the lower thrust level becomes 300 μN	L0-MI-R2, L0-MI-R7	High	PA	[9] μN	A, T	Thrust measurement using Indirect ToF analysis, and possibly direct thrust measurement	C
L2-TMS-FUN-R5	The propulsion specific impulse at full power shall be greater than or equal to [3000] sec for interplanetary exploration missions.	See parent requirement	L1-FUN-R2	High	A	[3000] s	A, T	Calculation based on ToF testing	NC
L2-TMS-FUN-R6	The TMS shall be able to deliver thrust during at least [17000] hrs.	See parent requirement	L1-FUN-R3	High	PA	1 month	T	1 month continuous testing in vacuum chamber, measuring currents downstream and at thruster module. NOTE: duration length may change due to operational feasibility.	NC
L2-TMS-FUN-R7	The TMS shall enable its refilling with propellant by the EPS in space	See parent requirement	L0-DR-R3	Medium	NA	-	-	-	
L2-TMS-FUN-R9	The TMS shall prevent spillage or leakage of propellant	All propellant should be used for propulsion and leakage will likely cause shorts and contamination of spacecraft	-	High	A	No visual leakage, no shorts/current leaks	T	General BB testing and inspection afterwards.	NC
L2-TMS-CON-R1	The TMS shall provide the needed insulation for 4 kV towards the spacecraft	In order to reach the 3000 s the TMS will have to work on 4 kV. Since the accelerator grid is grounded, the remaining part has to be safely and reliably insulated	-	High	A	4 kV	A, T	General BB testing and initial electrical tests.	C
L2-TMS-CON-R2	The TMS shall provide the needed insulation for 8 kV between the positive and the negative operating thruster parts	Operation in bipolar mode at 4kV leads to 8kV voltage difference between the two thruster parts on the TMS. Insulation between these two parts is crucial for the functionality.	L2-TMS-CON-R1	High	A	8 kV	A, T	General BB testing and initial electrical tests.	C
L2-TMS-CON-R3	The TMS shall have two electrically separated propellant tanks	A design choice is made in the project to go for bipolar operation (unless progress in knowledge shows unipolar is feasible for total propellant consumption and absence of unfavourable chemical degradation, etc.)	L2-TMS-FUN-R2	High	PA	4 tanks	A	BB design	C

MicroThrust VCRM (Verification and Cross-Reference Matrix)									
Version 3	Legend	Yellow Cells contain updated values w.r.t. previous version			A = Applicable	T = Test			C = Compliant
Date: 1-Nov-2013	Legend	Orange cells need elaboration of requirements in the future			NA = Non-Applicable	M = Measurement			NC = Non Compliant
	Legend	Deleted requirement			PA = Partial Applicable	A = Analysis			PC = Partial Compliant
Requirement ID	Requirement description	Justification	Parent Requirement	Functional criticality [High / Medium / Low / Goal]	Applicability for Breadboard [A/NA/PA]	Applicable values for breadboard	Verification Method (VM) if Applicable for BB	Description of verification	Breadboard Verification Status [C/NC/PC]
L2-TMS-INT-R1	The TMS shall fit on a cubesat	See parent requirement	L0-MI-R7	High	NA	-	-	-	
L2-TMS-INT-R2	The TMS shall electrically interface with the PCS	Design choice	L0-PR-R3	High	A	ICD	A	General BB testing and initial electrical tests.	C
L2-TMS-INT-R3	<del>The TMS shall fluidically interface with the EPS (in case an EPS is required by the mission)</del>	<del>Design choice</del>	<del>L0-PR-R3</del>	<del>Medium</del>	<del>NA</del>	<del>-</del>	<del>-</del>	<del>-</del>	
L2-TMS-PHY-R1	The dry mass of the TMS shall be less than [150] gram	Mass budget allocation from L1-PHY-R1	L1-PHY-R1	Medium	PA	< [150] g	M	Mass measurement of dry TMS	C
L2-TMS-PHY-R2	The envelope of the TMS shall be limited to 84x84x75 mm Figure 15	Volume allocation from L1-PHY-R3	L1-PHY-R3	Medium	PA	ICD	M	Measure dimensions of BB	C
L2-TMS-PHY-R3	The TMS shall consume less than [3]W of low voltage power	This [3] Watts is largely assigned for the heaters/coolers, but include all other possible users (like sensors etc.)	L0-MI-R7	Medium	NA	-	-	-	
L2-TMS-PHY-R4	Materials are selected on the basis of ECSS-E-30 Part 8	See parent requirement	L1-PHY-R6	Medium	NA	-	-	-	
L2-TMS-ENV-R1	As a first assumption, the TMS shall survive external temperatures in the range of [-80 to +90] oC (operational and non-operational).	See parent requirement	L1-ENV-R2	High	NA	-	-	-	
L2-PCS-FUN-R3	The PCS shall be able to handle a factor of 3 in input power	See parent requirement	L0-MI-R4	High	PA	3800V (in case accelerator is present) and 1 or 2 THC's	T	Vemitter on the BB performance, by measurement of currents. Variation of number of THC's in use input power, and the downstream current and which voltages.	NC
L2-PCS-FUN-R4	The power efficiency of the high voltage section of the PCS shall be more than 50% at its design envelope (factor of 3 input power range)	A 50% efficiency is assumed as a minimum for deducting the parent requirement	L1-FUN-R1	High	A	>50% power efficiency	T		NC
L2-PCS-FUN-R5	The PCS shall be able to provide and control a voltage difference of up to 4kV between the accelerator and the emitters	See parent requirement	L1-FUN-R2	High	A	4 kV	T	General BB testing and initial electrical tests.	C
L2-PCS-FUN-R6	The emitter to extractor voltage shall be controlled between 0 and 1kV	Current experience shows that 700V is a feasible value. 0-1kV is set for design margin	-	Medium	A	0 - 1 kV	T	General BB testing and initial electrical tests.	C
L2-PCS-FUN-R7	The extractor to accelerator voltage shall be controlled between 0 and 4 kV	This range results from a combination of required isp and factor of power input	L0-MI-R4, L1-FUN-R2	Medium	PA	0 - 4 kV	T	General BB testing and initial electrical tests.	C
L2-PCS-FUN-R8	The PCS shall be able to operate at a frequency of up to [1] Hz	Higher frequency reduces efficiency and is not likely to be needed to prevent chemical degradation of the propellant	-	Medium	A	[1] Hz	T	BB testing	TBC
L2-PCS-FUN-R9	The operating, idle or non-operating lifetime of the PCS shall be greater than [4] years.	See parent requirement	L1-FUN-R3	High	PA	1 month	T	1 month continuous testing in vacuum chamber. NOTE: duration length may change due to operational feasibility.	NC
L2-TMS-ENV-R2	The TMS shall survive the mechanical load and vibration environment as defined by the [TBD] launch vehicle.	See parent requirement	L1-ENV-R3	High	NA	-	-	-	
L2-TMS-OPE-R1	Temperature of the propellant inside the TMS shall during operation be kept within a TBD range.	See parent requirement	-	High	PA	Temperature monitoring on EIFB, optionally temperature regulation of BBTS	T	Temperature monitoring on EIFB, optionally experimental testing of effect of temperature on thruster operation	C
L2-TMS-SUP-R1	The TMS shall enable ground filling	The TMS needs to be filled on ground. Secondly, assuming a considerable amount of volume for propellant storage is present inside the thruster modules it a disadvantage not to use this.	-	High	PA	ICD, Filling via TSPF	T	General design/testing of TMS	C
L2-TMS-OPE-R	Sensors, do we need propellant sensing etc?	TBD							
L2-PCS-FUN-R1	The PCS shall provide and control the voltages and power to the other subsystems of the MTPS and do this in cooperation with the spacecraft control	The PCS is the interface between the spacecraft and the TMS. It is logical to let the PCS control the MTPS both operationally and electrically	L0-PR-R5	Medium	PA	control of TMS and communication with TSDC	T	Demonstration during BB testing that communication and control of TMS is possible	C
L2-PCS-FUN-R2	The PCS shall enable bipolar operation of the MTPS	See parent requirement	L1-FUN-R7	High	A	-	T	BB testing	C
L2-PCS-FUN-R10	The PCS shall bias the extractor voltages for neutral ion emission	biplar system) a neutral ion emission can be maintained	L1-FUN-R4	Medium	NA	Vemitter variation from ITBDI-		Investigation of the effect of reduced	
L2-PCS-FUN-R11	The operational lifetime of the PCS shall be greater than or equal to [17000] hrs	See D1.3 Mission Requirements and Propulsion System Specifications	L1-FUN-R3	High	PA	1 month	T	1 month continuous testing in vacuum chamber, measuring currents downstream and at thruster module. NOTE: duration length may change due to operational feasibility.	NC
L2-PCS-CON-R1	The PCS shall be able to operate and control up to [6] TMS	See parent requirement	L1-CON-R2	Medium	PA	1 TMS, 4 THC's	T	BB testing	TBC
L2-PCS-INT-R1	The PCS shall electrically interface with the TMS	Design choice	L0-PR-R3	High	A	ICD	T	General BB testing and initial electrical tests.	C
L2-PCS-INT-R2	<del>The PCS shall electrically interface with the EPS</del>	<del>Design choice</del>	<del>L0-PR-R3</del>	<del>Medium</del>	<del>NA</del>	<del>-</del>	<del>-</del>	<del>-</del>	
L2-PCS-INT-R3	The potential of accelerator grid shall be equal to external spacecraft, which is assumed to be ground level (= 0V)	See parent requirement	L1-INT-R3	High	A	Vacc=0V	M	General BB testing and initial electrical tests.	C
L2-PCS-INT-R4	The PCS shall accommodate a satellite [5] V or [12] V regulated bus.	See parent requirement	L1-INT-R1	Medium	PA	[12] V	T	General BB testing and initial electrical tests.	C
L2-PCS-INT-R5	The PCS shall mechanically interface with the spacecraft	Design choice	L0-PR-R3	High	PA	ICD	A	By design	C
L2-PCS-INT-R6	The PCS shall mechanically interface with the TMS	Design choice	L0-PR-R3	High	PA	ICD	A	By design	C

MicroThrust VCRM (Verification and Cross-Reference Matrix)									
Version 3	Legend	Yellow Cells contain updated values w.r.t. previous version			A = Applicable		T = Test		C = Compliant
Date: 1-Nov-2013	Legend	Orange cells need elaboration of requirements in the future			NA = Non-Applicable		M = Measurement		NC = Non Compliant
	Legend	Deleted requirement			PA = Partial Applicable		A = Analysis		PC = Partial Compliant
Requirement ID	Requirement description	Justification	Parent Requirement	Functional criticality [High / Medium / Low / Goal]	Applicability for Breadboard [A/NA/PA]	Applicable values for breadboard	Verification Method (VM) if Applicable for BB	Description of verification	Breadboard Verification Status [C/NC/PC]
L2-PCS-PHY-R1	The mass of the PCS shall be less than [150] gram (Single TMS configuration)	Mass budget allocation from L1-PHY-R1	L1-PHY-R1	Medium	PA	< [150] g	M	PCS mass measurement	C
L2-PCS-PHY-R2	The PCS envelope is limited to 80x80x20 mm (Single TMS configuration)	Volume allocation from L1-PHY-R3	L1-PHY-R3	Medium	PA	ICD	M	Measurement of dimensions	C
L2-PCS-PHY-R3	The PCS shall be designed for a maximum input power of [15]W per thruster module (TMS)	Power allocation from L1-PHY-R5	L0-MI-R7	High	PA	15W down rated with actual number of emitters	T	BB testing	C
L2-PCS-PHY-R4	The low power consumption of the PCS shall be less than [800] mW	Power allocation from L1-PHY-R5	L0-MI-R7	Medium	A	< 800 mW	T	BB testing	C
L2-PCS-PHY-R5	Materials are selected on the basis of ECSS-E-30 Part 8	See parent requirement	L1-PHY-R6	Medium	NA	-	-	-	-
L2-PCS-ENV-R1	As a first assumption, the PCS shall survive external temperatures in the range of [-30 to +60] oC (operational and non-operational).	See parent requirement	L1-ENV-R1	High	NA	-	-	-	-
L3-MSA-CON-R1	The MSA shall accommodate two electrically separated propellant tanks	See parent requirement	L2-TMS-FUN-R2	High	PA	4 tanks	A	BB design	C
L3-MSA-CON-R2	The MSA shall accommodate two (re)fill connectors (one per tank)	See parent requirement	L2-TMS-FUN-R7	High	PA	ICD	A	By design	C
L3-MSA-INT-R1	The MSA shall mechanically interface with a typical Cubesat structure	See parent requirement	L0-MI-R7	High	NA	-	-	-	-
L3-MSA-INT-R2	The MSA shall mechanically interface with the ESA	Design choice in order to keep a significant amount of cabling as short as possible	-	Medium	NA	-	-	-	-
L3-MSA-INT-R3	The MSA shall Fluidically interface with the EPS	Design choice	L0-PR-03	Medium	NA	-	-	-	-
L3-MSA-PHY-R1	The mass of the MSA shall be less than [100] gram	Mass budget allocation from L2-TMS-PHY-R1	L2-TMS-PHY-R1	Medium	A	< [100] g	M	Measurement of MSA mass	C
L3-MSA-PHY-R2	The envelope of the MSA shall be limited to 84x84x75 mm Figure 15	Volume allocation from L2-TMS-PHY-R2	L2-TMS-PHY-R2	Medium	PA	ICD	M	Dimensions of BB MSA	C
L3-MSA-PHY-R3	Materials are selected on the basis of ECSS-E-30 Part 8	See parent requirement	L1-PHY-R6	Medium	NA	-	-	-	-
L3-MSA-ENV-R1	As a first assumption, the MSA shall survive external temperatures in the range of [-80 to +90] oC (operational and non-operational).	See parent requirement	L1-ENV-R2	High	NA	-	-	-	-
L3-MSA-ENV-R2	The MSA shall survive the mechanical load and vibration environment as defined by the [TBD] launch vehicle.	See parent requirement	L1-ENV-R3	High	NA	-	-	-	-
L3-MSA-SUP-R1	The MSA shall enable ground filling	See parent requirement	L2-TMS-SUP-R1	High	PA	ICD, filling by TSPF	T	BB testing	C
L3-MSA-OPE-R	Sensors, do we need propellant sensing etc?	TBD							
L2-PCS-ENV-R2	The PCS shall survive the mechanical load and vibration environment as defined by the [TBD] launch vehicle.	See parent requirement	L1-ENV-R3	High	NA	-	-	-	-
L2-PCS-QUA-R1	The emitter to extractor voltage shall be controlled with an accuracy of 1V	It is estimated that this accuracy is needed based on current test results (d.d. JAN2012)	-	High	A	1V	T	Measurement of PCS output voltages using voltmeter before attachment to TMS	TBC
L2-PCS-QUA-R2	The extractor to accelerator voltage shall be controlled with an accuracy of 1%	This value seems reasonably feasible and this does not influence Isp significantly	-	Medium	A	1%	T	Measurement of PCS output voltages using voltmeter	TBC
L3-MSA-FUN-R1	The MSA shall mechanically support the subsystems of the TMS	Design choice	-	High	PA	ICD	A	General design and testing	C
L3-MSA-FUN-R2	The MSA shall enable bipolar operation mode of the MTPS	See parent requirement	L1-FUN-R7	High	A	-	T	BB testing	C
L3-MSA-FUN-R3	The lifetime of the MSA shall be greater than [4] years.	THE MSA shall remain functioning even after the operational life time of the TMS	L1-FUN-R3	High	NA	-	-	-	-
L3-MSA-FUN-R4	The MSA shall provide the needed insulation for 4 kV towards the spacecraft	In order to reach the 3000 s the TMS will have to work on 4 kV. Since the accelerator grid is grounded, the remaining part has to be safely and reliably insulated	L2-TMS-CON-R1	High	A	4 kV	A, T	BB design and initial electrical tests.	C
L3-MSA-FUN-R5	The MSA shall provide the needed insulation for 8 kV between the positive and the negative operating thruster parts	Operation in bipolar mode at 4kV leads to 8kV voltage difference between the two thruster parts on the TMS. Insulation between these two parts is crucial for the functionality.	L2-TMS-CON-R3	High	A	8 kV	A, T	BB design and initial electrical tests.	C
		A design choice is made in the project to go							

MicroThrust VCRM (Verification and Cross-Reference Matrix)									
Version 3	Legend	Yellow Cells contain updated values w.r.t. previous version			A = Applicable		T = Test		C = Compliant
Date: 1-Nov-2013	Legend	Orange cells need elaboration of requirements in the future			NA = Non-Applicable		M = Measurement		NC = Non Compliant
	Legend	Deleted requirement			PA = Partial Applicable		A = Analysis		PC = Partial Compliant
Requirement ID	Requirement description	Justification	Parent Requirement	Functional criticality [High / Medium / Low / Goal]	Applicability for Breadboard [A/NA/PA]	Applicable values for breadboard	Verification Method (VM) if Applicable for BB	Description of verification	Breadboard Verification Status [C/NC/PC]
L3-TBA-FUN-R1	The TBA integrates the EIFB, THC's, the connectors, the sensors and the heaters.	Design Choice	-	Medium	PA	ICD	A, T	By design and BB testing	C
L3-TBA-FUN-R2	The produced thrust to power ratio of the TBA shall be greater than [51] $\mu\text{N}/\text{W}$ (19.6mW/ $\mu\text{N}$ ) when considering the power as the total high voltage input power to the TBA	See D.2.5.1 (M36 update) Preliminary propulsion system design	L2-TMS-FUN-R3	High	A	[51] $\mu\text{N}/\text{W}$	A, T	Calculation based on Thrust and power testing	C
L3-TBA-FUN-R3	The TBA shall be able to deliver a minimum thrust of 300 $\mu\text{N}$ in its smallest configuration.	See parent requirement	L2-TMS-FUN-R4	High	PA	[9] $\mu\text{N}$	T	Thrust measurement	C
L3-TBA-FUN-R4	The propulsion specific impulse at full power shall be greater than or equal to [3000] sec for interplanetary exploration missions.	See parent requirement	L2-TMS-FUN-R5	High	A	[3000] s	A, T	Calculation based on ToF testing	NC
L3-TBA-FUN-R5	The lifetime of the TBA shall be greater than [4] years.	The TBA shall remain functioning even after the operational life time of the TMS	L1-FUN-R3	High	PA	1 month	T	1 month continuous testing in vacuum chamber. NOTE: duration length may change due to operational feasibility.	NC
L3-TBA-FUN-R6	The TBA shall enable bipolar operation mode of the MTPS	See parent requirement	L2-TMS-FUN-R2	High	A	-	T	General design/testing of TMS	C
L3-TBA-FUN-R7	The TBA shall be design to handle 4 kV voltage	In order to reach the 3000 s the TMS will have to work on 4 kV. Connectors, wires, components on different voltage levels are expected to be situated closely together. Sufficient distance or insulation has to be	L2-TMS-CON-					General BB testing and	
L3-TBA-FUN-R8	difference between its subcomponents	applied to avoid i.e. arcing or leak currents	R1	High	A	4 kV	A, T	Initial electrical tests.	C
L3-TBA-FUN-R9	The TBA shall provide the needed insulation for 8 kV between the positive and the negative operating thruster parts	Operation in bipolar mode at 4kV leads to 8kV voltage difference between the two thruster parts on the TMS. Insulation between these two parts is crucial for the functionality.	L2-TMS-CON-R3	High	A	8 kV	A, T	General BB testing and initial electrical tests.	C
L3-TBA-FUN-R9	The operational lifetime of the TBA shall be greater than or equal to [17000] hrs	See D1.3 Mission Requirements and Propulsion System Specifications	L1-FUN-R3	High	PA	1 month	T	1 month continuous testing in vacuum chamber, measuring currents downstream and at thruster module. NOTE: duration length may change due to operational feasibility.	NC
L3-TBA-CON-R1	The TBA shall accommodate two sets of THC's	A design choice is made in the project to go for bipolar operation (unless progress in knowledge shows unipolar is feasible for total propellant consumption and absence of unfavourable chemical degradation, etc.)	L2-TMS-FUN-R2	High	A	ICD	A,T	General design and testing of BB	C
L3-TBA-INT-R1	The TBA shall mechanically interface with the MSA	Design choice	L0-PR-03	High	A	ICD	A,T	General design and testing of BB	C
L3-TBA-INT-R2	The TBA shall mechanically interface with the CFA	Design choice	L0-PR-03	High	A	ICD	A,T	General design and testing of BB	C
L3-TBA-INT-R3	The TBA shall electrically interface with the PCS	Design choice	L0-PR-03	High	A	ICD	A,T	General design and testing of BB	C
L3-TBA-INT-R4	The TBA shall fluidically interface with the CFA	Design choice	L0-PR-03	High	A	ICD	A,T	General design and testing of BB	C
L3-TBA-PHY-R1	The mass of the TBA shall be less than [40] gram	Mass budget allocation from L2-TMS-PHY-R1	R1	Medium	PA	< [40] g	M	Mass measurement	C
L3-TBA-PHY-R2	The envelope of the TBA shall be limited to 80x80x2 mm	Best guess	L2-TMS-PHY-R2	Medium	PA	ICD	M	Dimensions measurement	C
L3-TBA-PHY-R3	The power consumption of subsystems on the TBA shall be less than [2.2]W.	Power budget allocation from L2-TMS-PHY-R3	L2-TMS-PHY-R3	Medium	NA	-	-	-	
L3-TBA-PHY-R4	Materials are selected on the basis of ECSS-E-30 Part 8	See parent requirement	L1-PHY-R6	Medium	NA	-	-	-	
L3-TBA-ENV-R1	As a first assumption, the TBA shall survive external temperatures in the range of [-80 to +90] oC (operational and non-operational).	See parent requirement	L1-ENV-R2	High	NA	-	-	-	
L3-TBA-ENV-R2	The TBA shall survive the mechanical load and vibration environment as defined by the [TBD] launch vehicle.	See parent requirement	L1-ENV-R3	High	NA	-	-	-	
L3-CFA-FUN-R1	The CFA shall transport the propellant towards the emitters by capillary forces	Design Choice	-	High	PA	ICD	A, T	General design and testing of BB	C
L3-CFA-FUN-R2	The lifetime of the CFA shall be greater than [4] years.	See parent requirement	L1-FUN-R3	High	PA	1 month	T	1 month continuous testing in vacuum chamber. NOTE: duration length may change due to operational feasibility.	NC
L3-CFA-FUN-R3	The CFA shall function as an electrode, conducting electrons towards or away from the propellant boundary layer	Dependant on the physics, charge build up between the propellant and the electrode will occur and is needed, or electrons will flow towards or away from the propellant dependant on the bipolar state (positive or negative)	-	High	PA	ICD	A, T	General design and testing of BB	C
L3-CFA-FUN-R4	The CFA shall function under bipolar operation	See parent requirement	L2-TMS-FUN-R2	High	A	-	T	BB testing	C
L3-CFA-FUN-R5	The operational lifetime of the CFA shall be greater than or equal to [17000] hrs	See D1.3 Mission Requirements and Propulsion System Specifications	L1-FUN-R3	High	PA	1 month	T	1 month continuous testing in vacuum chamber, measuring currents downstream and at thruster module. NOTE: duration length may change due to operational feasibility.	NC

MicroThrust VCRM (Verification and Cross-Reference Matrix)									
Version 3	Legend	Yellow Cells contain updated values w.r.t. previous version		A = Applicable	T = Test				C = Compliant
Date: 1-Nov-2013	Legend	Orange cells need elaboration of requirements in the future		NA = Non-Applicable	M = Measurement				NC = Non Compliant
	Legend	Deleted requirement		PA = Partial Applicable	A = Analysis				PC = Partial Compliant
Requirement ID	Requirement description	Justification	Parent Requirement	Functional criticality [High / Medium / Low / Goal]	Applicability for Breadboard [A/NA/PA]	Applicable values for breadboard	Verification Method (VM) if Applicable for BB	Description of verification	Breadboard Verification Status [C/NC/PC]
L3-CFA-CON-R1	The CFA shall consist of the PFIC and the PFC	Design choice	-	High	PA	ICD	A	By design	C
L3-CFA-CON-R2	The CFA shall allow the option of placement of a refill connector to th HLOW	Design choice	L2-TMS-FUN-R7	High	A	ICD	A	By design	C
L3-CFA-INT-R1	The CFA shall mechanically interface with the HLOW	Design choice	L0-PR-03	High	A	ICD	A,T	General design and testing of BB	C
L3-CFA-INT-R2	The CFA shall mechanically interface with the THC	Design choice	L0-PR-03	High	A	ICD	A,T	General design and testing of BB	C
L3-CFA-INT-R3	The CFA shall mechanically interface with the EIFB	Design choice	L0-PR-03	High	A	ICD	A,T	General design and testing of BB	C
L3-CFA-INT-R4	The CFA shall electrically interface with the EIFB	Design choice	L0-PR-03	High	A	ICD	A	BB design and initial electrical tests.	C
L3-CFA-INT-R5	The CFA shall fluidically interface with the THC	Design choice	L0-PR-03	High	A	ICD	A,T	General design and testing of BB	C
L3-CFA-PHY-R1	The mass of the CFA shall be less than [10] gram	Mass budget allocation from L2-TMS-PHY-R1 The propellant storage efficiency inside the TMS should be efficient to allow as much as possible local storage. [80]% seems a reasonable value for the smallest configuration. For larger configurations the efficiency is expected to be higher.	L2-TMS-PHY-R1	Medium	PA	<[10] g	M	Mass measurement	C
L3-CFA-PHY-R2	The combined storage efficiency of the propellant and the CFA should be larger than [80]% w.r.t. volume available inside the HLOW in the smallest TMS configuration.		L2-TMS-PHY-R2	Medium	NA	-	-	-	
L3-CFA-PHY-R3	Materials are selected on the basis of ECSS-E-30 Part 8	See parent requirement	L1-PHY-R6	Medium	NA	-	-	-	
L3-CFA-ENV-R1	As a first assumption, the CFA shall survive external temperatures in the range of [-80 to +90] oC (operational and non-operational).	See parent requirement	L1-ENV-R2	High	NA	-	-	-	
L3-CFA-ENV-R2	The CFA shall survive the mechanical load and vibration environment as defined by the [TBD] launch vehicle.	See parent requirement	L1-ENV-R3	High	NA	-	-	-	
L3-CPCB-FUN-R1	The CPCB shall provide and control the voltages and power to the other subsystems of the MTPS and do this in cooperation with the spacecraft control	The CPCB is the interface between the spacecraft and the TMS. It is logical to let the CPCB control the MTPS both operationally and electrically	L0-PR-R4	High	PA	In cooperation with TSDC	T	By design and BB testing	C
L3-CPCB-FUN-R2	The CPCB shall be able to function in uni- and bipolar operation mode	See parent requirement	L1-FUN-R5	High	A	-	A, T	By design and BB testing	C
L3-CPCB-FUN-R3	The CPCB shall be able to handle a factor of 3 in input power	See parent requirement	L0-MI-R4	High	PA	Vemitter variation from [TBD]-3800V (in case accelerator is present) and 1 or 2 THC's	T	Investigation of the effect of reduced Vemitter on the BB performance, by measurement of currents. Variation of number of THC's in use	TBC
L3-CPCB-FUN-R4	The power efficiency of the high voltage section of the CPCB shall be more than 50% at its design envelope (factor of 3 input power range)	A 50% efficiency is assumed as a minimum for deducting the parent requirement	L1-FUN-R1	High	A	> 50%	T	BB testing	NC
L3-CPCB-FUN-R5	The CPCB shall consume (for its own functioning) less than [400] mW per kg of launch mass.	See parent requirements	L0-MI-R7, L1-FUN-R1	Medium	PA	<[400] mW	T	Testing of power input	
L3-CPCB-FUN-R6	The CPCB shall be able to provide and control a voltage difference of up to 4kV between the accelerator and the emitters	See parent requirement	L1-FUN-R2	High	A	4 kV	T	General BB testing and initial electrical tests.	C
L3-CPCB-FUN-R7	The CPCB shall control the total voltage between the emitter and the accelerator up to 4 kV	See parent requirement	L2-PCS-FUN-R7	High	A	0-4 kV	T	BB testing	C
L3-CPCB-FUN-R8	The CPCB shall be able to operate at a frequency of up to [1] Hz	Higher frequency reduces efficiency and is not likely to be needed to prevent chemical degradation of the propellant	L2-PCS-FUN-R8	Medium	A	1 Hz	T	BB testing	TBC
L3-CPCB-FUN-R9	The operating, idle or non-operating lifetime of the CPCB shall be greater than [4] years.	See parent requirement	L1-FUN-R3	High	PA	1 month	T	1 month continuous testing in vacuum chamber. NOTE: duration length may change due to operational feasibility.	TBC
L3-CPCB-CON-R1	The CPCB shall be able to operate and control up to [6] TMS	See parent requirement	L1-CON-R2	Medium	PA	1 TMS	T	BB testing	C
L3-CPCB-INT-R1	The CPCB shall electrically interface with the TMS	Design choice	L0-PR-R3	High	A	ICD	M	General BB testing and initial electrical tests.	C
L3-CPCB-INT-R2	The CPCB shall electrically interface with the ESA	Design choice	L0-PR-R3	High	A	ICD	M	General BB testing and initial electrical tests.	C
L3-CPCB-INT-R3	The CPCB shall electrically interface with the EPS	Design choice	L0-PR-R3	High	NA	-	-	-	
L3-CPCB-INT-R4	The potential of accelerator grid shall be equal to external spacecraft, which is assumed to be ground level (= 0V)	See parent requirement	L1-INT-R3	High	A	Vacc=0V	T	General BB testing and initial electrical tests.	C
L3-CPCB-INT-R5	The CPCB shall accommodate a satellite [5] V or [12] V regulated bus.	See parent requirement	L1-INT-R1	Medium	PA	12 V	T	General BB testing and initial electrical tests.	C
L3-CPCB-INT-R6	The CPCB shall mechanically interface with the spacecraft	Design choice	L0-PR-R3	High	PA	ICD	M	By design	C
L3-CPCB-INT-R7	The PCS shall mechanically interface with the TMS	Design choice	L0-PR-R3	High	NA	-	-	-	

MicroThrust VCRM (Verification and Cross-Reference Matrix)									
Version 3	Legend	Yellow Cells contain updated values w.r.t. previous version			A = Applicable		T = Test		C = Compliant
Date: 1-Nov-2013	Legend	Orange cells need elaboration of requirements in the future			NA = Non-Applicable		M = Measurement		NC = Non Compliant
	Legend	Deleted requirement			PA = Partial Applicable		A = Analysis		PC = Partial Compliant
Requirement ID	Requirement description	Justification	Parent Requirement	Functional criticality [High / Medium / Low / Goal]	Applicability for Breadboard [A/NA/PA]	Applicable values for breadboard	Verification Method (VM) if Applicable for BB	Description of verification	Breadboard Verification Status [C/NC/PC]
L3-CPCB-PHY-R1	The mass of the CPCB shall be less than [100] gram (Single TMS configuration)	Mass budget allocation from L1-PHY-R1	L1-PHY-R1	Medium	A	< [100] g	M	Mass measurement	C
L3-CPCB-PHY-R2	The CPCB envelope is limited to 80x80x(15) mm (Single TMS configuration)	Volume allocation from L1-PHY-R3; High components on both the CPCB and the ESA should not interfere	L1-PHY-R3	Medium	PA	ICD	M	Dimensions measurement	C
L3-CPCB-PHY-R3	The CPCB shall be designed for a maximum power throughput of [6]W per thruster module (TMS) at High Voltage	Power allocation from L1-PHY-R5	L0-MI-R7	High	PA	[0.18] W	T	BB testing	TBC
L3-CPCB-PHY-R4	The low power consumption of the CPCB shall be less than [400] mW	Power allocation from L1-PHY-R5	L0-MI-R7	Medium	A	< [400] mW	T	General BB testing and initial electrical tests.	C
L3-CPCB-PHY-R5	Materials are selected on the basis of ECSS-E-30 Part 8	See parent requirement	L1-PHY-R6	Medium	NA	-	-	-	-
L3-CPCB-PHY-R3	The CPCB shall be designed for a maximum power throughput of [2.6]W per thruster module (TMS) at Low Voltage	Power allocation from L1-PHY-R5	L0-MI-R7	High	A	[2.6] W	T	BB testing	TBC
L3-CPCB-ENV-R1	As a first assumption, the CPCB shall survive external temperatures in the range of [-30 to +60] oC (operational and non-operational).	See parent requirement	L1-ENV-R1	High	NA	-	-	-	-
L3-CPCB-ENV-R2	The CPCB shall survive the mechanical load and vibration environment as defined by the [TBD] launch vehicle.	See parent requirement	L1-ENV-R3	High	NA	-	-	-	-
L3-CPCB-QUA-R2	The CPCB shall control the emitter to accelerator voltage with an accuracy of 1%.	This value seems reasonably feasible and this does not influence Isp significantly	-	Medium	A	1%	T	Measurement of PCS output voltages using voltmeter	TBC
L3-ESA-FUN-R1	The ESA shall control emitter to extractor voltages	See parent requirement	L2-PCS-FUN-R1	High	A	-	T	BB testing	C
L3-ESA-FUN-R2	The ESA shall communicate directly with the CPCB	Design choice	L2-PCS-FUN-R1	Medium	A	-	T	General BB testing and initial electrical tests.	C
L3-ESA-FUN-R3	THE ESA shall control the on/off functionality of the THC's	Design choice	L2-PCS-FUN-R1	High	A	-	T	General BB testing and initial electrical tests.	TBC
L3-ESA-FUN-R4	The ESA shall be able to function in uni- and bipolar operation mode	See parent requirement	L1-FUN-R7	High	A	-	T	General BB testing and initial electrical tests.	C
L3-ESA-FUN-R5	The ESA shall be able to handle at least [9] THC's per polar side	Addressing several THC's should be able to adjust power matching and extend MTPS functional life time.	L0-MI-R4, L1-FUN-R3	Medium	PA	[2]	T	General BB testing and initial electrical tests.	C
L3-ESA-FUN-R6	throughput of [6]W high voltage per thruster module (TMS) at High Voltage	See parent requirement	L2-PCS-PHY-R3	High	PA	[0.18]W	T	General BB testing and initial electrical tests.	TBC
L3-ESA-FUN-R7	The ESA shall be designed for a maximum power throughput of [2.2]W low voltage per thruster module (TMS)	See parent requirement	L2-TMS-PHY-R3	High	NA	-	-	-	-
L3-ESA-FUN-R8	The ESA shall transport the high voltage power provided by the CPCB towards its assigned TBA	This solution prevents separate cabling from a CPCB towards the TBA's	L2-PCS-FUN-R5	Medium	A	-	T	General BB testing and initial electrical tests.	C
L3-ESA-FUN-R9	The ESA shall control the emitter to extractor voltage between 0 and 1kV	Current experience shows that 700V is a feasible value. 0-1kV is set for design margin	-	High	A	0 - 1 kV	T	General BB testing and initial electrical tests.	C
L3-ESA-FUN-R10	The ESA shall be able to operate at a frequency of up to [1] Hz	Higher frequency reduces efficiency and is not likely to be needed to prevent chemical degradation of the propellant	L2-PCS-FUN-R8	Medium	A	[1] Hz	T	BB testing	NC
L3-ESA-FUN-R11	The operating, idle or non-operating lifetime of the ESA shall be greater than [4] years.	See parent requirement	L1-FUN-R3	High	PA	1 month	T	1 month continuous testing in vacuum chamber. NOTE: duration length may change due to operational feasibility.	TBC
L3-ESA-FUN-R12	The ESA shall bias the extractor voltages for neutral ion emission	By biasing the extractor voltages with respect to each other (positive and negative sides of bipolar system) a neutral ion emission can be maintained	L2-PCS-FUN-R10	Medium	NA				
L3-ESA-CON-R1	The ESA shall be able to operate and control up to [6] TMS	See parent requirement	L1-CON-R2	Medium	PA	1 TMS	T	BB testing	C
L3-ESA-CON-R2	The ESA consists of the HVESM, the LVEC and the DCI	Design choice	-	Medium	A	-	M	Inspection	C
L3-ESA-INT-R1	The ESA shall electrically interface with the TMS	Design choice	L0-PR-R3	High	A	ICD	A,T	General BB testing and initial electrical tests.	C
L3-ESA-INT-R2	The ESA shall electrically interface with the CPCB	Design choice	L0-PR-R3	High	A	ICD	A,T	General BB testing and initial electrical tests.	C
L3-ESA-INT-R3	The potential of accelerator grid shall be equal to external spacecraft, which is assumed to be ground level (= 0V)	See parent requirement	L1-INT-R3	High	A	Vacc = 0V	T	General BB testing and initial electrical tests.	C
L3-ESA-INT-R4	The ESA shall mechanically interface with the TMS	Design choice	L0-PR-R3	High	PA	ICD	M	General design/testing of BB	C
L3-ESA-PHY-R1	The mass of the ESA shall be less than [50] gram	Mass budget allocation from L1-PHY-R1	L1-PHY-R1	Medium	PA	< [50] g	M	Weighting of ESA	C
L3-ESA-PHY-R2	The ESA envelope is limited to 80x80x(15) mm (Single TMS configuration)	Volume allocation from L1-PHY-R3; High components on both the CPCB and the ESA should not interfere	L1-PHY-R3	Medium	PA	ICD	M	Dimensions measurement	C
L3-ESA-PHY-R3	The ESA shall consume less than [400] mW for its own use	Budgetted power allocation	L0-MI-R7, L1-FUN-R1	Medium	A	< [400] mW	T	Testing of power input	C
L3-ESA-PHY-R4	Materials are selected on the basis of ECSS-E-30 Part 8	See parent requirement	L1-PHY-R6	Medium	NA	-	-	-	-
L3-ESA-ENV-R1	As a first assumption, the ESA shall survive external temperatures in the range of [-30 to +60] oC (operational and non-operational).	See parent requirement	L1-ENV-R1	High	NA	-	-	-	-
L3-ESA-ENV-R2	The ESA shall survive the mechanical load and vibration environment as defined by the [TBD] launch vehicle.	See parent requirement	L1-ENV-R3	High	NA	-	-	-	-
L3-ESA-QUA-R1	The emitter to extractor voltage shall be controlled individually for each THC with an accuracy of 1V	It is estimated that this accuracy is needed based on current test results (d.d. JAN2012)	L2-PCS-QUA-R1	High	A	1V	T	BB testing	TBC

## Appendix C Heat dissipation

During tests in the local laboratory the board is always tested in an aerial environment. This means that heat dissipation will happen through convection. In a vacuum environment all heat dissipation will depend on thermal radiation meaning that, depending on the load and the efficiency, the CPCB board might overheat. Although the temperature of the different components might be significantly higher than the overall board temperature, it is interesting to at least get an idea on average board temperatures.

The radiative emissivity of a body is determined by the Stefan-Boltzmann equation which states that the radiation is equal to the emissivity  $\epsilon$  of the material, times the Stefan-Boltzmann  $\sigma$  constant, times the fourth power of the temperature.

$$Q_{emitted} = \epsilon \sigma T^4$$

With  $\sigma = 5.67 * 10^{-8} W/m^2$

If one takes an average constant of 0.9 for the emissivity of PCB board and a worst case 6W power with 50% efficiency for the CPCB board will leave 3W of dissipation.

The size of the CPCB board is 80x80 with one side covered by the ESA board so for simplicity only single side dissipation is taken into account. The dissipation per  $m^2$  will be  $3W * \frac{10000}{64} = 469W$ . The

temperature will then be  $\sqrt[4]{\frac{469W}{0,9 * \sigma}} = 309K$  which is equal to  $309-273 = 36$  degrees Celsius, but in a

room temperature environment this temperature can easily be much higher as the board also absorbs thermal radiation from the chamber wall.

This shows that the temperature might be a factor when a large load is present and that it is advisable to keep this in mind during high load tests in vacuum. To account for this during our tests stickers were applied to certain components that would change color when the board reached high temperatures (e.g. 85 degrees Celcius)

## Appendix D Calibration table negative

Using a high voltage power supply a voltage is injected into the system and the resulting measurement values are noted. The difference then is used to fill the calibration table and compensate for measured values.

In (V)	Out (ADC)	Out (V)	expected	difference
0			0	0
98	16	91,04	20,48	-4,48
198	36	188,3	40,96	-4,96
298	56	285,9	61,44	-5,44
398	76	383,5	81,92	-5,92
498	96	481,2	102,4	-7,4
598	117	579,2	122,88	-7,88
698	137	677,6	143,36	-7,36
798	157	776	163,84	-7,84
898	177	874,6	184,32	-8,32
998	198	973,5	204,8	-7,8
1098	218	1073	225,28	-8,28
1198	239	1172	245,76	-7,76
1298	259	1271	266,24	-8,24
1398	280	1371	286,72	-7,72
1498	301	1471	307,2	-7,2
1598	321	1571	327,68	-7,68
1698	342	1672	348,16	-7,16
1798	363	1773	368,64	-6,64
1898	384	1874	389,12	-6,12
1998	404	1975	409,6	-5,6
2098	426	2076	430,08	-5,08
2198	447	2178	450,56	-4,56
2298	468	2280	471,04	-4,04
2398	489	2383	491,52	-3,52
2498	510	2485	512	-3
2598	532	2589	532,48	-1,48
2698	553	2693	552,96	-0,96
2798	574	2796	573,44	0,56
2898	596	2900	593,92	1,08
2998	617	3004	614,4	2,6
3098	639	3109	634,88	4,12
3198	660	3215	655,36	4,64
3298	682	3320	675,84	6,16
3398	704	3425	696,32	7,68
3498	726	3531	716,8	9,2
3598	748	3638	737,28	10,72
3698	769	3744	757,76	12,24
3748	780	3798	0	13

As the ADC has 10 bits, an interpolation of the 'difference' values gives a full coverage for all correction values for every ADC result. To save space and since the calibration values vary only in small increments, the values are grouped in sets of 4 which are then averaged, resulting in an more manageable array of 256 bytes.

## Appendix E List of commands

The full list of commands is given in the table below. All the commands directed at the ESA are sent to the CPCB and will be passed to the ESA board through the serial bus.

	CPCB COMMANDS		
increase channel A	a+	10x increase	a9
increase channel B	b+		b9
decrease channel A	a-	10x decrease	a*
increase channel B	b-		b*
ON	<b>1</b>		
OFF	<b>0</b>		
start positive	w		
start negative	q		
get current	ai		
get voltage	av		
	bi		
	bv		
start swichtimer	<b>p</b>		
halt swichtimer	<b>o</b>		
increase sw interval (500ms)	s+		
decrease sw interval (500ms)	s-		
	ESA COMMANDS		
increase/decrease ESA channels	e1p+	request voltages	e1v
	e1p-		e2v
	e1n+		e3v
	e1n-		e4v
	e2p+		
	e2p-		
	e2n+		
	e2n-		
	e3p+		
	e3p-		
	e3n+		
	e3n-		
	e4p+		
	e4p-		
	e4n+		
	e4n-		
enable/disable ESA channels	e1E		
	e1D		
	e2E		
	e2D		
	e3E		
	e3D		
	e4E		
	e4D		

## Appendix F Test driven development

One of the topics that eventually has not been incorporated in this thesis is test driven development. Test driven development is a form of software development where writing and designing software is 'driven' by its specifications, which are enforced by iterations of writing tests, and creating software that complies to these tests.

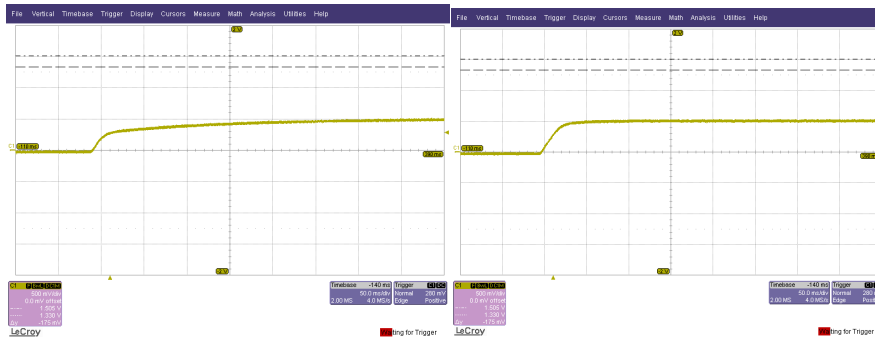
An often cited advantage is a reduced number of bugs and debugging time, as well as a sounder software design as inconsistencies are often caught during test development. Another advantage is the possibility of safer code refactoring as the tests help keep the software functioning correctly. The major disadvantage is the tests themselves as they require usually more time to write than the software itself.

Although theoretically a sound principle, test driven development is a major challenge when interacting with hardware as the tests are running locally and some functions rely or wait on input of peripherals. This can be solved by creating mock-ups that mimic some hardware functionality and provide inputs.

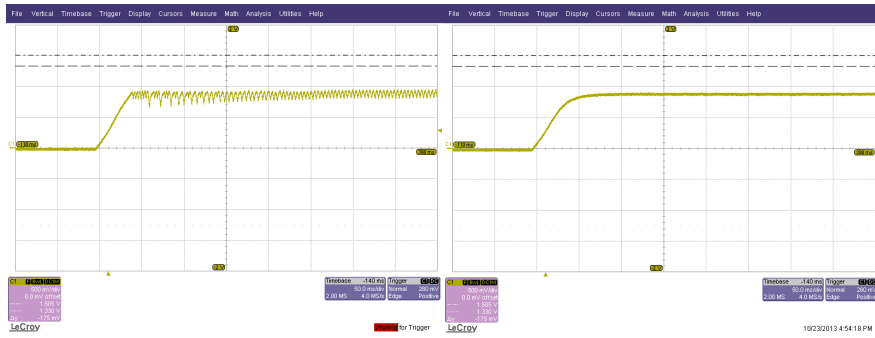
Another microthruster specific problem is the fact that hardware has evolved during the project meaning a change of requirements and the change of tests alongside.

In the course of this project I have looked into this topic during hours where hardware was under repair, or being developed, in order to find a way to incorporate unit-testing and test-driven-development into the project. An Eclipse/Cygwin environment was set up using Unity to run tests and some functional tests have been written using variables with register names to mock the registers but eventually it was difficult to fit into the workflow.

# Appendix G Behavior extractor control settings



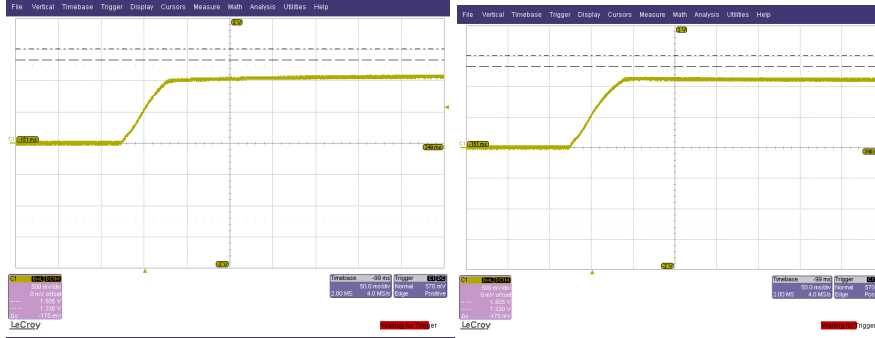
(a)  $P=2, i=1/32$ , (b)  $i=1/16$



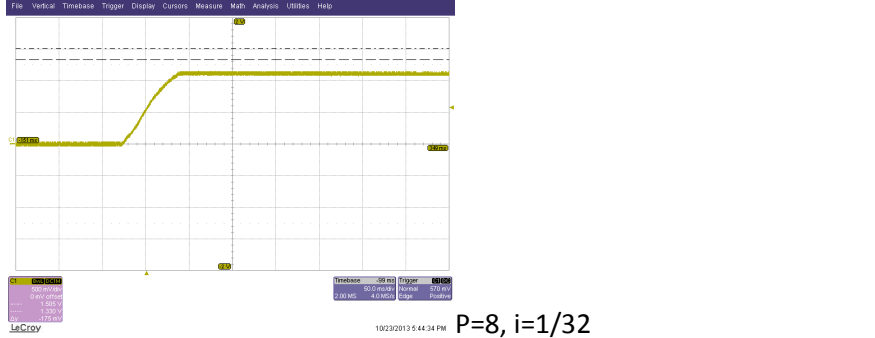
(a)  $P=1, i=1/16$ , (b)  $i=1/32$



(a)  $P=2, i=1/64$ , (b)  $i=1/32$



(a)  $P=2, i=1/64$ , (b)  $i=1/32$



$P=8, i=1/32$

Figure 43: Tests using different control variables. 50 ms/division.

Figure 43 shows an excerpt of various extractor control setting at 35%, 60% and 75% of its control range with their corresponding control variables. The P and I factors correspond to the P and I variables in the controller. These tests have been performed at the buffered measurement input of the board so do not necessarily correspond directly to the output.

## Miniaturized HV Power Supply

**IEPC-2013-258**

Presented at the 33rd International Electric Propulsion Conference,  
The George Washington University • Washington, D.C. • USA  
October 6 – 10, 2013

Richard Visee<sup>1</sup>, Martin de Jong<sup>2</sup> and Jan Timmerman<sup>3</sup>  
SystematIC design b.v., Delft, 2623CR, the Netherlands

### Abstract:

The advances in MEMS are enabling technology for miniaturized electrospray colloid thruster designs. These thrusters can be advantageously applied in small, low mass, sizeable electric propulsion systems with high specific impulse. To fully exploit the capabilities of MEMS colloid thruster propulsion technology a small and low mass HV electronic power supply and control circuit is needed. In the European FP7 funded MicroThrust project a consortium works towards the goal of a MEMS colloid thruster breadboard. In this project SystematIC design develops the miniaturized HV power supply and control unit.

The power and control system operates in dual bipolar operation. Two independently controllable HV power supplies with opposite polarity operate in bipolar mode to drive a colloid thruster and expel equal amounts of positive and negative charged ions.

The electronic design is split into two functional parts: a Central Power and Control Board (CPCB), where HV supplies are generated and an Extractor Switch Assembly (ESA), which controls the colloid extractor grids. The ESA design is modular and flexible and can be extended to control additional extractor grids, whereas the CPCB board can drive multiple ESA boards. The HV power supply architecture covers a dual bipolar setup and is scalable in power to accommodate various missions.

The electronic circuits are laboratory tested for electrical functionality. Initial test results of the circuits and their operation when assembled to an actual colloid thruster prototype are presented in this paper.

In the MicroThrust breadboard design target is a HV power supply (HVPS) with 0.4-5W output power. The bipolar emitter voltage is designed for  $\pm 3.8$  kV. The CPCB and ESA boards measure 80mm by 80mm and have a height of 35mm when stacked. The total mass of the boards excluding cables is 115 grams. On the S/C side the electrical interface applies the I<sup>2</sup>C protocol and requires a single supply voltage of 12V.

### Nomenclature

BB	= BreadBoard (model)
CPCB	= Central Power and Control Board
COTS	= Commercial off the shelf
ESA	= Extractor Switch Assembly
EIFB	= Electrical Interface Board
FM	= Flight Model
HVPS	= High Voltage Power Supply
IA	= Instrumentation Amplifier
$I_{sp}$	= Specific Impulse
I <sup>2</sup> C	= IIC, inter integrated circuit communication protocol
PCB	= Printed Circuit Board
PCS	= Power and Control System
S/C	= Space Craft

<sup>1</sup> Director SystematIC design b.v., r.visee@systematic.nl, <sup>2</sup> HW engineer, m.djong@systematic.nl, <sup>3</sup> MsC student TU Delft, j.timmerman@systematic.nl

THC = Thruster chips (microfabricated thruster arrays)  
 TRL = Technology Readiness Level  
 UART = Universal asynchronous receiver/transmitter

## I. Introduction

In the European FP7 funded MicroThrust project<sup>1</sup> a consortium of universities, knowledge institutes and SME's work towards the goal of a MEMS colloid thruster Bread Board (BB). The BB includes all relevant functional blocks of the thruster, in scaled format and allows a straightforward path to extend the design to a Flight Model (FM). Due to the MEMS technology applied in these colloid thrusters the thrusters can be miniaturized and advantageously applied in small, low mass, sizeable electric propulsion systems with high specific impulse  $I_{sp}$ . While the target missions require a small size and low mass Thruster Module, there are challenges for the electronic Power and Control Systems. HV operation is to be combined with small size and low mass. In the MicroThrust project SystematIC design develops the miniaturized HV power supply and control electronics. A 3D impression of the MEMS colloid thruster with power and control electronics for application in Nano satellites is shown in figure 1. The CPCB and ESA boards measure 80mm by 80mm and have a height of 35mm when stacked.

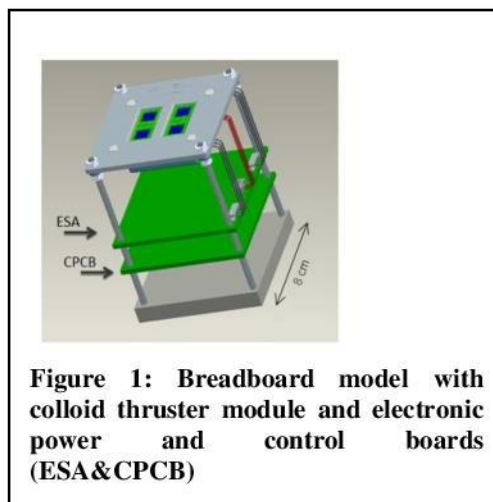


**Figure 1: Breadboard model with colloid thruster module and electronic power and control boards (ESA&CPCB)**

## II. Power and Control System concept

The Power and Control System (PCS) operates in dual bipolar operation. Two independently controllable HV power supplies with opposite polarity operate in bipolar mode to drive a colloid thruster and emit equal amounts of positive and negative charged ions. In this way propellant tank damage due to electrolysis is prevented, propellant is optimally (fully) used and the need for an electric S/C neutralizer is absent.

The electronic system concept<sup>2</sup> of the dual bipolar thruster is depicted in figure 2. The electronic design is split into two functional parts: a Central Power and Control Board (CPCB) and an Extractor Switch Assembly (ESA). In figure 2 simultaneous emissions of positive and negative propellant ions is indicated, it is to be noted that polarity of each ion stream alternates over time.

On the CPCB board HV power supplies (HVPS) generate the positive and negative HV. The load currents of both bipolar HVPS are measured so that the ion output can be measured and balanced.

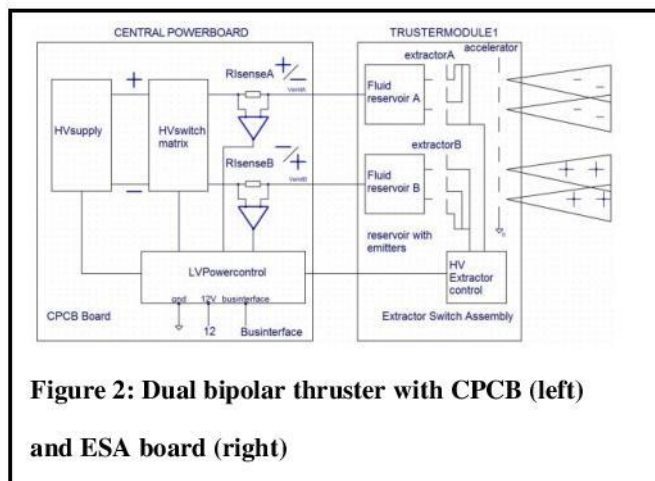


**Figure 2: Dual bipolar thruster with CPCB (left) and ESA board (right)**

The ESA board controls the Thruster Chip (THC) extractor grids and is dimensioned for the BB to control four THC's independently, two THC's per tank. The ESA design is modular and flexible and can be extended to control additional THC's, whereas the CPCB board can drive multiple ESA boards and can be scaled in power. This HV power supply architecture<sup>2</sup> covers a dual bipolar setup and is scalable in power to accommodate various missions.

## III. Power and Control System implementation

The constraints on maximum board size and mass dictated some of the design choices, where other implementation choices were dictated by limitations in availability or even existence of HV components. Solid state switching

components were used in the form of COTS high voltage FET's. To save area for all low voltage interconnections the smallest sized suitable space qualified Omnetics<sup>3</sup> connector was chosen.

Figure 3 below shows the conceptual arrangement of the building blocks of the PCS, with just one of the two HVPS's of a CPCB shown, and just one of the four extractor circuits of an ESA board.

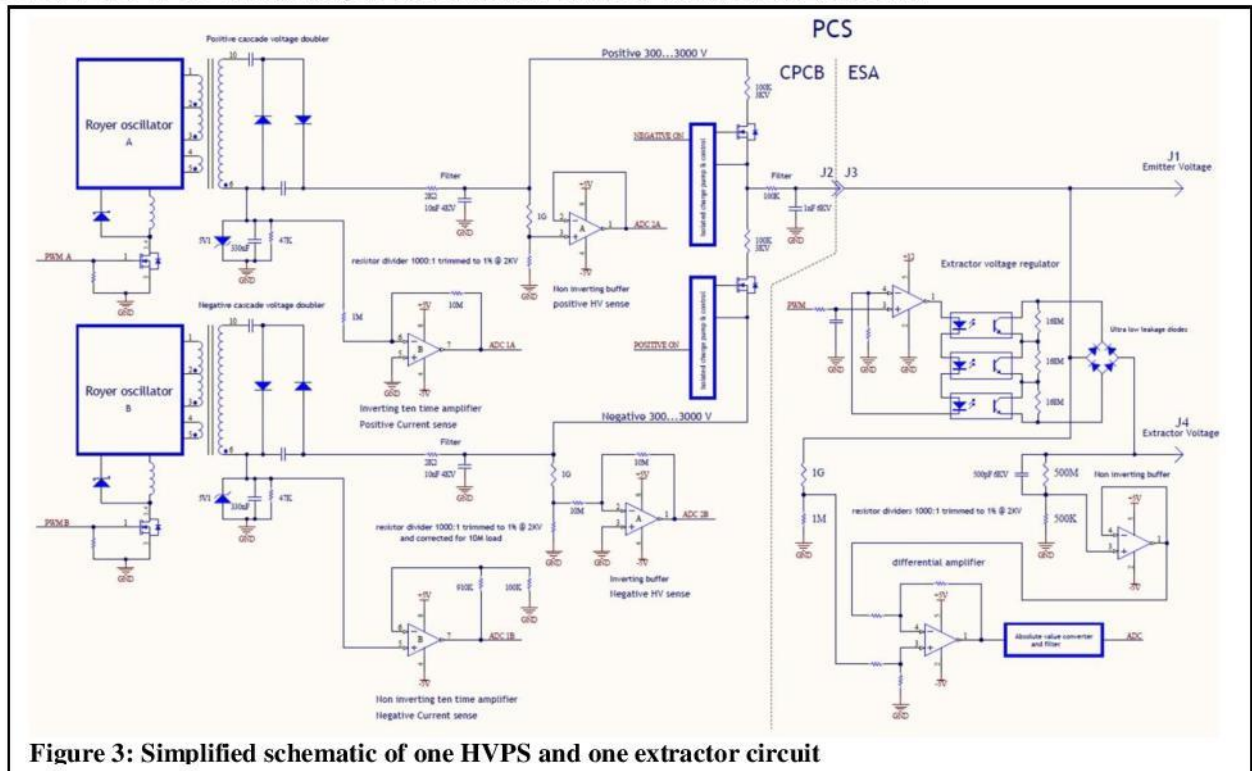


Figure 3: Simplified schematic of one HVPS and one extractor circuit

### A. Central Power and Control Board

A practical way to generate alternating positive and negative high voltages applies a separate HV generator for positive and another generator for negative high voltages. A commonly used H-bridge configuration requires at least twice the number of the large HV FET's and driver circuits.

The HV FET's switch between the generated positive and negative high voltages and also fully discharge one generator before turning on the other generator. This is mandatory to prevent momentarily having twice the high voltage which would exceed the breakdown voltage of applied components. To accommodate the high voltages, while the device is tested in air, the design uses at least 3mm creeping space for the high voltage signal routings, mutually and between high voltage signals and ground.

Because the FET's must be controlled on the high voltage side of the isolation barrier, an isolated gate voltage generator is developed. For gate control an opto-isolator is used to quickly switch the gate voltage on or off.

The basic topology used for the HV generator is based on a resonant converter, also known as a Royer circuit<sup>4</sup>, of which the output voltage could be controlled by regulating a DC bias current. The Royer is dimensioned to generate about 2kV and is followed by a single Villard cascade stage, to double the output voltage to 3.8kV maximum. By design and dimensioning of the transformer each Royer can generate about 6 Watt of power. The analog circuitry of the converter is simplified as much as possible, and replaced by digital control, to save PCB space. As can be found in figure 3 the generated and filtered high voltage is divided by a factor thousand using a precision compensated resistor dividers. Voltage non-linearity of the high ohmic HV resistors is compensated in the digital domain. Converter control is implemented in software. The second HPVS on the CPCB operates completely independent; the CPBC contains four HV generators in total.

Initially current detection on the high voltage side was considered, first in the form of a COTS high side powered and controlled A/D converter and an Instrumentation Amplifier (IA) to measure the current, but this approach was power inefficient. Later a design that transmitted the analog output of the IA across the isolation barrier using an analog opto-isolator was proposed. This design required an isolated power supply that was implemented with a charge pump to transfer about 10mW to the high side. This circuit performance deteriorated due to voltage non-linearity of the high voltage charge pump capacitors and operated unreliable in vacuum. Finally a simpler low side current measure mechanism was used. By measuring the total average DC current flowing into the Villard cascade, the HVPS output current can be calculated. The required precision of about 1% can be reached by mathematically removing the known non emission currents.

#### **B. ESA:**

To save mass, the design of the ESA extractor voltage generators does not use a separate HV generator for the extractor voltage a controllable resistive voltage divider to regulate the extractor voltage. This concept is found in figure 3. With a high side resistor that is software controllable from 0 to 500M $\Omega$  and a fixed low side resistor of 500M $\Omega$ . The 500M $\Omega$  “variable resistor” consists of a series connection of three phototransistors. In parallel to each Phototransistor a 166M $\Omega$  resistor is mounted so that fully dark the total resistance of the string will be approximately 500M $\Omega$ . The PWM control signal from the microcontroller is low pass filtered and converted into current by a transadmittance amplifier to control current through the opto-isolator LEDs. Because the photo transistors are polarity sensitive a diode bridge is applied to provide the correct polarity. The voltage over the diode bridge is the extractor voltage, and can be controlled from zero volt up-to half the emitter voltage. To quickly and precisely regulate this voltage we measure as well the emitter voltage as the extractor voltage as indicated in figure 3. Each voltage is divided by a factor thousand using a compensated precision 1:1000 resistive divider. These signals, now in the range of several volts, are subtracted, resulting in a voltage proportional to  $V_{emitter}-V_{extractor}$ . This signal can be positive or negative and a precision absolute voltage generator is used to convert this into a positive voltage  $|V_{emitter}-V_{extractor}|$ . The rectified signal is low pass filtered (anti-aliasing) and input to one of the ESA microcontroller’s analog inputs. In software an algorithm compares the sensed voltage to a set level and controls a PWM signal accordingly to regulate the extractor voltage. A logic “wired or” configuration is used so that multiple ESA boards can communicate with the CPCB over one serial connection. The CPCB communicates to all ESA boards. For other inter-board communications, temperature measurements on the Electrical interface board (EIFB) and communication with the spacecraft, the I<sup>2</sup>C protocol interface is used.

In figure 4 the assembled CPCB and ESA boards are depicted. All Low Voltage interconnections are made using the Omnetics connectors. The connection to the S/C consists of 12V power, GND and I<sup>2</sup>C signals. The inter-board connection adds 5V for ESA’s and EIFB’s, which is generated on the CPCB board, and the serial interconnections. Lastly the connection to the EIFB of the thruster chip (THC) consists only of 5V, GND and I<sup>2</sup>C signals. For HV interconnects between CPCB, ESA and the EIFB flexible wires are used that are isolated with Kapton tape. These HV wires are soldered to the board, and use strain relieves for mechanical stability.

The CPCB and ESA boards measure 80mm by 80mm and have a height of 35mm when stacked. The total mass of the boards excluding cables is 115 grams.

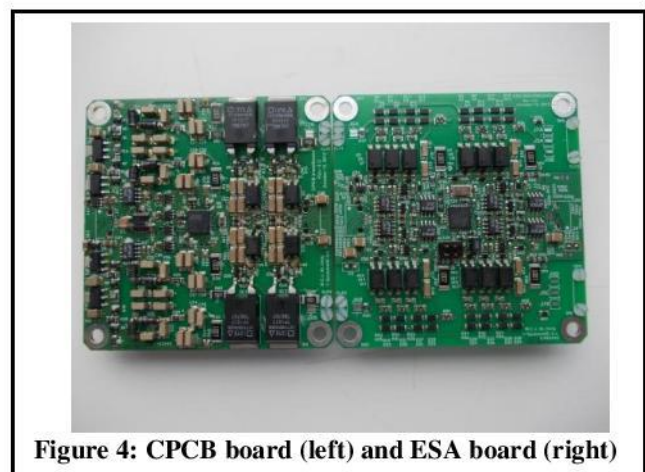


**Figure 4: CPCB board (left) and ESA board (right)**

#### IV. CPCB and ESA Software

The modular setup of a CPCB board with multiple extractor switching assembly (ESA) boards requires that hardware and control are split across multiple boards therefore control is distributed over two microcontrollers. The controller implement two basic functions: control of the generation of high voltage and control of extractor regulation.

Controller functionality consists of:

CPCB:

- HV generator control
- HV polarity switching
- Overvoltage and short circuit protection
- Current measurement
- Compensation of non-linear HV resistive divider errors
- Communication and error reporting with S/C
- Communication with ESA modules

ESA:

- Extractor voltage controls
- Communication with CPCB

Communication

To communicate between CPCB and ESA boards a separate dedicated serial UART bus is used. The UART protocol is used since only one I<sup>2</sup>C bus and one UART bus is available and the I<sup>2</sup>C bus is used for communication with the main controller board.

CPCB Control

The CPCB microcontroller controls the power supplied to the HV generation circuit to generate a stable high voltage level. The ADC of the microcontroller generates an interrupt when a new measurement sample of the high voltage supply output is available. The control algorithm in the interrupt handler adjusts the power input in the high voltage generation circuit if necessary.

This means that delays in handling of ADC interrupts can potentially cause a voltage outside the specs which can even be damaging. To ensure proper handling of the delays, all the interrupt routines are short and, as the worst case delay is the sum of all interrupts, also the number of interrupts have been kept to an absolute minimum resulting in only two other interrupt sources with a total of less than 1100 cycles (estimated, as they are subject to change, but well within this limit) resulting in an absolute worst case response time of 70µs which is still an order of magnitude faster than the HV generation circuit. To ensure maximum accuracy and low measurement noise levels the frequency of the interrupts is around 9600 samples/s divided over two high-voltage ADC's and two current detection circuits with an effective update rate of 2400 Hz.

Additionally, to prevent accidental damaging during development and also to provide an extra safeguard during space operation, all HV generation will be aborted when an overvoltage is detected which is set at |300V| above the set level, to account for possible measurement noise and the slight control variations. This is based on noise tests in a laboratory environment.

High voltage polarity switching is implemented in the CPCB controller with a period that can be set to any multiple of 0.5 seconds with a maximum of 127 seconds. Polarity switching follows a number of strict consecutive states. Failing to adhere to this order will damage to the circuit.

These states are:

- Disabling negative/positive HV generation
- Open both positive and negative voltage switches to discharge the circuits
- Closing positive/negative switches
- Starting positive/negative HV generation

Access to polarity switching in software is restricted to a single method thus reducing software complexity and no errors in polarity switching will occur.

#### Current measurement

The emitter current measured correlates with the power output of the board and is measured using two of the ADC inputs. The current measurements are also used to detect short circuits.

#### ESA Control

The ESA controllers each control four extractors and control operation is interrupt based like the CPCB. The ADC of the microcontroller generates an interrupt when a new measurement sample of one of the extractor output is available and adjusts the voltage accordingly. As there are no other interrupt sources, the interrupt response time of the ESA controller is instantaneous. Each of the extractor channels is connected to a separate ADC channel which is sampled with a frequency of approximately 2400 Hz. This is the maximum sample speed for four channels on the microcontroller. The resolution of the measurements is 1.62V which originates in the resolution of the microcontroller ADC of 10 bits and the hardware implementation of the circuit which provides a 3times amplification over the measured 1:1000 volts circuit, thus allowing for a maximum measuring range of 1667 volts. This exceeds the control range of the extractor therefore allowing for possible overvoltage detection. As soon as the supply voltage is stable the CPCB will send a command through the UART interface to generate an extractor voltage of a set level. The voltage levels can be set separately for each extractor channel and also separately for both the positive and negative cycle. The controller ensures the  $|V_{emitter} - V_{extractor}|$  voltage does not exceed 1000V

#### Calibration table for hardware compensation

There is a notable non-linear effect present in the system, which is voltage coefficient (VCR) of the 1:1000 resistor divider used to transfer voltages to the low voltage domain. The specification of VCR of the high ohmic resistors used is up to 7ppm/V so at 3kV and corresponds to  $7\text{ppm/V} * 3000\text{V} = 2\%$ .

The solution in the microthrust project is the use of a lookup-table with compensation for ADC values is generated based on measurements in a controlled test environment.

#### Controlling the PCS

For easy control and tests at project partners a graphical user interface is provided to control part of the board functionality. A screenshot is found in figure 5. One in every 2000 samples is provided to the interface to report on the current status and optionally the measurement results are returned as text only for later analysis.

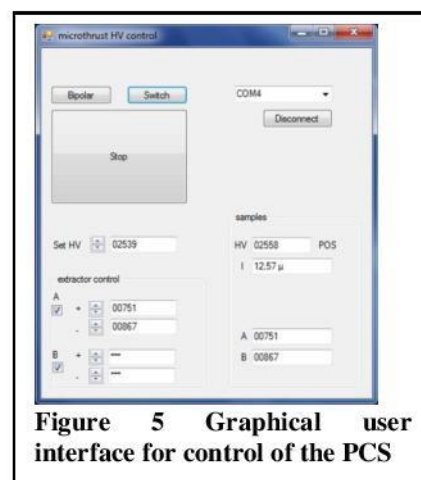


**Figure 5 Graphical user interface for control of the PCS**

## V. TEST results

The design target for the MicroThrust breadboard is a dual bipolar 3.8kV power supply with 0.4-5W output power capability. In figure 6 a typical PCS measurement result is shown in bipolar operation. The curve in red displays  $V_{emitter}$  for a programmed value set at 2558V and corresponds to the values found in figure 5. In yellow  $V_{extractor}$  is measured, in this set up  $V_{emitter} - V_{extractor}$  is set at 751V for positive  $V_{emitter}$  and 867V for negative  $V_{emitter}$ . It is to be noted that during polarity switching initially  $V_{emitter}$  and  $V_{extractor}$  are intentionally regulated to an equal voltage and the thruster will be off. When  $V_{emitter}$  has settled the controller starts regulating  $V_{emitter} - V_{extractor}$  to the programmed value. Just before polarity changing  $V_{emitter}$  and  $V_{extractor}$  are regulated to an equal voltage again to turn the thruster off. Then the same procedure repeats for the opposite polarity. The displayed waveforms are accurate representations

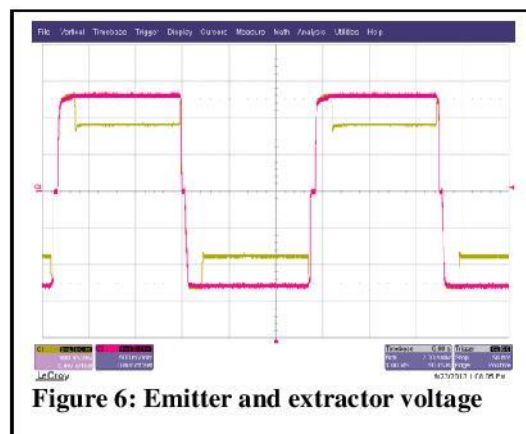


**Figure 6: Emitter and extractor voltage**

of the actual  $V_{emitter}$  and  $V_{extractor}$  but scaled to LV domain with calibrated probe networks. At 0V the switch over from positive supply to negative supply can be noticed.

At 3kV under ambient conditions measured ripple of  $V_{emitter}$  is  $<10 V_{pp}$  at  $100\mu A$  (0.3W) load. The measured ripple waveform is displayed in figure 7. Bipolar operation frequency is programmable in 0.5s steps and has a default setting of 12s which equals 0.083 Hz. The supply can be operated in a dual static HVPS mode for application in a unipolar thruster system. The  $|V_{emitter}-V_{extractor}|$  voltage is programmable in the range of 0-1kV.  $V_{emitter}$  voltage accuracy is calibrated to 0.1% at 3kV.  $V_{emitter}$  ripple is 4 V<sub>p</sub>. By design the accelerator grid is 0V and acceleration voltage equals  $|V_{extractor}|$ . Target electric power conversion efficiency is 50% at 0.4W. Measured electrical efficiency of the HV part of the PCS in figure 4 is 36% at this output power. The HVPS efficiency improves at higher output power and the supply has an efficiency of 44% at 3W and 3kV. Measurements on a

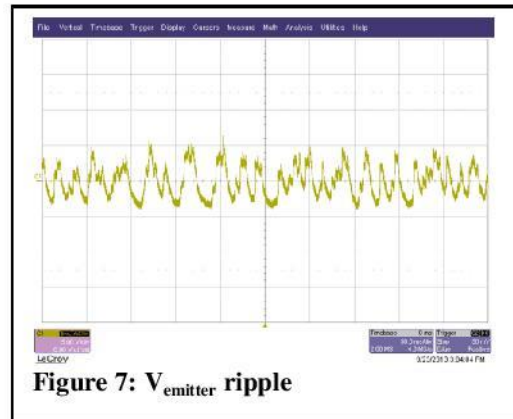


**Figure 7:  $V_{emitter}$  ripple**

single HVPS with an improved control result in efficiencies of 45% at 0.4W and 3kV and 73% at 2.4W and 3kV.

Initial tests with a single emitter thruster with the PCS outside vacuum were fully functional<sup>5</sup>. Figures 8 and 9 display some results of these tests. In figure 8 the emitted current during a single cycle is shown. Bipolar operation is clearly visible. It is to be noted that the electrical current in single emitter operation is in the 200 to 300nA range and is very small. Some switching spikes are visible on this scale and can be correlated to the HVPS electrical switching and are harmless for the thruster is off at these moments in time. In figure 9 the bipolar currents are shown

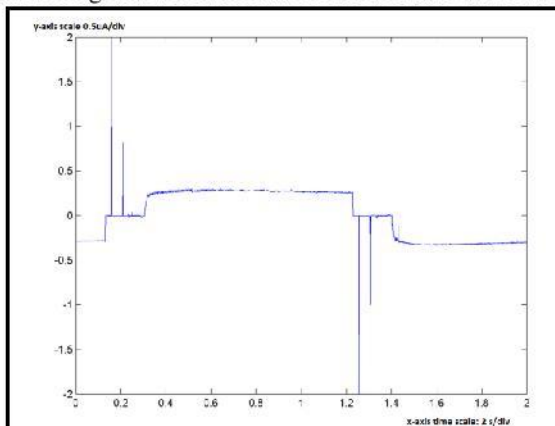


**Figure 9: Emitted current in bipolar operation, single switch cycle**

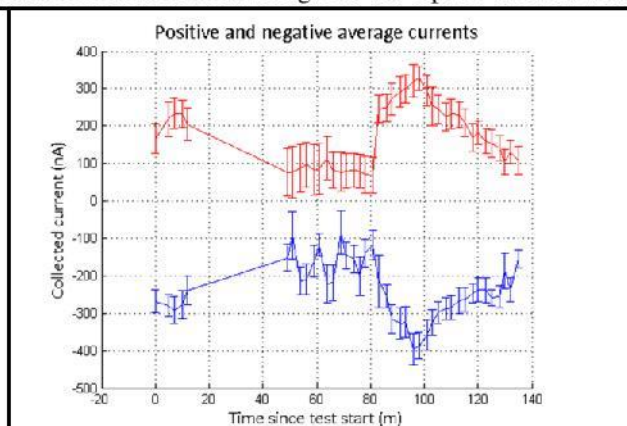


**Figure 8: Emitted current in bipolar operation over time**

over time for more than 2 hours of operation.

In vacuum the PCS operation is functional. In the months to come further work will be done to combine the PCS with an actual Thruster array.

The emitter current is measured to have an accuracy of 4% of the maximum current. The required precision of about 1% can be reached by mathematically compensating for the ESA HV bias current in software, which load the HVPS but do not contribute to emission current. This functionality needs to be implemented.

Measurement results are summarized in the table 1 below.

**Table 1: PCS measurements versus specifications**

	Specification	Measurement
$V_{emitter}$ vacuum	$\pm 3.8kV$	$\pm 3.8kV$
$V_{emitter}$ air	-	$\pm 3kV$
Ripple $V_{emitter}$	$< 4V_p$	$4V_p$
HV output power	$0.4W (100 \mu A)$	$> 0.4W (100\mu A)$
$V_{emitter}$ accuracy		0.1%
Current sensor accuracy	$< 1\%$	4%
Bipolar operation frequency	$< 0.1Hz$	$< 0.25Hz$
Target power conversion efficiency in operation	$> 50\%$ at 0.4W	36% at 0.4W
$(V_{emitter}-V_{extractor})$ voltage	0-1kV	0-1kV
Ripple $V_{extractor}$	$< 4V_p$	$4V_p$
$V_{emitter}$ accuracy	0.1%	2.3%
Acceleration voltage	$V_{extractor}$ V	$V_{extractor}$ V

### Conclusion

In this article a HV PCS for application with a colloid Thruster is presented, both on conceptual level as well as implemented in hardware with cubesat size PCB dimensions. Actual hardware is tested outside vacuum with a single emitter colloid Thruster. Inside vacuum the PCS is tested and functional. Further integration tests with the colloid Thruster are planned for the months to come. The electrical performance of the PCS is in the right ball park but requires further work on the design to meet the intended specifications and to improve efficiency and accuracy of the PCS breadboard.

### Acknowledgments

This work has been supported by the MicroThrust project, grant agreement number 263035, funded by the EC Seventh Framework Program theme FP7-SPACE-2010.

### References

1. Consortium website: [www.microthrust.eu](http://www.microthrust.eu)
2. Development of the microthrust breadboard: a miniaturized electric propulsion system for nano satellites, AAAF-ESA-CNES Space Propulsion 2012 7th – 10th May 2012, Bordeaux, France
3. Omnetics connector MNSO-09-AA-ETH2, <http://www.omnetics.com/products/bilobe-cots-dualrow>
4. Royer topology is invented by Richard L. Bright and George H. Royer, U.S. Patent 2783384, filed 26 Feb. 1957.
5. Measurement results obtained with colloid thruster setup of consortium partner at EPFL in Neuchatel.

## Appendix I Lab results using a 91 emitter thruster chip

Figure 44 shows results for a 91 emitter array using a laboratory supply. In this configuration an extractor load current of 125nA is present. This is equivalent to a load of 10M $\Omega$  which is likely to negatively impact as shown in Figure 23 on page 35 this is controlled with a variable resistor of 500M which is a magnitude higher so the resistor that is intended to control the extraction voltage has little influence in reality.

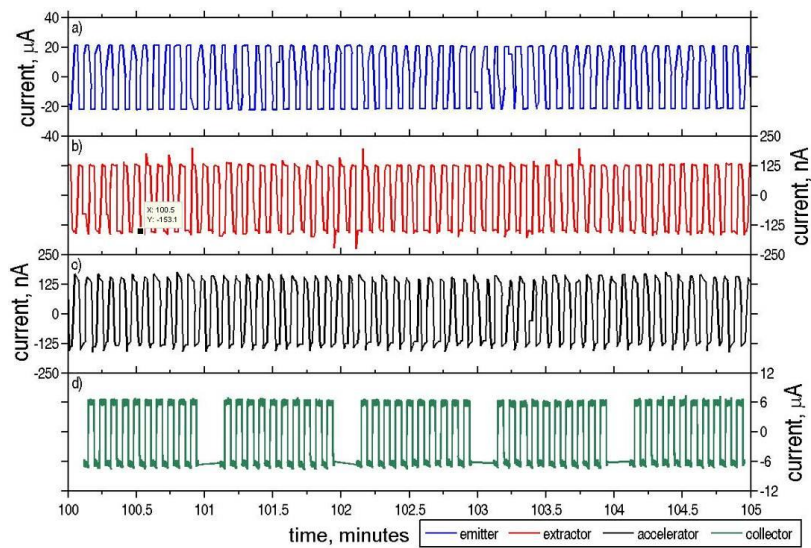


Figure 44: 91 emitter chip, using lab supply at 800 V<sub>emitter</sub>, 0 V<sub>extractor</sub> and 0 V<sub>emitter</sub>